THE

NATURE AND PROPERTIES

OF

GHATTI GUM.

A Thesis presented by

THOMAS MARSHALL GEORGE

in fulfilment of the requirments

of the degree of

MASTER OF SCIENCE

of the

UNIVERSITY OF GLASGOW.

Department of Pharmacy,

Royal College of Science

and Technology,

Glasgow.

September , 1963.

SUMMARY

In the first section the source, history and formation of ghatti gum and its physico-chemical properties and molecular structure were outlined. A general outline of the physical chemistry of polyelectrolytes was given together with an account of such polyelectrolytes as gum acacia, gum tragacanth, carrageenin and sodium carboxymethylcellulose, which are important in pharmacy. The theory of light scattering was also reviewed.

In the experimental sections of the thesis work was reported on an authenticated sample of ghatti gum from Anogeissus latifolia (Combretaceae) which was fractionated by acidic alcoholic precipitation (Fraction 1) and chromatography on silica gel (Fractions 2 and 3). The equivalent weights of the three fractions were found to be 1750, 1800 and 2040 respectively.

The sodium salts of the three fractions were studied in aqueous solutions and in various concentrations of sodium chloride. The molecular weights of the fractions were determined from the Zimm plots constructed from the light-scattering results. From the light-scattering experiments an idea of the radii of gyration and molecular weight were obtained. The molecules of sodium ghattate appear to be rod-shaped in both aqueous solutions and in solutions of sodium chloride. The molecular weights of Fractions 1, 2 and 3 were found to be 2.1, 2.7 and 2.6 x 10^6 respectively.

The viscosity of the sodium salts of the fractions in aqueous solutions and in solutions of sodium chloride were determined using

a suspended level dilution viscometer and a Couette viscometer. All the solutions appeared to exhibit Newtonian flow over the range of shear rates investigated. The effect of added salt in the solutions was to decrease the viscosity.

From the light-scattering and viscosity experiments the expansion factors of the molecules were calculated. Values for this calculated from each of these experimental results showed reasonable agreement with each other. The molecules were considerably affected by the concentration of sodium chloride; in solutions of high salt concentration considerably contraction of the molecules was observed.

Reasons for the difference in the observed and calculated values of the second virial coefficients for the various systems were discussed.

The absorption and desorption of water-vapour by the fractions was investigated at 25° and 40°C. From the isotherms obtained from these experiments values of the amount of water present in the macromolecules in the first and second layers and at saturation were calculated. The values of the partial enthalpies and entropies of adsorption were calculated and possible mechanisms for the sorption of water vapour were suggested.

The sodium salts of all the fractions were found to be fairly surface-active. The effect of the addition of sodium chloride and the effect of time on the surface tension of the solutions was determined using the sessile drop method. This was found to have

certain advantages over the Wilhelmy plate method for the determination of surface tension. A possible mechanism for the surface activity and a possible structure for the surface film were suggested.

ACKNOWLEDGEMENTS

I would like to record my appreciation to Dr. P.H.Elworthy for his guidance and help during the course of this work and to Professor J.B.Stenlake for his interest.

I would also ~~lá~~ thank Dr. F.Fish for the authentification of the ghatti gum , Mr. A.G.Kenyon , the Tropical Products Institute , and Professor P.V.Bole , St. Xavier's College , Calcutta for arranging the supply of a genuine sample of ghatti gum , and Mr. G.Cochrane for building the apparatus.

I would also like to thank Evans Medical Ltd. for the gift of ghatti gum and for the award of an Evans Medical Fellowship and Dr. Glaser and Dr. Thomas for their interest and encouragement.

CONTENTS

SECTION 1

INTRODUCTION

PROPERTIES OF GHATTI GUM

Introduction

Many plants produce gums either on injury or as an integral part of their natural biochemical mechanisms. The general properties of these gums have been known for many centuries and they have been employed in a wide diversity of processes.

There are still a number of naturally occurring plant gums which are of considerable importance in pharmacy and in industry in general. Most of these widely used gums have been fully investigated and their structure and physico-chemical properties have been elucidated.

The important plant gums are polysaccharides and many are polyelectrolytes. Because of these basic similarities many of the physical properties of these gums are similar. It is now possible to synthesise polyelectrolytic poly-:saccharides, for example sodium carboxymethyl cellulose, to replace these natural products. This has the advantage that the nature of the molecules of these synthetic substances can be largely predetermined.

However, there are a number of gums, like ghatti gum, which have a more limited use in pharmacy and in industrial applications and which have not been studied with the same

intensity as the more common gums like gum acacia and gum tragacanth.

The main properties which make these substances useful are the facts that they are largely water-soluble and that their aqueous solutions have a high viscosity. Many of them also have good emulsifying properties.

To explain and understand these properties it is essential to understand the nature of the molecules of the substances and the properties of their solutions. Hence studies on the molecular properties of ghatti gum have been undertaken and are reported in this thesis.

Source

Ghatti gum is the translucent, water-soluble, exuded gum from Anogeissus latifolia (Combretaceae). This large deciduous tree is indigenous to India and Ceylon. It is common in the dry deciduous forests there excepting East Bengal and Assam. It is found in the sub-Himalayan tract from the Ravi to Nepal, Bihar, Chota Nagpur, Madhya Bharat and southwards to Ceylon. It grows ~~up to~~ at a height of 3,000 to 4,000 feet above sea level in the Himalayas and the South Indian Hills. [1]

The leaves, which turn bright red during the dry season, yield a black dye and are widely used in the leather tanning industry. A tanning extract containing 48.3% tannin has also been prepared from the bark by Hooper [2].

The timber is tough and strong and, though it splits on seasoning and will not stand damp, is used in axe-handles, furniture making and has been recommended for railway sleepers[3].

The gum varies from light-brown to dark-brown and consists of round or vermiform pieces of varying size. It has a glassy fracture and is transparent. The surface of the gum nodules, however, may be roughened and opaque.

The gum is produced as a sealing mechanism when the bark is injured and the yield may be increased by artificial incisions. However, this process must be carefully carried out to prevent permanent injury to the tree.

The gum is hand-picked by natives and then dried in the sun for two or three days before being taken to Bombay for sorting and export.

After classification the gum is hand-sorted into

grades. The grading is done by means of colour and appearance. The lighter gum nodules are the best grade.

The gum is picked during the dry season as the rain during the wet season would spoil the unpicked gum. Normally the largest crop of gum is picked in April.

History

During the latter half of the nineteenth century there was a severe shortage of gum arabic due to the fact that the exports of this gum from the Sudan were virtually stopped as a result of hostilities between France, Britain and Egypt. The trade routes from the Sudan did not reopen until the Sudan came under British Control in 1898.

This shortage of gum arabic, a very important pharma:ceutical substance at this time, lead to the investigation of various gums to find a substitute for gum arabic in pharmaceutical preparations. A great number of Indian gums were considered for this purpose such as Ocmrawhatti, Glassy Amrad, East Indian Amrad, Pale Amrad, Ghatti and some Australian gums such as wattle gum and Kauri gum 4 - 10 .

It appears that at this time there was some considerable confusion and uncertainty in the nomenclature of the Indian gums and obviously some difficulty in obtaining authenticated

samples of gums due, presumably, to the haphazard methods of collection and distribution.

Birdwood[12] stated that ghatti was the gum from Feronia elephantum, Magnifera indica, Azadirachta indica, Terminalia bellerica and Acacia arabica.

Rideal and Youle[8] mentioned a number of gums to which they referred as "ghattis".

Watt stated that the gum from Anogeissus latifolia constituted the bulk of the gum ghatti sold in Bombay[3] and that gum ghatti was so named because it was brought by train down the Ghatts of Bombay. Gum ghatti referred to a wide range of gums.

Proble[4] in 1823 gave the source of ghatti gum as Anogeissus latifolia while Rideal and Youle[8] described the physical appearance of ghattis without giving any botanical source. In fact the physical properties of the gum described by them bear very little or no resemblance to the properties of the proper ghatti gum. The authors described the gum of Anogeissus latifolia as being of very little use. This statement does not agree with the findings of other authors.

Rideal and Walker maintained that ghatti gum could very well be used instead of gum arabic. They stated that

solutions of gum ghatti were more viscous than comparative gum arabic solutions and that it produced good white emulsions with excellent keeping properties.

Hander[5] stated that "if more care were taken in the gathering and selection (of ghatti gum) there seems little doubt that picked qualities would speedily rise to considerable commercial value and pharmaceutical interest". He also stated that the emulsions made from a mucilage of ghatti gum were equal to those made with acacia.

The main disadvantage of ghatti gum was the fact that although described as a "water-soluble gum" it was actually only partially soluble in water. Henry[13] and Rideal and Youle[6,8] stated that the gum was only 75% soluble in water. The insoluble 25% was referred to as "metarabin" and methods were tried to convert this to the soluble "arabin" by boiling in water for long periods. Rideal and Youle attempted to convert ghatti gum by fractional precipitation with alcohol into a gum which could be identified as ordinary gum arabic. This high percentage of insoluble matter also indicates that the picking and sorting of gums at this time were not particularly efficient, and that a considerable amount of other gums were present in the samples of ghatti gum available.

Ghatti gum was first officially recognised in the "Indian and Colonial Addendum" 1900 to the 1898 British Pharmacopoeia for use in Eastern and Colonial countries[14]. This monograph was transferred to the British Pharmacopoeia 1914[15] but was not included in the 1932 edition. It was known in the British Pharmacopoeia 1914 and in Squire's Companion[16] as Indian gum with a synonym of ghatti gum and was defined as "the exudation from the stem of Anogeissus latifolia".

Indian gum was allowed to describe Bassora of gum sterculia. Bassora was a collective term for a group of highly coloured gums collected in the neighbourhood of Bassora on the Gulf of Persia. The two main sources of Bassora gum were Cochlospermum gossypium (Bixaceae) and Sterculia urens (Sterculiaceae).

The term "Indian gum" was also applied to the exudate from Acacia arabica. It is possible that ghatti gum was also confused both in picking and sorting with gum shiraz to which it bears some resemblance. Eventually however the term ghatti came to mean specifically the gum produced by Anogeissus latifolia[11,17].

Possibly this variety of meanings for the term ghatti and the uncertainty of the name of the gum from Anogeissus latifolia were not only due to erratic picking and uncertain

sorting but also due to the origins of the name.

Clusius in 1605[3] speaks of "Gummi Gutti" being brought from China to Europe and so it is possible that this was derived from some Chinese or Malayan dialect.

However, the more reasonable explanation is that the word ghatti was derived from the Indian word "ghátí" which meant a strait or a pass through the mountains. Therefore, in India, drugs of local origin were called ghátí to dis: :tinguish them from drugs imported from a distance. Since a great variety of gums were collected in India it is quite conceivable that a considerable amount of confusion resulted from this basis of drug nomenclature.

Eventually after British Control of the Sudan in 1898 the export of gum acacia restarted and there was no need to search for substitutes. Though ghatti gum had been used quite considerably in pharmacy its use was then dis: :continued.

Formation of Gums

Many plants produce or contain some form of gum or mucilage and these plant products have been used in their country of origin for many and various purposes. Their use spread from one area to another and many of them achieved considerable economic importance. Such gums

and mucilages have been used for food, in medicine, in embalming and in many other arts and crafts.

The use of these plant gums has developed and diversified and at the present time many gums are used in the pharmaceutical industry, in mining, in textiles, in paint manufacture, in confectionery, in the food industry, in cosmetics and in many other industries. It has been estimated that more than a billion pounds of gum are used for these various purposes in the United States of America every year[18].

The mechanism whereby plants produce gums is as yet not certain though various theories have been put forward to account for it.

There is the possibility that these gums are formed by the natural metabolic activities of the plants and that injury to the plant merely causes them to appear on the surface.

It may be that plants only produce gums as a result of a pathological condition and there is some evidence for this. Acacia trees which were grown under favourable climatic and ecological conditions did not produce very much gum but Acacia trees grown under arduous and unfavourable conditions produced copious amounts of gum[19]. Wallis[20] stated that gums are abnormal products resulting from pathological conditions brought about by injury or unfavourable conditions of growth, and that gums were formed by the conversion of the cell walls by an enzyme.

Thaysen and Bunker[21] stated that gums were produced by the plants as a protection against invading organisms[22].

Another suggestion is that gums were produced by the injured trees to act as sealants to prevent water-loss.

It would seem, however, that no matter what the mechanism for the instigation of gum production, the actual production of the gum is due to enzymatic polymerisation rather than chemical polymerisation. If the gum were produced by enzymatic means then it is reasonable to assume that the enzymes responsible for the production would be found in the tears of gum produced and that these enzymes would, under suitable conditions, be capable of reconverting the gum into its constituent materials.

It has, in fact, been shown by several workers that gums under suitable conditions will be broken down by the enzymes present in them to their original components.

Molecular Structure

Ghatti gum was found to be the calcium salt of an acidic polysaccharide which was called ghattic acid[23,24]. The soluble portion of the gum had a molecular weight of 11,860 when calculated from osmotic pressure measurements.

The ghattic acid which was prepared by alcoholic precipitation of an acidified alcoholic solution of the

crude gum had an equivalent weight of between 1340 and 1735.

From complete hydrolysis of the gum it was shown that it contained 41% L-arabinose, 27% D-galactose, 12% D-glucuronic acid, 8% D-mannose, D-xylose and 6 deoxyhexose[25]. Ghatti gum resembled damson and cherry gums in the composition of their component sugars[26, 27, 28]. (Fig. 1).

Partial hydrolysis of the gum with dilute sulphuric acid gave two aldobiuronic acids which were shown to be 6,0 (β-D-glucopyranosyluronic acid) D-galactose and 2,0 (β-D-glucopyranosyluronic acid) D-mannose.

The former aldobiuronic acid's analogue 4β-(β-D-glucopyranosyluronic acid) D-galactose has been isolated from Type III pneumococcus polysaccharide[29] while the latter has been isolated from some Acacia gums.

With periodic oxidation of ghatti gum three moles of formic acid were formed for each equivalent of the gum, and it was found that 33% of the galactose and 80% of the arabinose residue were oxidised. Periodic oxidation breaks the bond between two adjacent carbon atoms if each has a hydroxyl group. The results of the periodic oxidation of ghatti gum could be explained if it were assumed that the labile L-arabinose residue were present in the furanose form with an α,L type of linkage, and if most of the D-galactose units were joined through C_1 and C_3 and the remainder by 1,6 - linkage.

If the gum were methylated and then subjected to hydro: :lysis then, as well as the constituents listed above, small amounts of 2,3,4 tri-O-methylxylose, 2,3,4 tri-O-methyl: :rhamnose and 2,3,5 tri-O-methylarabinose were obtained.

From this hydrolyzate the acid components were removed largely as a mixture of methylated aldobiuronic acids with an equivalent weight of 370. This gave, on further hydro: :lysis, a mixture of 2,3,4 tri-O-methyl-D-glucuronic acid, 2,3 di-O-methyl-D-glucuronic acid, 3,4,6 tri-O-methyl-D-mannose, 2,3,4 tri-O-methyl-D-galactose and 2,3 di-O-methyl-D-galactose.

It would appear from this that some of the glucuronic residues in the degraded gum were present in non-terminal positions and linked through C_3 and C_4. Since the main neutral products on hydrolysis of the methylated aldobiuronic acid were 2,3,4 tri-O-methyl-D-galactose and 3,4,6 tri-O- :methyl-D-mannose the aldobiuronic acid groups were present in the degraded gum as terminal groups.

The point of attachment of the aldobiuronic acid side chains to the main galactose framework could be deduced from the products of hydrolysis of methylated degraded gum. On hydrolysis the methylated gum gave 2,3 di-O-methyl-D-galactose which indicated that the main framework of D-galactose units contained 1,6- linkages. From this it appeared that the

aldobiuronic acid chains were attached to C_4 of the D-galactose framework.

The galactose residues which gave rise, on methylation and hydrolysis, to the 2,3,4,6 tetra-O-methyl-D-galactose were attached to those units of glucuronic acid which gave 2,3 di-O-methyl-D-glucuronic acid.

The galactose residue may have been the terminal units of a side chain as they were found to be in the case of gum acacia[30] or they may have formed the non-reducing ends of the D-galactose framework, and were generated by cleavage of the main chain during autohydrolysis.

Most of the side-chains were attached to the C_4 of the D-galactose framework. This was shown by the presence of 2,3 di-O-methyl-D-galactose. However, this was accompanied by some 2,4 di-O-methyl-D-galactose which indicated that some of the side chains were attached to C_3 in the main framework.

Hydrolysis of the methylated undegraded gum gave 2,3,4,6 tetra-O-methyl-D-galactose, 2,3,4 tri-O-methyl-D-galactose, 2,O-methyl-D-galactose, 2,4 di-O-methyl-D-galactose, 4,O-methyl-D-mannose, 2,3,4 tri-O-methyl-D-glucuronic acid, 2,3 di-O-methyl-D-glucuronic acid, 2,3,4 tri-O-methyl L-rhamnose, 2,3,5 tri-O-methyl-L-arabinose, 2,3 di-O-methyl L-arabinose, 2,4 di-O-methyl-L-arabinose, 2,5 di-O-methyl- L-arabinose and 2,3 di-O-methyl-L-arabinose.

The presence of the two glucuronic acid residues indicated that some of the glucuronic acid was present as terminal units and others as non-terminal units joined through C_4.

The D-galactose residues of the 6,0 (β-D-glucopyranosyl-uronic acid) D-galactose gave the 2,4 di-O-methyl D-galactose and the D-mannose from the 2,0 (β-D-glucopyranosyluronic acid) D-mannose gave the 4,0-methyl D-mannose. From this it appeared that arabinose side chains are attached to the aldobiuronic acid groups through C_3 of D-galactose and through C_3 and C_6 of D-mannose. Side chains of L-arabinose, D-galactose, D-xylose and L-rhamnose may be attached through C_4 of some of the D-glucuronic acid units as in the case of the degraded gum.

Because the D-galactose units which gave rise to 2,3 di-O-methyl D-galactose on methylation of the degraded gum, gave rise to 2 mono-O-methyl-D-galactose on hydrolysis of the methylated undegraded gum, it was assumed that a side-chain, probably of arabinose, must have been joined to the C_3 of the D-galactose units which were joined by the 1,6- linkage and to which the side chain aldobiuronic acids were attached.

On hydrolysis of the methylated undegraded gum the L-arabinose gave rise to 2,3,5 tri-O-methyl-L-arabinose and smaller amounts of the 2,3; 2,4; 2,5; and 3,5 di-O-methyl

others. Only the 2,3 di-O-methyl-L-arabinose arose from L-arabinose which was attacked by periodic acid oxidation. This was agreed with the fact that only 20% of the L-arabinose residues were susceptible to periodate oxidation .

It may be that the 2,4 di-O-methyl L-arabinose was formed from the arabopyranose units interspersed in the main D-galactose framework as suggested by studies on acacia.

Ghatti gum resembled cherry, damson, acacia and mesquite gums since it contained a high proportion of terminal L-arabo-:furanose units but differed from them in possessing a 1,6-linked galactose framework.

From these results it would appear that ghatti gum is composed of a framework of D-galactose units joined by 1,3- and 1,6- linkages. This framework is interspersed occasionally with arabopyranose units. The aldobiuronic acid side chains are mainly joined to the C_4 of the galactose units in the main framework and occasionally to C_3. Arabinose side chains are also attached to the aldobiuronic acid groups through C_3 of D-galactose or C_4 and C_6 of the D-mannose.

Arabinose side chains are also attached to the C_3 on the 1,6- linked D-galactose to which the aldobiuronic acid groups are attached. Some uronic acid groups terminate other side chains or form the non-reducing ends of the D-galactose framework.

Physical Chemistry

During the period when gum arabic was difficult to obtain ghatti gum was widely used as a substitute in pharmaceutical preparations. Because of the fact that solutions of ghatti gum were twice as viscous as comparative solutions of gum arabic, one part of ghatti was used in place of two parts of gum arabic. Its use for this purpose has been officially recognised.

Though some work had been done on ghatti gum[4,5,7-10,13] in the late nineteenth century, it was mainly on the appearance and means of identification of the gum, and some on the viscosity of aqueous solutions. Many of the results obtained at this time are rather dubious due to the uncertain nomenclature and methods of sorting.

The chemistry of ghatti gum was studied by E.H. Shaw Jr. and others [23, 24, 31-33] who found that the gum was only 90% soluble in water. They were unable to make the unsoluble portion soluble either by Folin's suspension method[34] or by boiling it in water.

The soluble portion of ghatti gum consisted almost entirely of colloidal material. This solution of ghatti gum was dialysed against distilled water for ten days. From the dialysed solution the colloid was separated by evaporation

to low volume in a water-bath and final dehydration by boiling with carbon tetrachloride in a continuous cycle dehydrator.

The pH of this aqueous solution was 5.5 and the sample contained no phosphorus when tested by the Youngburg procedure for total phosphorus. The total nitrogen in the sample was found by the Koch-McMeekin micro-method[36] to be 0.72%. The total ash was 1.9% and the sulphated ash was 3.2%.

The molecular weight of the sample was determined by freezing point depression to be 2,878 and by osmotic pressure to be 11,920. This discrepancy between these results may have been due to the loss of low molecular weight constituents through the osmometer membrane.

A second solution of ghatti gum was dialysed against N sulphuric acid and again dehydrated as for the previous sample. In aqueous solution this sample had a pH of 2.9. The equivalent weight of the material was found to lie in the range 1340 - 1735.

They found that the sample contained 12% galactose and the crude gum contained 26% pentosans. This value for the content of galactose does not agree with the value of 27% that was obtained by Aspinall, Hirst and Wickstrom[25].

The optical rotation of solutions of the sample changed from -42° to +58° during hydrolysis with sulphuric acid.

Carhart and Shaw also studied the coagulation of solutions of Prussian Blue and ghatti gum[31-33]. They found that the pH of the solution affected the rate and extent of coagulation markedly. In acid solutions, pH 2.7 - 5.5 the gum acted as a neutral colloid but, as the pH was raised it was converted to the sodium salt which acted as a negative colloid. Above a pH of 4.2 the Prussian Blue ghatti gum systems were very stable to coagulating agents.

It has been found[37] that ghatti gum is not a homogeneous material. A solution of ghatti gum was revealed to be heterogenous by electrophoresis. The electrophoresis was carried out in borate buffer at pH 9.0 - 10.0 on glass-fibre paper. This type of paper was found to be preferable to ordinary cellulose paper because no complexes were formed by the polysaccharide as they were with cellulose paper.

Kulshrestha[38] has studied various gums and their acids by differential thermal analysis techniques which consist of heating the material in a furnace and comparing the temperature of the material with that of an inert reference material.

It was found that ghattic acid had endothermic peaks at 130, 235 and 325°C and an exothermic peak at 300°. These peaks were due to removal of -OH groups and elimination of H_2O and CO_2. It was proposed that the analysis graphs so formed by this process could be used as a means of identifi: :cation and characterization.

Uses

Ghatti gum has been used as an additive to drilling fluids to reduce the water loss[39,40]. Ghatti gum was useful in preventing the drilling mud coagulating when it came into contact with salt water. With unprotected muds there was a danger of the mud coagulating and so causing the drill to stick.

Ghatti gum has many similar uses to gum acacia and it may be used to replace acacia in certain countries.

It has also been used in the manufacture of certain explosives especially those to be used in damp surroundings. The explosive mixture is admixed with a proportion of powdered ghatti gum. If any moisture does penetrate the outer wrappings then the gum swells and prevents any further water entering[41].

It is used as a binder in coating compositions. Mixtures of ghatti gum and a flexibilising agent can be used as adhesives, oil-resistant protective films, impregnants for woven fabrics, paints for concretes and varnishes for artificial leather[18].

In India and in this country it is used in the textile industry as a thickener in cloth printing processes, a sizing agent for yarns and an adhesive to bind cloth to the printing tables.

It has also been used in ceramics as a binder to enhance the wet strength of the clay prior to the firing process.

OUTLINE OF POLYELECTROLYTE BEHAVIOUR

General

A polyelectrolyte[42] is a high molecular weight substance which is also an electrolyte. The range of substances which can be classed as polyelectrolytes is very large and spreads from synthetic materials to naturally occurring proteins and polysaccharides.

Just as there can be weak and strong electrolytes so the polyelectrolytes can be classified according to their ionising strength. A strong polyelectrolyte is one which, in solution, is in a permanent state of ionisation while a weak polyelectrolyte may exist as a neutral molecule capable of ionisation.

While polyelectrolytes are essentially electrolytes, they have certain differences from simple electrolytes. In a solution of simple electrolyte the positive and negative ions are distributed evenly throughout the bulk of the solution and any particular volume element of that solution will very probably contain equal numbers of cations and anions. Also, on addition of solvent to such a solution of simple electro: :lyte the average distance between each charge will increase.

This is not the case in solutions of polyelectrolytes. In an ionized solution of a polyelectrolyte the arrangement of the charges on the polyelectrolyte is governed by the

configuration of the polyelectrolyte molecule. The solvent surrounding the polyelectrolyte molecule contains only the oppositely charged counter-ions which are held close to the polyelectrolyte molecule by electrostatic interaction.

However, not only does the configuration of the poly:electrolyte chain affect the arrangement of the polyion groups in the solution, but the degree of ionization of the polyelectrolyte chain affects the spatial arrangement of the macromolecule.

If the polyelectrolyte is in dilute solution in a fully ionized state then each charged group repels similarly charged neighbouring groups, and there is, under these conditions, the maximum electrostatic repulsion possible along the polyelectrolyte chain. Consequently the macromolecule expands to its maximum size and the polyelectrolyte is fully extended.

However, if, when the macromolecule is in its fully extended position, the degree of ionization is lowered due to an increase in concentration or some other factor, then the electrostatic repulsion along the chain is decreased. With this decrease in ionic interaction the polyelectrolyte chain contracts slightly in size.

This process can be continued until there are no ionized groups present in the polyelectrolyte chain and therefore no repulsion between the various ionizable groups. Under these

conditions the polyelectrolyte is fully contracted and behaves like a neutral polymer molecule.

This progressive change of molecular size and shape with concentration will affect the hydrodynamic volume, and this change will be reflected in the various physico-chemical properties which rely on the movement of the polyelectrolyte molecules in solution.

The effect of the ionised groups on the molecular dimensions can also be demonstrated by the addition of extraneous salt to the polyelectrolyte solutions.

When the polyelectrolyte is fully ionised then obviously the molecule will be at its maximum size. If, under these conditions, some salt is added to the solution then the molecule will contract slightly due to a diminution of the repulsive forces between the charges, because of the shielding effect of the added salt on the ionised groups in the polyelectrolyte. If sufficient salt is added then the polyelectrolyte behaves as if it were unionised; i.e. behaves as a neutral polymer.

It is mainly these two characteristics of polyelectrolytes which govern their physico-chemical properties.

Various attempts have been made to calculate the degree of expansion and various other properties from theoretical considerations.

In the early theories the polyion was considered as a sphere of charges. This was modified by Hermans and Overbeek[49] who calculated the free energy and electrostatic potential as a function of the size and shape of the polyion.

Kimball and others [43] calculated the distribution of the small ions for this model using the Donnan equilibrium. Flory [44] considered that the system was determined by the osmotic effect of the small ions in the presence of the bound charges on the polyelectrolyte, and assumed that the equilibrium position was found by minimising the free energy of this system.

Katchalsky and others[45,46] attempted to deduce the properties of the polyelectrolyte by considering a chain model. They assumed the probability of the various configurations of such a chain depended only on the end-to-end distance of the chain.

Rice and Harris[47,48] extended the theoretical treatment of Katchalsky's chain model by considering the electrostatic interaction energy between the charges of the polyelectrolyte. It was assumed that not all of the electrostatic energy expanded the chain and that the probability of the configuration of the chain depended on more than the end-to-end distance. In the calculation of the configuration of the chain Rice and Harris also took into account the effects

of each charged group, and also calculated the entropy of the chain molecule from the distribution of charged and uncharged sites.

Viscosity

The viscosity of a large number of polyelectrolytes has been studied both in the presence of salt and in aqueous solution[49-68]. The viscosity of polyelectrolytes differed very much from the viscosity behaviour of simple electrolytes and neutral polymers due to the charges distributed along their molecular chains and to the various effects of these charges.

When a graph of reduced viscosity against concentration was drawn for a neutral polymer then a straight line relationship was obtained. The quantity $\eta_{sp/c}$ decreased with increased dilution and a finite value for the intrinsic viscosity, $[\eta]$, that is $\eta_{sp/c}$ extrapolated to zero concentration, was obtained from the graph.

This was, however, not true of the viscosity curves of polyelectrolytes in aqueous solutions. The $\eta_{sp/c}$ against concentration graph curved steeply upwards as concentration decreased.

The reason for this increase in $\eta_{sp/c}$ was due to the fact that in aqueous solutions of polyelectrolyte without added salt the only mobile ions present were the counterions which accompanied each macro-ion.

When such a solution was diluted by the addition of more solvent then the ionic strength of these counterions decreased. This decrease in ionic strength was accompanied by a corresponding increase in the size of the molecule and therefore an increase in the viscosity.

Another contributory cause of this upward curve of the graph may be that, since the molecules were so greatly expanded in the absence of salt they tend to interfere with each other. Thus the concentration of the polyelectrolyte may influence the configuration of each molecule.

While the viscosity data from neutral polymers obeyed the equation

$$\frac{\eta_{sp}}{c} = [\eta] + k'c$$

where $[\eta]$ was the intrinsic viscosity and k' was a constant, polyelectrolyte solutions gave[52]

$$\frac{\eta_{sp}}{c} = \frac{A}{1 + B\sqrt{c}}$$

in which A was the limiting value of $\frac{\eta_{sp}}{c}$ and B was a constant. Therefore a plot of $\frac{c}{\eta_{sp}}$ against $\sqrt{c}$ provided a straight line relationship from which the value of the intrinsic viscosity could be calculated.

If however some simple electrolyte were added to the solution of a polyelectrolyte then the viscosity decreased

due to the corresponding decrease in the molecular extension. Also the general shape of the $\frac{\eta_{sp}}{c}$ against c graph changed. The graph, instead of turning upwards, formed a maximum.

This maximum has been exhibited for various synthetic polyelectrolytes[53,60] and for other polyelectrolytes[56]. Fuoss and Strauss[53] stated that the maximum in the $\frac{\eta_{sp}}{c}$ against c graph appeared for poly-N-n-butyl-4-vinylpyridinium bromide when the concentration of bromide ions from the polymer was of the same order of magnitude as the bromide ion concentration in the solvent. It was also shown that this maximum decreased on increasing the salt concentration.

When the polyelectrolyte was relatively concentrated in such a salt solution, the molecule was compact and the solvent contained both the gegenions of the polyelectrolyte and the ions of the added salt. Both these ionic types affected the spatial arrangement of the polyelectrolyte.

However at medium concentrations the ionic strength of the solution depended on the gegenions of the polyelectrolyte and of the added salt, and so dilution affected the number of ions in the solvent. Since a number had been removed due to dilution, the polyelectrolyte expanded and the viscosity increased.

At low concentrations, however, the ionic strength was fairly constant due to the relatively small number of macromolecules present. Since the ionic strength remained comparatively stable there was no change in the shape of the polyelectrolyte and therefore no increase in viscosity.

As was shown by Pals and Hermans[58] this maximum in the $\frac{\eta_{sp}}{c}$ against c graph could be avoided by measuring the viscosity at various polyelectrolyte concentrations in a series of electrolyte solutions such that the total ionic strength of the solution was kept constant. This type of dilution was called iso-ionic dilution.

By plotting $\frac{\eta_{sp}}{c}$ against c graphs for various systems of sodium pectinate in sodium chloride solutions they showed that straight line relationships between the reduced viscosities and concentrations could be obtained for polyelectrolytes.

At normal concentrations of polyelectrolyte, that is down to about 0.001%, at which viscosity measurements have been made, the upward curve of $\frac{\eta_{sp}}{c}$ against c graph in the absence of salt showed no tendency to decrease with increased dilution. However it was found[63,69] that if the viscosity measurements were continued to very low polyelectrolyte concentrations then the graph described a maximum and subsequently decreased sharply with decreased polyelectrolyte concentration. For partially

quaternised poly-4-vinylpyridine in water the maximum of the curve appeared at a concentration of approximately 0.00005 g./ml. Considerable uncertainty existed[63] concerning the validity of such experiments because of the obvious difficulties in measur: :ing viscosities at such very low concentrations.

Terayama and Wall[63] also investigated a method of dilution of polyelectrolyte in salt solution different from the two methods of diluting the polyelectrolyte solution with a salt solution of constant ionic strength, and of diluting the poly: :electrolyte with salt solutions of varying concentration to keep the total concentration of counterions in the system constant, i.e. iso-ionic dilution.

In the former method a maximum appeared on the $\frac{\eta sp}{c}$ against c graph. The concentration at which the maximum appeared decreased with increased salt concentration until the graph became linear at high salt concentrations. In the second case it has been reported that a straight line relation: :ship was obtained[58,70]. Doty and Steiner[71] also used this method of iso-ionic dilution for the light-scattering experi: :ments on aqueous solutions of albumin in hydrochloric acid.

Terayama and Wall did not obtain straight line graphs with this process for the viscosity experiments on potassium polyvinyl alcohol sulphate, potassium cellulose sulphate and potassium polyacrylate in the present of potassium halides.

Rather, the curves were sharply curved at the early stages of dilution. They attributed this to the fact that since many polyelectrolytes behaved as being only partially ionised[72-75] it was very difficult to ascribe to any parti: :cular polyelectrolyte solution a definite ionic strength. They diluted the polyelectrolytes on a trial and error basis until they obtained the correct salt concentration, c_1 , which gave a straight line relationship. The ratio $\frac{c_1}{c_o}$ where c_o was the concentration of counterions from the original polyelectrolyte solution gave some indication of the counter-ion fixation of the polyelectrolyte.

From the viscosity measurements of the polyelectrolytes in various solvents it was possible to determine some idea of the shape of the molecule.

Einstein[76,77] showed that the addition of spherical particles to a solvent increased the viscosity from η to η' and the relative viscosity η_r ,

$$\eta_r = 1 + 2.5\phi$$

where ϕ was the volume fraction of the solute.

Onsager[78] modified Einstein's factor of 2.5 to $\frac{4}{15}.f^2.\ln f$ where $f = \frac{a}{b}$, the ratio of the major to the minor axes of ellipsoids of revolution.

It was also shown that

$$[\eta] = \frac{\bar{v}\left(\frac{4}{15}\right).\pi^2}{\ln f}$$

where $[\eta]$ was the intrinsic viscosity.

Simha and others[79,80] extended Einstein's treatment to include particles which were ellipsoids of revolution and showed that

$$\eta' = \eta\,(1 + v\phi)$$

where v was Simha's shape factor and equal to 2.5 for suspended spheres but larger than 2.5 for ellipsoids. The shape factor has been evaluated in terms of the axial ratios for prolate and oblate ellipsoids of revolution[80]. It was found that v increased as the axial ratio increased.

The volume fraction, ϕ, was not an experimentally determinable quantity. It was necessary to replace it with known factors. If v_h were the hydrodynamic volume of the dissolved macromolecule then

$$\phi = \frac{N c v_h}{M}$$

However the hydrodynamic volume of any particle is

$$v_h = \frac{M}{N}\left(\bar{v} + w_1 \cdot v_1^{0}\right)$$

From this it was possible to derive a value for the

intrinsic viscosity, $[\eta]$, of rigid macromolecules

$$[\eta] = v(\bar{v}_2 + w_1 \cdot v_1^{\circ})$$

where v = Simha's shape factor

$\bar{v}_2$ = specific volume of solute

v_1° = specific volume of solvent

and w_1 = hydration of the macromolecule in g water/g material.

Flexible polymers, however, can be considered[256] to behave as equivalent spheres of radius

$$R_e = \xi R_g$$

where ξ = proportionality factor.

The hydrodynamic volume of the flexible polymers would, therefore, be

$$v_h = \frac{4}{3} \cdot \pi \xi^3 \cdot R_g^3$$

From this the intrinsic viscosity of the flexible polymer is

$$[\eta] = \frac{10 \cdot \pi \cdot N}{3 \cdot M} \xi^3 \cdot R_g^3$$

$$= \frac{10 \cdot \pi \cdot N \cdot \alpha^3 \cdot \beta^3 \cdot \xi^3 \cdot M^{1/2}}{3(6M_o)^{3/2}}$$

where α = empirical expansion factor

β = effective bond length of the polymer chain.

From this relationship it is obvious that the viscosity of flexible polymers is directly proportional to α^3 .

Conductance

The conductance of an electric current through a solution is a characteristic phenomenon of electrolytes and involves such variables as the amplitude and the frequence of the applied electrical field, the charge, size and geometry, and concen: :tration of the ions present in the solution, and the dielectric constant, viscosity, and temperature of the system.

Since the conductance depends on the ionization of the solute in the solution it is obvious that polyelectrolytes will also exhibit the property of conducting electricity in a solution. However in polyelectrolyte solutions the problems are greater than in simple electrolyte solutions[81]. In fact it has been stated that the phenomenon of polyelectrolyte conductance was not completely understood[81].

Various models have been put forward to explain theoreti: :cally the results obtained from experimental study. Huizenga and others[72] proposed that in conductance studies the polyelectrolyte molecule should be considered as an association model.

Hermans and others have considered polyelectrolyte con: :ductance as the result of a porous model with[82] and without[83] electrostatic relaxation effects. Eigen and Schwarz[84] con: :sidered the effects on the conductivity of polyelectrolyte solutions of the polarization of the ionic atmosphere around

rigid anisotropic polyelectrolyte particles and the associated orientation phenomenon in solutions.

It was found[81] in salt-free dilute aqueous solutions of partially neutralised polymethacrylic acid that the equivalent conductance did not depend very much on frequence between 10 and 50,000 cycles per second, and that the equivalent conductance increased with decreased polyelectrolyte concentration[42,81,85].

It was also stated that, though the equivalent conductance was virtually independent of the molecular weight of the polyelectrolyte[81,86] in the molecular weight range 129,000 to 464,000, it increased for molecular weights around 17,000.

The equivalent conductance was found to decrease with increased degree of neutralisation[72,73,75,81].

Eisenberg[81] stated that the change in the equivalent conductance with temperature in the temperature range 0°C to 50°C was related to the change of the conductivity of the counterions. However Wall and Doremus[75] found that the polyion mobility increased with increased temperature and ascribed this increase to be due to a decrease in the viscosity of the medium.

From studies on synthetic polyelectrolytes it was found that the conductance of the polyelectrolyte solution was less than that of a solution of the corresponding electrolytic

monomers at the same concentration[85] and that the equivalent conductance of a polyelectrolyte solution increased with decreased molecular weight of the fraction[81].

It has also been shown that a high molecular weight polyelectrolyte molecule contributed only negligibly to the conductance of the solution except at high concentrations and that most of the measured conductance was due to the free counterions[87-90].

For a given charge a small ion moved faster and therefore had a higher conductance than a large ion. The higher the charge of an ion of a given size the higher the conductance and at a given concentration a given electrolyte has a lower conductance in a solution of lower dielectric constant. It has been shown[91] that the dielectric constant of a poly-electrolyte solution increased sharply on dilution.

The upward curve of the equivalent conductance against concentration graph was due to the proportionately greater number of free counterions present in dilute solutions.

In concentrated polyelectrolyte solutions a considerable proportion of the counterions were held close to the poly-electrolyte chain. During conductivity measurements these counterions moved with the polyion. The remainder of the counterions behaved normally and contributed to the conduct-ance although slightly impeded by long-range interionic interactions from the polyions.

On dilution of this solution there was more volume between each macromolecule and therefore counterions left the vicinity of the polyions.

With each counterion which left the macromolecule the charge on the macromolecule increased and therefore more current was carried by each polyion. Also since there were more free counterions available the current carried by them was also proportionately increased. This increase in conductance, though sufficient to cause the upward slope, was impeded by an increase in the frictional coefficient since the macromolecule expanded as a result of increased intramolecular repulsion.

The effect on the conductivity of polyelectrolyte solutions of addition of simple electrolyte has been studied[82,86,92,89]. It was found that the mobility of the polyion decreased on addition of simple electrolyte[86,93] and that there was strong interaction between the polyelectrolyte and the simple electrolyte.

In this type of system it was found that the mobility of the polyion depended on the concentration of the polyelectrolyte more so than the concentration of the simple electrolyte.

Nagasawa, Soda and Kagawa[92] found that at zero simple electrolyte concentration the mobility of the polyion agreed

with the mobility of the monomer and at the limit of sufficient simple electrolyte concentration, the mobility also approached that of the monomer. Between these two values the mobility of the polyions was always larger than the mobility of monomers.

From conductivity measurements it is possible to determine some idea of the shape of the polyelectrolyte molecule. The equivalent conductance of the polyelectro-:lyte can be measured readily and a molecular shape can be assumed for the polyelectrolyte. Theoretical equivalent conductances can be calculated for the hypothetical models and the extent of agreement between the observed and calcu-:lated values give some measure of the validity of the molecular model chosen.

Surface Tension

Polyelectrolytes in solution cause a lowering of the surface tension. According to Gibb's absorption isotherm, a decrease in surface tension is due to the adsorption of the solute at the surface.

Jorgensen and Strauss[94] studied the surface activity of polysoaps and a polyelectrolyte from poly-4-vinylpyridine. Though the polysoaps caused a relatively high decrease in surface tension, the polyelectrolyte did not, even in the presence of salt.

For the polysoaps, however, the surface tension decreased sharply on increased concentration and eventually reached a constant value.

The addition of salt to the solutions of polysoaps further decreased the value of the surface tension of the solution. This reduction was due to the fact that the simple electrolyte reduced the electrical charge of the polysoaps and, in addition, to the fact that the polysoaps were less soluble in salt solutions than in water. Presumably this had the effect of introducing more of the molecules at the interface and so causing a decrease in surface tension.

While these authors[94] found that the polysoaps reduced the surface tension, they stated that the polyelectrolyte studied only reduced the surface tension of water by ½ dyne and that addition of salt to this polyelectrolyte solution did not affect the surface tension further.

However it has been shown that other electrolytes, for example acacia[95-98] quite definitely reduced the surface tension of solutions.

Light Scattering

Due to the peculiar properties to polyelectrolyte molecules on dilution of the solutions or on addition of simple electrolyte, the results obtained from light-scattering experiments are characteristic of this type of material.

The light-scattering theory assumes that the molecules are largely independent of each other. This, however, is not true when ionised groups are present.

The turbidity of polyelectrolyte solutions increased rapidly on dilution due to the molecular expansion. This effect has been noted by various workers[99-101].

It was also found that the turbidity of aqueous polyelectrolyte solutions increased on the addition of salt to the solutions[102].

The reason for this was, as Doty and Steiner[103] pointed out, that fluctuations in concentration could not be independent in solutions of polyelectrolytes because of the necessity of maintaining electrical neutrality. Therefore, in aqueous solutions or in solutions in which the macromolecules were highly ionized, the electrostatic interactions between neighbouring molecules tended to establish an ordered distribution.

This caused destructive interference between the light

scattered from various particles with a corresponding decrease in the intensity of the scattered light.

However, when salt was added to such a solution, the effect of the ionized groups was restricted and the molecules tended to take up random positions in the solution. Because of this loss of order in the polyelectrolyte solution, there was less destructive interference and so the turbidity of the solution increased.

In aqueous solutions of polyelectrolyte it was found that $\frac{H_c}{\pi}$ against concentration graphs decreased on increased dilution and that it was difficult to extrapolate this graph to zero concentration[99,100,104].

It was possible, however, to obtain straight-line graphs for $\frac{Hc}{\pi}$ against concentration if the polyelectrolyte were studied in buffer solutions[100], in salt solutions[102], or if the polyelectrolyte were completely unionized[99].

Under these conditions the effect of the charges on the molecules was minimized and the solutions scattered like neutral polymers.

With linear graphs, extrapolation of $\frac{Hc}{\pi}$ to zero concentration was facilitated and accurate results obtained.

The dissymmetry of polyelectrolytes in aqueous solutions was found to decrease[99,103] with concentration, pass through

a minimum and increase. This was presumably caused by the change in size and configuration of the polyelectrolyte molecules on dilution, as well as by the ordering effects discussed above.

The dissymmetry of an aqueous solution was also found to decrease on addition of salt to the solution[105]. This was caused by the molecules contracting.

For polymethacrylic acid[99], it was found that as the degree of neutralisation increased so the dissymmetry increased. This again was due to the increased effect of the ionized groups on the molecular configuration.

The addition of simple electrolyte to solutions for light scattering removed some of the effects of the charged groups and facilitated the interpretation of the results. As was shown by Vrij and Overbeek[106], however, the polyelectrolyte in such a salt solution would adsorb the salt ions which were oppositely charged to itself and repulse similarly charged salt ions. When the light-scattering of such a solution was being considered by the fluctuation theory then it should be assumed that the particle and the adsorbed salt fluctuate together. It was, therefore, necessary to calculate the refractive index increment of the system at constant chemical potential and this was done by a membrane equilibrium process.

Acacia

It has been shown by immunilogical and electrophoretic experiments that gum arabic was not a homogenous substance but rather a mixture of related polysaccharides. This has been supported by work recently carried out on a gum from Acacia seyel[108].

The component sugars of gum arabic have been found by hydrolysis to be D-galactose, L-arabinose, L-rhamnose and D-glucuronic acid. The position of some of the L-rhamno-:pyranose residues has been established by reduction of the D-glucuronic acid residues and acetylation procedures[114].

Many attempts have been made to determine a definite structure for arabic acid[113, 115, 116]. Hirst and Jones[117] came to the conclusion that the arabic acid molecule con-:sisted of a backbone of 1,6 - linked D-galactose residues with side-chains of D-galactose, D-glucuronic acid and L-rhamnose or L-arabinose. This conclusion resulted from the fact that on partial hydrolysis the two aldobiuronic acids, 6.0.(β. D-glucopyranosyluronic acid) D-galactose[115,116] and 3.0.(β. D-glucopyranosyluronic acid) -L-arabinose were obtained; they were found in the products of hydrolysis before and after methylation.

While Hirst[113] proposed that the galactose units in the arabic acid molecule were linked in the 1,3 - position, other

workers[118] have proposed that they are alternately joined by 1,6 - and 1,3 - linkages.

It would seem that a possible structure of gum arabic[119] is that the main D-galactose framework is joined by 1,3 - linkages and that, interspersed along this chain, are arabo-furanose units and that the side-chains of D-galactose, D-glucuronic acid and L-rhamnose or L-arabinose are joined through the C_6 of the galactose units in the main chain. However the possibility of the presence of 1,6 - linked D-galactose units at the end or near the middle of this main chain is not invalidated by the known experimental facts.

It can be seen that the structure of gum arabic is consistent with the structure of a polyelectrolyte. It is a large molecule, along which are distributed ionisable groups. The physico-chemical properties of arabic acid and its salts clearly demonstrate their polyelectrolytic nature.

Gum acacia is freely soluble in water and when in the acid form it is a moderately strong acid with a pH of between 2.2 and 2.7. Its equivalent weight, when determined by potentiometric titration was found to be in the region of 1000 - 1400[88, 120-126].

Various methods have been used to determine the molecular weights of gum arabic, arabic acid and the salts of arabic acid.

By osmotic pressure investigations the molecular weights of arabic acid and its salts were found to be between 217,000 and 245,000[120, 127, 128].

Sedimentation experiments gave the molecular weight to be 300,000 while light-scattering results showed it to be 0.58×10^6 [104] and $1.0 \pm 0.05 \times 10^6$ [105]. The discrepancies between these figures may be due to polydispersity.

Veiss and Eggenberger[105] also showed that the arabic acid molecule was in the form of a stiff coil with many side-chains. The root mean square end-to-end distance varied between 1050 Å when the molecule was completely uncharged to 2400 Å when fully charged. Mukherjee and Deb[104] found that the expansion was from 1090 Å to 2400 Å which is remarkably good agreement with Veiss and Eggenberger's results.

When the gum arabic or the arabic acid molecules were highly charged the graph of $\frac{Hc}{\tau}$ against $\sin^2 \frac{\theta}{2}$ curved downwards as the concentration decreased. This effect which is common to all polyelectrolytes is due to the change in the polyelectrolyte charge and shape on dilution.

It was also shown by Veiss and Eggenberger that the contraction of the arabic acid molecules was hindered by the size of the molecules and that the monosaccharide units in the chain were too bulky to allow complete contraction. In most cases any other considerations of molecular interaction

do not affect the results to a great extent. However in the light-scattering experiments of arabic acid it was evident from the shape of $\frac{Hc}{\tau}$ against concentration curves that this molecular interaction was modifying the results and that virial coefficients higher than the second had to be considered.

As was shown by Katchalsky and Eisenberg, if the ionization of the macromolecules could be repressed than the plot of $\frac{Hc}{\tau}$ against concentration became a straight line and extrapolation of this graph to zero concentration was made more easy and accurate.

This was done by Mukherjee and Deb[104] by the addition of potassium chloride or a mixture of other electrolytes and by Veiss and Eggenberger[105] by the addition of hydrochloric acid to the solutions.

The idea of considering the molecules of arabic acid as flexible chains was suggested by Basu and others[121] from their viscosity experiments. The peculiar viscosity properties of arabic acid could be explained if it were assumed that they were long molecules with a high charge density and a flexible structure[52-55].

The change in viscosity of arabic acid solutions on the addition of electrolytes was due to the effect of the charges along the macromolecule chain. When sufficient

salt was added the arabic acid molecule acted as a neutral polymer[121, 129-131].

Various experiments have been carried out on the viscosity of arabic acid and its salts[121, 129, 130, 132-135], and in all of these the viscosity was shown to be reduced on the addition of simple electrolyte to the solutions[136]. Thus arabic acid and its salts acted, in the viscosity experiments, as typical polyelectrolytes.

Conductivity experiments on arabic acid[88,131,137,138] also demonstrated the polyelectrolytic nature of the macromolecules, and Briggs demonstrated that the conductance of arabic acid was due primarily to the hydrogen ions.

The surface tension of arabic acid and its salts have been studied by various methods. Clark and Mann[136] found that the surface tension of a gum arabic solution increased up to a gum arabic concentration of 0.1% and then fell until the surface tension had a value of 61.49 dynes/cm. for a 10% solution and 69.69 dynes/cm. for a 5% solution.

Banerji[139] used Traube's stalagmometer to determine the surface tension of gum arabic solutions and found that a 4% solution had a surface tension of 63.16 dynes/cm.

Both Clark and Mann and Banerji found that the surface tension of gum arabic solutions was decreased by the addition of electrolytes.

The interfacial tension of gum arabic solutions with cyclohexane[140] and benzene[96,97,98] has been studied. Shotton showed that the results given for the interfacial tension between solutions of gum arabic and benzene from the ring method and the drop-volume method were unsatisfactory due to certain disadvantages in these methods. It was difficult to measure the results of ageing by these methods because of the disturbance caused in the surface layer by each reading.

It was stated that a static method of determining surface tension, such as the sessile drop method, gave more accurate and reproducible results.

The lowering of the surface tension between benzene and gum arabic solutions was shown[96,97,98,141] to be due to an adsorbed multilayer of gum arabic molecules at the interface. It was stated[98,142,143] that such a film would exhibit the physical properties which would explain the emulsifying characteristics of gum arabic.

Gum Tragacanth

Gum tragacanth is the exudate from various shrubs belonging to the genus Astragalus.

It has been indicated by fractionation[144], electrophoresis[37] and structural[145,146] experiments that the gum is heterogenous and is a complex mixture of polysaccharides.

The gum is only 30 - 40% soluble in water and the insoluble portion was called "bassorin"[147].

The constituent sugars of gum tragacanth have been found by hydrolysis with dilute mineral acid to be L-arabinose, D-xylose, L-fucose and D-galactose.

Crude gum tragacanth was a mixture[145] of an acidic polysaccharide, a neutral polysaccharide and a small amount of a glycoside. It has been found that the acidic polysaccharide had an equivalent weight of between 442[145] and 550[148]. The neutral polysaccharide could very readily be separated by precipitation of an aqueous solution of the gum by alcohol since it was soluble in 70% alcohol.

The acid nature of gum tragacanth was due to the presence in the macromolecules of D-glucuronic and D-galacturonic acids.

The structure of the tragacanthic acid has been studied[149] by degredation with acid and enzymes. The component sugars

of this tragacanthic acid were D-galacturonic acid (43%), D-xylose (40%), L-fucose (10%) and D-galactose. Various oligosaccharides were obtained on degradation, including 2 0 α L-fucopyranosyl D-xylose; 2.0 β D-galactopyranosyl-D-xylose; 3.0 β D-xylopyranosyl-D-galacturonic acid and oligomers of D-galacturonic acid.

The structure of the tragacanthic acid was said to be based on linear chains of 1,4 - linked D-galacturonic acid residues. Most of these D-galacturonic acid residues were connected through C_3 to side chains containing xylose. Three types of side chains were found, namely single β D-xylopyranose residues and disaccharide units of 2.0 α L-fucopyranosyl D-xylopyranose and 2.0 β D-galacto-:pyranosyl-D-xylopyranose. It was also possible, however, that branched side-chains were present.

The structure of the arabinogalactan from gum tragacanth was studied by hydrolysis and methylation techniques[150]. The constituent sugars were found to be L-arabinose, D-galactose, L-rhamnose, D-galacturonic acid and traces of other sugars.

From the products of methylation and hydrolysis it was stated that the arabinogalactan from gum tragacanth was composed of chains of D-galactopyranose residues which were mainly linked through 1,6 - linkages but with some 1, 3 -

linkages present. Highly branched chains of L-arabo-furanose residue joined by 1,2 -; 1,3 - and 1,5 - linkages were joined through the C_3 of the galactopyranose residues to the main chain.

This arabogalactan also contained proportions of D-galacturonic acid and L-rhamnose but the precise way in which these residues were connected to the main chain was not known.

The molecular weight of the water-soluble fraction was found from diffusion experiments[151] to be 840,000 and from osmotic pressure measurements to be in the range 80,000 to 100,000[148].

The viscosity experiments on the free acid[148] exhibited the typical viscosity behaviour of polyelectrolytes. In aqueous solutions the graph of reduced viscosity against concentration rose sharply on increased dilution and the addition of small amounts of simple electrolyte produced a maximum in the curve which eventually disappeared at higher simple electrolyte concentrations.

However, viscosity experiments on the sodium salt of the tragacanthic acid showed some anomalous behaviour. The reduced viscosity/concentration curve showed a decrease at low concentrations.

At any particular concentration however the reduced

viscosity of the sodium salt was higher than that of the acid. Thus the molecules of the sodium salt of tragacanthic acid must have been more expanded than the corresponding free acid form. It was also shown that the pH of a solution of the sodium salt increased on dilution, presumably due to hydro-:lysis of the sodium salt. Since the acid groups were less dissociated than the sodium salt this hydrolysis would tend to lower the viscosity. It was thought that this may have a greater effect on the solution than the uncoiling effect of the macromolecules on dilution.

From these viscosity experiments[148] and sedimentation and viscosity experiments[151] it was deduced that the molecule was linear. The length of the macromolecule was calculated to be 4500 $\mathring{A}$ and the diameter 19 $\mathring{A}$.

The viscosity of tragacanth solutions was also measured on a rotational viscometer. The graphs obtained were curved which indicated a structural viscosity which increased with concentration. At low concentrations and at low rates of shear, the solutions of gum tragacanth did not deviate significantly from the behaviour of Newtonian fluids.

Carrageenin

Carrageenin is the complex polysaccharide which is extracted by water from various red sea-weeds and in particular from Chondrus crispus, Gigartina stellata and Chondrus ocellatus[152,153].

Carrageenin was found to be mainly composed of D-galactose units[154,155] and to contain 3-6 anhydro-D-galactose[156, 157] and small amounts of D-glucose[154,155], pentoses[155,158] and L-galactose[154,159]. Carrageenin also contained about 30% mono-esterified sulphuric acid.

Extraction of C.crispus with hot and cold water appeared to give two separate polysaccharides[155,160,161] though the galactose parts of each substance were structurally similar.[154]

This proposal that carrageenin was heterogenous was supported by evidence from various physico-chemical measurements. It appeared that it was composed of a major component with a linear molecular structure and a minor component which was suggested to have a branched molecular structure[162]. These two components have been separated by fractional precipitation with potassium chloride[163-165].

These fractions were found to differ in sulphate content, optical rotation, and content of 3,6-anhydro-D-galactose[156,157].

It would appear that a possible structure of carrageenin is that the main framework was composed of D-galactose and

3,6 -anhydro-D-galactose joined through 1,3 - linkages with a sulphate group on C_4. The order in which these and the other sugar residues existed in the chain was not fully known[119].

It was found that the viscosity of aqueous solutions of carrageenin exhibited the peculiarities of polyelectrolyte viscosity[166,167], especially those fractions of carrageenin which had relatively low molecular weights. For extracts with higher molecular weights the viscosity became dependant on the rate of shear[167].

In aqueous solutions[166] the reduced viscosity against concentration graphs curved upwards on dilution and on addition of simple electrolyte the behaviour of the solution was like that of neutral polymers.

The reduced viscosity/concentration curves for carrageenin in aqueous solution[166] exhibited a maximum at very low concentrations. This had been noted by previous authors for polyelectrolytes in salt solutions[55]. Masson and Goring ascribed this phenomenon to traces of inorganic impurities present in the water.

The maximum in the viscosity curve for carrageenin in salt solutions had been observed by Masson and Caines[167]. It appeared when the solution had a salt concentration of 0.000231M $NaHSO_4$, and at a salt concentration of 0.1M sodium chloride it disappeared.

The main component of carrageenin was found to be composed of linear molecules with a molecular weight of between 110,000 and 530,000[162,168]. The macromolecule was assumed to be rod-shaped and appeared to have an axial ratio of 160 - 340 and a diameter of 9.9 - 13.5 Å. The molecular weight has also been calculated to be between 800,000 and 1,000,000 by sedimentation[169] and 2,500,000 by osmotic pressure measurements[166].

By light-scattering measurements the molecular weight of sodium carrageenate in sodium acetate buffer solutions was found[170] to be $1.7 \pm 0.1 \times 10^5$.

Sedimentation experiments[162,170,171] and viscosity experiments[166,167] also indicated that the carrageenin molecule was rod-like.

Goring and Chepeswick[171] suggested that the molecule was, in fact, coiled and was capable of considerable expansion. It was also suggested that sodium carrageenate existed in solution as a molecular network which broke up in dilute solutions. This would explain the gelling tendency of certain fractions of carrageenin.

The light-scattering experiments[170] suggested that the sodium carrageenate molecules were stiff rods with a length of 3700 Å. Since structurally a stiff rod was not possible,

it was suggested that the molecule had an extended branched structure which was flexible in its major axis. It was suggested that the light-scattering envelope was distorted by a small concentration of aggregates which were not removed by the centrifugation treatment.

Goring and Chepeswick[171] found that the molecular weight of sodium carrageenate 790,000 and the length of the rod was 2400 Å by sedimentation.

Sitaramaiah and Goring[172] ascribed Masson and Goring's[167] results to be due to a rod-coil transformation on increased ionic strength.

Sodium Carboxymethylcellulose

Sodium carboxymethylcellulose is a derivative of cellulose in which some of the cellulose hydroxy groups have been transformed into $-O.CH_2COONa$ groups.

The carboxymethyl ether of cellulose was first prepared by the interaction of alkali cellulose and chloroacetic acid[173,174]. This reaction was normally carried out with an excess of alkali so that the sodium salt, sodium carboxymethylcellulose, was formed.

Sodium carboxymethylcellulose was therefore composed of the long cellulose molecule along which were distributed sodium carboxymethyl groups. Structurally therefore it fitted the definition of a polyelectrolyte.

The viscosity of sodium carboxymethylcellulose solutions naturally exhibited the peculiar viscosity properties of polyelectrolytes and this type of viscosity behaviour has been reported by various workers[93,175-182].

In aqueous solutions the graph of reduced viscosity against concentration increased on dilution of the solutions. Fujita and Homma[176,181], Inoue[182], and Inagaki[183] found that in aqueous solutions this graph formed a maximum below a sodium carboxymethylcellulose concentration of 0.008% and that the position and appearance of this maximum depended on the molecular weight of the sodium carboxymethylcellulose

fraction used. For relatively low molecular weight fractions the maximum and subsequent decrease in the graph were very marked. In higher molecular weight fractions the maximum disappeared and the reduced viscosity against concentration curve appeared to be almost flat over a wider range of concentration than before.

The appearance of this maximum was explained to be due to the antagonistic effects of the shape effect and the electrostatic interaction effect.

At very low concentrations the electrical interaction effect predominated and the reduced viscosity increased with concentration. At slightly higher concentrations, however, the effect of the shape of the molecule overcame the primary effect and the curve gradually fell with increased concentration.

Basu and Dasgupta[175] did not measure the viscosity of sodium carboxymethylcellulose solutions at sufficiently low concentrations to demonstrate the maximum in the reduced viscosity curve though maxima were obtained for sodium carboxymethylcellulose in dilute salt solutions.

At a sodium chloride concentration of around 8.75×10^{-4} g.eq./lt. the maximum disappeared and the sodium carboxymethylcellulose acted as a neutral polymer and the reduced viscosity decreased with decreased concentration.

Fuoss[55] had already shown that the rise in the reduced viscosity against concentration curve would be proportional to the dielectric constant of the medium. This was confirmed by Basu and Dasgupta[175] who dissolved the sodium carboxymethylcellulose in various mixtures of dioxane and water and measured the viscosity.

This relation between the dielectric constant of the medium and the change in the reduced viscosity was stated to be due to the increased contraction of the polyelectrolyte molecule when the dielectric constant of the medium was decreased, since the electrostatic interaction between the ionized groups along the polyelectrolyte chain decreased with the fall of dielectric constant.

It was found that iso-ionic dilutions[179,184,185] of sodium carboxymethylcellulose gave straight line viscosity graphs[181,93,186,187] as had been reported for other polyelectrolytes[58,70].

It was found[172] that if the sodium carboxymethylcellulose were assumed to be fully ionized and if the solutions were diluted isoionically then straight line viscosity graphs were not obtained. However if the method of Terayama and Wall[63] were used in which the solutions were diluted with a concentration of sodium chloride chosen by trial and error then straight line graphs were obtained. This failure of the

iso-ionic dilution technique to give straight line reduced viscosity graphs was said to be due to the effect of the counterion binding activity of the polyelectrolyte molecules which left only a fraction of the counterions free in solution.

The light-scattering experiments[186,188] demonstrated typical polyelectrolyte behaviour. As had been found before the $\frac{Hc}{\tau}$ graph was curved downwards on increased dilution. On addition of sufficient salt this line became straight and extrapolation to zero concentration became easier.

Schneider and Doty[188] found the weight average molecular weight of a particular fraction to be about 440,000 with a $M_z : M_w : M_N$ distribution of 5.15 : 2.65 : 1.0. The root mean square end-to-end distance of the coil changed from 2300 Å in 0.5M sodium chloride to 3350 Å in 0.005M sodium chloride.

This increase of 45% in the range of ionic strengths studied could not be explained by the Hermans-Overbeek, Flory or Katchalsky-Kuhn theories of polyelectrolyte expansion.

They assumed that the intrinsic viscosity, $[\eta]$, was proportional to α^2, the coil expansion factor.

The disagreement between their experimental results and the theoretical predictions was said to be due to the neglect of counter-ion binding in the latter.

It was also found that the second virial coefficient increased as the ionic strength decreased. If it were assumed that the counterions distributed themselves between the atmosphere and the solution the Donnan term calculated for this condition did not agree with the experimental results. However, if it were assumed that the counterions were held close to the polymer chain and the second virial coefficient calculated from the Flory[44] theory of molecular configuration then reasonable agreement between the calculated and observed results was obtained. Schneider and Doty assumed that in the case of sodium carboxymethylcellulose the counterions must be held close to the macromolecule.

Trap and Hermans[186] also studied sodium carboxymethyl-:cellulose by light-scattering in aqueous hydrochloric acid and sodium chloride solutions. The molecular weight of the sample of sodium carboxymethylcellulose was found to be 86,000 and the length was 2000 Å if the molecule were assumed to be rod-shaped.

They also found little agreement between the Donnan term and the observed second virial coefficient. It was found that the second virial coefficient was approximately propor-:tional to the square of the charge density and to the 2/3 power of the reciprocal ionic strength.

Sitaramaiah and Goring[172] attempted to study sodium

carboxymethylcellulose by light-scattering techniques but found that the molecular weights obtained were irregular and unreliable.

The inaccuracies of the molecular weights obtained from the light-scattering experiments were stated to be due to the presence of small amounts of high molecular weight aggregates which were formed during the synthesis of the sodium carboxymethylcellulose and which could not be removed. This difficulty has been noted before for carrageenin[170] and has been stated to be the main cause of inaccuracies in the light-scattering experiments on biological macromolecules[189-192].

Because of the effect of these aggregates on the light-scattering results and since they had virtually no effect on the results of the sedimentation or viscosity experiments Sitaramaiah and Goring regarded the results from the light-scattering experiments of sodium carboxymethylcellulose as unrealistic.

The same authors suggested that at high ionic strength the sodium carboxymethylcellulose molecules were in a coiled shape but that at low ionic strengths the molecules expanded to a rod-like shape.

Pharmaceutical Applications

The applications of the polyelectrolytes described above to the pharmaceutical industry depend on their peculiar physico-chemical properties. They are all, to some extent, soluble in water and their aqueous solutions have very high viscosity. This high viscosity and the fact that they are adsorbed at interfaces makes them good emulsifiers and stabilisers.

Gum arabic, perhaps the most commonly used pharmaceutical polyelectrolyte, has been used for many years as an emulsifying agent and its excellent properties of emulsification have been shown[96-98, 141-143] to be due to the adsorption of the gum arabic molecules at the interface of the aqueous and non-aqueous phase. This eventually forms an elastic layer of gum arabic between the disperse and the continuous phases.

Gum tragacanth, carrageenin and sodium carboxymethyl-cellulose have also been used as emulsifying agents.

These polyelectrolytes have been used as stabilising agents for pharmaceutical suspensions.

It has been shown that these polyelectrolytes very effectively stabilise suspensions of such insoluble medica-ments as kaolin and calamine. The stabilisation is effected in two ways. Firstly the polyelectrolyte increases the viscosity of the medium and so retards the

sedimentation of the material[193]. Secondly the poly-
:electrolyte acts as a protective colloid. Each particle becomes surrounded with a layer of the polyelectrolyte and so becomes charged due to the ionized groups present on the polyelectrolyte. Since each particle and adsorbed layer of polyelectrolyte has the same charge they tend to repel each other. This also prevents any sedimentation or agglomeration of the particles in the suspension.

THEORY OF LIGHT-SCATTERING

Introduction

The scattering of light has a very important position in the determination of molecular weights and molecular properties. It is an invaluable technique when studying substances with a high molecular weight.

One of the first observations of the results of scattered light was made by Lord Rayleigh[194] when he proposed that the blue colour of the sky was due to the small particles suspended in the air which diverted light, especially light of low wave length, from its normal course.

Richter[195] noticed that light was scattered when it was passed through a solution of colloidal gold.

Tyndall[196] found that the direction of the scattered light was dependant on the polarisation of the incident light. He suggested that the phenomenon of light-scattering was due to reflection of the incident beam. However, Rayleigh pointed out that the light scattered was due to diffraction.

Lord Rayleigh stated that the oscillating field of the incident beam gave rise to an induced oscillating electric moment in the small particles through which the beam was passing. Such induced electric moments, in turn, acted as secondary light sources of the same wavelength provided that the induced oscillations were far removed from the natural frequency of the electrons.

Some of the incident beam, however, was absorbed by the

particle and this caused the molecules to be raised to a higher energy level. This absorbed energy was re-emitted by the molecule at certain specific wavelengths as Raman spectra.

Rayleigh's original treatment of light-scattering was for independent transparent particles that were optically isotropic and small compared with the wavelength of the incident light.

There are two methods of considering the theory of light-scattering.

Firstly, the scattered light may be treated as being due to fluctuations in density and concentration which result in fluctuation in the optical dielectric constant of the solution. In a perfect crystal lattice each similar volume contains the same number of scattering points. In this case complete destruction of the scattered light occurs. However in a solution the fluctuations ensure that there is no complete destruction of the scattered light. This theory was developed by Schmoluchowski[197] and Einstein[198].

The second approach to light-scattering is to consider the light scattered from each independent particle. The total light scattered is then calculated by a summation over all particles. The final answer is modified by taking into account interference producing phase differences in the scattered light. This method is called the Interference theory and was developed by Rayleigh. Debye[199] showed that this theoretical approach could be applied to dilute solutions of high molecular weight polymers provided that the molecules of the polymers did not interact very strongly.

Light Scattering of Small Particles

If any particle in space be subjected to an electric field of strength, E, then a dipole is induced in the particle which is parallel to the electric field.

The magnitude of the induced dipole is proportional to the electric field strength. The proportionality factor, α, is called the polarizability of the particle.

$$p = \alpha E \quad \ldots\ldots\ldots\ldots (1)$$

The equation for the electric field of such a light-wave is

$$E = E_o \cos 2\pi \left(\nu t - \frac{x}{\lambda}\right) \ldots\ldots (2)$$

where E = amplitude
E_o = maximum amplitude
ν = frequency
t = time
x = position in the direction of propogation
and λ = wavelength

The incident beam induces an oscillating dipole and from equations (1) and (2) it will be seen that the oscillating dipole is such that

$$p = \alpha E_o \cos 2\pi \left(\nu t - \frac{x}{\lambda}\right) \ldots\ldots\ldots (3)$$

An oscillating dipole is, however, itself a source of light and in this case the light produced is the scattered light. The field strength of the scattered light is proportional to $\frac{d^2p}{dt^2}$ and is dependant on the direction.

The value of E_s at a distance, r, from the dipole where r

is very large compared to the wavelength, will be proportional to sin ϕ_1 where ϕ_1 is the angle between the axis of the dipole and the line from the dipole to the point at which E_s is being measured.

E_s must also vary as $\frac{1}{r}$.

$$E_s \propto \frac{d^2p}{dt^2} \cdot \frac{\sin \phi_1}{r} \quad \ldots\ldots\ldots (4)$$

By differentiating equation 3 to obtain $\frac{d^2p}{dt^2}$ and by introducing the proportionality constant which in this case is $\frac{1}{\bar{c}^2}$ where $\bar{c}$ is the velocity of light, equation 4 becomes

$$E_s = \frac{4\pi^2 \nu^2 \alpha E_o \sin\phi_1}{\bar{c}^2 \cdot r} \cos 2\pi(\nu t - \frac{x}{\lambda}) \ldots\ldots\ldots (5)$$

The intensity of a light-wave is the quantity which is measured experimentally and this is proportional to E^2 which has been averaged over one fluctuation. From equation 5 and equation 2 the ratio of the intensity of the scattered light, i_s, to the intensity of the incident light, I_o, can be obtained.

$$\frac{i_s}{I_o} = \frac{16\pi^4 \alpha^2 \sin^2\phi_1 \nu^4}{\bar{c}^4 \cdot r^2} \quad \ldots\ldots (6)$$

Since the wavelength of light in vacua, λ, is equal to $\frac{\bar{c}}{\nu}$ equation 6 becomes

$$\frac{i_s}{I_o} = \frac{16\pi^4 \alpha^2 \sin^2\phi_1}{\lambda^4 r^2} \quad \ldots\ldots (7)$$

For experimental purposes the quantity α^2 must be evaluated.

It may be related to the dielectric constant, E, of the medium by

$$E - 1 = 4\pi N\alpha \qquad \ldots\ldots\ldots(8)$$

Where N is the number of molecules per cubic centimetre.

It can also be shown that

$$E = n^2 \qquad \ldots\ldots(9)$$

where n is the refractive index of the material.

By combining equations 8 and 9 it is possible to relate to the refractive index of the material.

$$n^2 - 1 = 4\pi N\alpha \qquad \ldots\ldots\ldots(10)$$

$$(n - 1)(n + 1) = 4\pi N\alpha$$

If n is close to unity

$$(n - 1) = 2\pi N\alpha$$

If this equation is divided by the concentration in grammes/ml.

$$\frac{(n - 1)}{C} = \frac{2\pi N\alpha}{C} \qquad \ldots\ldots\ldots (11)$$

$\frac{n - 1}{C}$ represents the change in refractive index with concentration and is therefore dn/dc .

Therefore by substituting $\mathcal{N}$, Avogardo's number and M the molecular weight for N and C

$$\alpha = \frac{(dn/dc).M}{2\pi\mathcal{N}} \qquad \ldots\ldots\ldots(12)$$

This value of α can be used to eliminate α^2 from equation 7 to give

$$\frac{i_s}{I_o} = \frac{4\pi^2(dn/dc)^2 M^2 \sin^2\phi_1}{r^2\lambda^4\mathcal{N}^2} \qquad \ldots\ldots(13)$$

For a system with N molecules per cubic centimetre

$$\frac{i_s}{I_o} = \frac{4\pi^2(dn/dc)^2 M^2 N \sin^2\phi_1}{r^2\lambda^4 N^2} \quad \ldots\ldots(14)$$

However $M = \frac{Mc}{N}$ and therefore by substitution equation 14 becomes

$$\frac{i_s}{I_o} = \frac{4\pi^2(dn/dc)^2 Mc.\sin^2\phi_1}{r^2.\lambda^4.N} \quad \ldots\ldots(15)$$

Figure 2 shows diagrammatically the angular dependence of the scattered light. The oscillating dipole at O, which is set up by the light, plane polarized in the XZ plane, sets up a secondary wave. The intensity of the secondary wave is proportional to the sine of the angle between the observer and the Z axis.

It will be seen that the intensity of the scattered light is symmetrical about the Z axis and that the intensity reaches a maximum in the XY plane and becomes zero along the Z axis.

If, however, the incident light is unpolarized, as in figure 2, then the vertical ZX wave behaves as before. The light, plane polarised along the XY plane sets up a secondary wave. The intensity of this wave is symmetrical about the Y axis, reaches a maximum in the XZ plane and becomes zero along the Y axis.

Equation 15 for unpolarized light becomes

$$\frac{i_s}{I_o} = \frac{2\pi^2(dn/dc)^2.M.c}{\lambda^4.r^2.N}(\sin^2\phi_1 + \sin^2\phi_2) \quad \ldots(16)$$

In this case, ϕ_2 is the angle made by the direction of observation and the dipole produced by the horizontally polarized wave.

By replacing $(\sin^2\phi_1 + \sin^2\phi_2)$ by $(1 + \cos^2\theta)$ where θ is the angle between the line of observation and the X axis equation 16 becomes

$$\frac{i_s}{I_o} = \frac{2\pi^2(dn/dc)^2.M.c.(1+\cos^2\theta)}{\lambda^4.r^2.N} \qquad .....(17)$$

For dilute solutions some account must be taken of the refractive index of the solvent.

If equation 10 is written as

$$n^2 - n_o^2 = 4\alpha\pi N \qquad .....(18)$$

where n_o is the refractive index of the solvent and n is the refractive index of the solution then

$$n^2 - n_o^2 = 2 n_o \left(\frac{dn}{dc}\right) c \qquad .....(19)$$

This redetermination of α^2 gives

$$\frac{i_s}{I_o} = \frac{2\pi^2.n_o^2.(dn/dc)^2.M.c}{\lambda^4.r^2.N}(1+\cos^2\theta) \qquad .....(20)$$

This equation can only be used to obtain the molecular weight at infinite dilution, as no account of non-ideality is taken in deriving it.

Fluctuation Theory of Light-scattering

In liquid systems a great deal of the light scattered is lost by destructive interference. The remainder of the scattered light can be regarded as arising from random fluctuations in the local concentration in small elements of the volume δV.

The solution may be divided into N such elements per cubic centimetre

$$N \delta V = 1 \quad \ldots\ldots(21)$$

The dimensions of each element are assumed to be small compared with the wavelength of the incident light.

If the concentration of the solute over all the solution is C^1 then the concentration of any element is

$$C = C^1 + \delta C \quad \ldots\ldots(22)$$

where δC is a small positive or negative increment in the concentra: :tion of the volume element.

Since the polarizability of the solute depends on the concentra: :tion then with any change, δC, in the concentration there will be an accompanying change, $\delta \alpha$, in the polarisability such that

$$\alpha = \alpha' + \delta \alpha \quad \ldots\ldots(23)$$

Equation 23 can be inserted into equation 7 to give the ratio of the intensity of the scattered light to the intensity of the incident light for such a volume element,

$$\frac{i_s}{I_o} = \frac{16\pi^4 (\alpha' + \delta\alpha)^2 \sin^2 \phi_1}{\lambda^4 . r^2} \quad \ldots\ldots(24)$$

However

$$(\alpha' + \delta\alpha) = \alpha'^2 + 2\alpha' \delta\alpha + (\delta\alpha)^2 .$$

The average fluctuation which gives rise to α'^2 is zero. The term $2\alpha' . \delta\alpha$ will be zero also as there is an equal probability of the value of $\delta\alpha$ being positive or negative. Therefore the only term in the expansion of $(\alpha' + \delta\alpha)^2$ which has any significance in equation 24 is $(\delta\alpha)^2$ for in this case all values of $\delta\alpha$ will

become positive due to squaring the term.

$$\frac{i_s}{I_o} = \frac{16\pi^4.(\delta\alpha)^2.\sin^2\phi_1}{\lambda^4.r^2} \qquad \ldots\ldots(25)$$

Since there are N elements per cubic centimetre and from 21 $N = \frac{1}{\delta V}$, equation 25 becomes

$$\frac{i_s}{I_o} = \frac{16\pi^4.(\delta\bar{\alpha})^2.\sin^2\phi_1}{\lambda^4.r^2.\delta V} \qquad \ldots\ldots(26)$$

where $(\delta\bar{\alpha})^2$ is the average value of $(\delta\alpha)^2$ for a large number of elements.

Temperature, pressure and concentration will all affect α and from the partial differential theorem

$$\delta\alpha = \left(\frac{\partial\alpha}{\partial P}\right)_{T,c}\delta P + \left(\frac{\partial\alpha}{\partial T}\right)_{P,c}\delta T + \left(\frac{\partial\alpha}{\partial c}\right)_{T,P}\delta c \qquad \ldots\ldots(27)$$

In dilute solutions the changes of α with pressure and temperature can be ignored since they are virtually the same as the changes of solvent alone

$$\delta\alpha = \left(\frac{\partial\alpha}{\partial c}\right)_{T,P}\delta c \qquad \ldots\ldots(28)$$

Equation 18 is

$$n^2 - n_o^2 = 4\alpha\pi N$$

If, in the derivation of equation 12 from equations 8 and 9 n_o^2 is substituted for 1 then it can be shown that

$$n_o\left(\frac{dn}{dc}\right) = \frac{2\pi N\alpha}{C} \qquad \ldots\ldots(29)$$

By substituting equation 28 in equation 29 it becomes

$$n_o\left(\frac{dn}{dc}\right) = 2\pi N\left(\frac{\partial\alpha}{\partial c}\right)_{T,P} \qquad \ldots\ldots(30)$$

However from equation 21 $N = \frac{1}{\delta V}$

$$n_o\left(\frac{dn}{dc}\right) = \frac{2\pi}{\delta V}\left(\frac{\partial \alpha}{\partial c}\right)_{T,P}$$

$$\left(\frac{\partial \alpha}{\partial c}\right)_{T,P.} = \frac{n_o\left(^{dn}/_{dc}\right)\delta V}{2\pi} \qquad \ldots\ldots(31)$$

From equations 28 and 26

$$\frac{i_s}{I_o} = \frac{16\pi^4.\left(\frac{\partial \alpha}{\partial c}\right)^2(\delta c)^2 \sin^2\phi_1}{\lambda^4.r^2.\delta V} \qquad \ldots\ldots(32)$$

By squaring equation 31 and substituting this relationship in equation 32

$$\frac{i_s}{I_o} = \frac{4\pi^2.(\overline{\delta c}).\sin^2\phi_1.n_o^2.\left(^{dn}/_{dc}\right)^2.\delta V}{\lambda^4.r^2} \qquad \ldots.(33)$$

where $(\delta \overline{c})^2$ is the average value of $(\delta c)^2$.

As in equation 16, equation 23 for unpolarized light becomes

$$\frac{i_s}{I_o} = \frac{2\pi^2.(\overline{\delta c})^2.n_o^2.\left(^{dn}/_{dc}\right)^2.\delta V.(1+\cos^2\theta)}{\lambda^4.r^2} \qquad \ldots\ldots(34)$$

If, in a system at equilibrium, there is a change in any thermodynamic quantity from a mean value $\overline{x}$ to another value x , then there will be a change in the free energy, ΔG , associated with that change such that

$$\Delta G = f(x) - f(\overline{x})$$

and the probability of such a change is given by a Boltzmann relationship, $e^{-\Delta G/kT}$ .....(35).

Large fluctuations in concentration are not expected, nor are large values of δG , therefore the expansion of δG gives

$$\delta G = \left(\frac{\partial G}{\partial x}\right).\delta x + \frac{1}{2!}\left(\frac{\delta^2 G}{\delta x^2}\right)(\delta x)^2 + \frac{1}{3!}\left(\frac{\partial^3 G}{\partial x^3}\right)(\delta x)^3 \ldots \qquad \ldots\ldots(36).$$

If in the above equation, the function x is related to the

concentration and if terms higher than squared are ignored equation 36 becomes

$$\delta G = \frac{1}{2!}\left(\frac{\partial^2 G}{\partial c^2}\right)_{T,P}(\delta c)^2 \qquad \ldots\ldots (38)$$

From this equation it can be deduced that

$$(\overline{\delta c})^2 = \frac{kT}{\left(\frac{\partial^2 G}{\partial c^2}\right)_{T,P}} \qquad \ldots\ldots (39)$$

which can be substituted in equation 34 to give

$$\frac{i_s}{I_o} = \frac{2\pi^2 n_o^2 \cdot \left(\frac{dn}{dc}\right)^2 \cdot \delta V \cdot (1+\cos^2\theta)}{\lambda^4 r^2} \cdot \frac{kT}{\left(\frac{\partial^2 G}{\partial c^2}\right)_{T,P}} \qquad \ldots (40)$$

If n_1 and n_2 are the number of moles of solvent and solute respectively in a volume δV and $\bar{V}_1$ and $\bar{V}_2$ are the partial molar volumes then

$$n_1\bar{V}_1 + n_2\bar{V}_2 = \delta V \qquad \ldots\ldots (41)$$

$$dn_1 = -\left\{\frac{\bar{V}_2}{\bar{V}_1}\right\} \cdot dn_2 \qquad \ldots\ldots (42)$$

By definition

$$dG = \mu_1 dn_1 + \mu_2 dn_2$$

where μ_1 and μ_2 are the chemical potentials of the solvent and solute respectively.

$$dG = -\mu_1\left(\frac{\bar{V}_2}{\bar{V}_1}\right)dn_2 + \mu_2 dn_2$$

$$= dn_2\left[\mu_2 - \frac{\bar{V}_2}{\bar{V}_1}\mu_1\right] \qquad \ldots\ldots (43)$$

The number of moles of solute per cubic centimetre is

$$-\frac{n_2}{\delta V} = \frac{C}{M}$$

$$dn_2 = \left(\frac{\delta V}{M}\right) dC$$

$$\therefore \quad \left(\frac{\partial^2 G}{\partial C^2}\right)_{T,P} = \frac{\delta V}{M}\left[\left(\frac{\partial \mu_2}{\partial C}\right)_{T,P} - \frac{\bar{V}_2}{\bar{V}_1}\left(\frac{\partial \mu_1}{\partial C}\right)_{T,P}\right] \quad \ldots\ldots\ldots(44)$$

By the Gibbs-Duhem equation

$$n_1 d\mu_1 + n_2 d\mu_2 = 0$$

$$\left(\frac{\partial^2 G}{\partial C^2}\right)_{T,P} = -\frac{\delta V}{M}\left(\frac{\partial \mu_1}{\partial C}\right)_{T,P} \cdot \left(\frac{n_1 \bar{V}_1 + n_2 \bar{V}_2}{n_2 \cdot \bar{V}_1}\right)$$

and since

$$\frac{n_2 M}{n_1 \bar{V}_1 + n_2 \bar{V}_2} = C$$

then

$$\left(\frac{\partial^2 G}{\partial C^2}\right)_{T,P} = -\frac{\delta V}{C \bar{V}_1} \cdot \left(\frac{\partial \mu_1}{\partial C}\right)_{T,P} \quad \ldots\ldots\ldots(45)$$

This can be inserted in equation 40 to give

$$\frac{i_s}{I_o} = \frac{2\pi^2 n^2 \cdot (dn/dc)^2 \cdot (1 + \cos^2\theta) \cdot C}{\lambda^4 r^2 - \left(\frac{1}{\bar{V}_1 kT}\right)\left(\frac{\delta \mu_1}{\delta C}\right)_{T,P}} \quad \ldots\ldots\ldots(46)$$

Since the deviation from non-ideality can be expressed as a power series in C

$$\mu_1 - \mu_{const.} = -RT\bar{V}_1\left(\frac{c_2}{M} + Bc_2^2 + Cc_2^3\right) \quad \ldots\ldots(47)$$

$$\left(\frac{\partial \mu_1}{\partial C}\right)_{T,P} = -RT\bar{V}_1\left(\frac{1}{M} + 2Bc + 3Cc_2^2 \ldots\right) \quad \ldots\ldots(48)$$

As $k = \frac{R}{N}$

$$-\frac{1}{\bar{V}_1 kT}\left(\frac{\partial \mu_1}{\delta C}\right)_{T,P} = N\left(\frac{1}{M} + 2Bc + 3Cc^2 \ldots\right) \quad \ldots\ldots\ldots(49)$$

Equation 49 can be included in equation 46 to give

$$\frac{i_\theta}{I_o} = \frac{2\pi^2 n_o^2 \cdot (dn/dc)^2 \cdot (1 + \cos^2\theta) \cdot C}{\lambda^4 \cdot r^2 \cdot N (\frac{1}{M} + 2Bc + 3Cc^2)} \qquad \ldots(50)$$

In very dilute solution equation 50 will become equation 20.

The Rayleigh ratio, R_θ, can be written

$$R_\theta = \frac{r^2 i_\theta}{I_o}$$

$$= \frac{2\pi^2 \cdot n_o^2 \cdot (dn/dc)^2 \cdot (1 + \cos^2\theta)}{\lambda^4 N (\frac{1}{M} + 2Bc + 3Cc^2)} \qquad \ldots.(51)$$

The turbidity, T, of a solution is

$$T = \frac{16\pi}{3} R_\theta \qquad \ldots\ldots(52)$$

$$T = \frac{32\pi^3 \cdot n_o^2 \cdot (dn/dc)^2 \cdot (1+\cos^2\theta)}{3 N \lambda^4 (\frac{1}{M} + 2Bc + 3Cc^2)} \qquad \ldots.(53)$$

If $$\frac{32\pi^3 n_o^2 \left(\frac{dn}{dc}\right)^2}{3N\lambda^4} = H \qquad \ldots.(54)$$

$$\frac{Hc}{T} = \frac{1}{M} + 2BC + 3Cc^2 \qquad \ldots.(55)$$

Equations 51 or 53 can be used to determine the molecular weight and the second virial coefficient of solute in solvent.

The second virial coefficient is a measure of the deviation of the system from ideality. For solutions of macromolecules the deviations are largely due to the molecular size and shape. Rod-shaped and coil molecules will give much larger values for the second virial coefficient than spherical molecules of the same molecular weight, provided the coiled molecules are in a good solvent.[201]

Depolarization

The theoretical treatment of light-scattering assumes that the particles which scatter the light are optically isotropic. Therefore in the practical interpretation of light-scattering data some compen: :sation must be made for molecules which are anisotropic.

If the molecule is completely isotropic and if unpolarized incident light is used then two independent oscillating dipoles are set up in the scattering particle. These dipoles are perpendicular to the electrical vectors of the incident light and are at 90° to the direction of the incident light in the horizontal and the vertical planes. The former dipole will not affect the intensity of the light scattered at 90° in the horizontal plane and therefore this scattered light will be completely polarized. Consequently, when the scattering particle is isotropic the ratio of horizontally polarized to vertically polarized scattered light will be zero.

However when the scattering particle is not absolutely isotropic then the oscillating dipoles induced by the unpolarized incident light are not parralel to the electric vector of the incident light. In this case the light scattered at 90° in the horizontal plane will not be completely polarized and the depolarization ratio, p_u , will not be zero.

It has been shown by Cabannes that the excessive scattered light due to the anisotropy of the scattering particle is related to the depolarization ratio. The intensity of light scattered is greater than the intensity due to fluctuations in concentration alone.

The correction factor used, Cabannes'[202] factor, is

$$\frac{6 - 7\,p_u}{6 + 6\,p_u}$$

where p_u is the depolarization ratio and the subscript "u" indicates that the incident light is unpolarized.

However while anisotropy of the scattering particles will give rise to a measurable depolarization ratio this ratio may also be affected by various other factors. Geiduschek[203] has stated that the depolarisation ratios quoted to be due to anisotropy may not be due to anisotropy but due to secondary scattering and various other factors.

Molecular Weight Averages

The distribution of the molecular weights of a system of macromolecules can be calculated in a number of ways to give a number of molecular weight averages for the same system. It is not possible to define any one particular system with one molecular weight average value because different physical properties demand the use of different molecular weight averages.

The three most important and appropriate molecular weight averages are considered. These are the number average, the weight average and the "Z"-average molecular weights.

The number average molecular weight, M_n, is obtained by dividing the sum of the products of the number of molecules and the molecular weight by the total number of molecules.

$$M_N = \frac{N_1M_1 + N_2M_2 + N_3M_3 + \cdots\cdots}{N_1 + N_2 + N_3 + \cdots\cdots}$$

$$= \frac{\sum_i N_i M_i}{\sum_i N_i}$$

where N_i is the number of molecules with a molecular weight M_i .

The weight average molecular weight, M_w , is defined as the sum of the products of the number of grammes of material and the molecular weight divided by the total number of grammes of the material

$$M_w = \frac{g_1M_1 + g_2M_2 + g_3M_3 + \cdots}{g_1 + g_2 + g_3 + \cdots}$$

$$= \frac{\sum_i g_i M_i}{\sum_i g_i}$$

where g_i is the number of grammes of material with molecular weight M_i .

However $g_i = \frac{N_iM_i}{N}$ where N is Avogardo's number.

Therefore the equation for the weight average molecular weight can be rewritten as

$$M_w = \frac{\sum_i N_i M_i^2}{\sum N_i M_i}$$

The third average molecular weight is the "Z" average molecular weight and is defined as

$$M_z = \frac{N_1M_1^3 + N_2M_2^3 + N_3M_3^3 + \cdots}{N_1M_1^2 + N_2M_2^2 + N_3M_3^2 + \cdots\cdots}$$

$$= \frac{\sum_i N_i M_i^3}{\sum_i N_i M_i^2}$$

To define the average radius of gyration it is necessary to

consider the macromolecule as a collection of units of mass M_i each at a distance r_i from the centre of mass of the macromolecule.

Equation 55 gives[20] at the intercept of the axis a measure of the weight average molecular weight since the limiting value of T_1 at the limit of zero concentration is proportional to $H\sum c_i M_i$ where C_i is the concentration of the dissolved molecules of molecular weight M_i .

From this

$$\lim_{c=0} \frac{Hc}{T} = \frac{\sum c_i}{\sum c_i M_i} = \frac{1}{\bar{M}_w}$$

Radius of Gyration

The radius of gyration, R, of the macromolecule is then

$$R^2 = \frac{\sum_i M_i r^2_i}{\sum_i M_i}$$

and the root-mean-square-average, R_g, is

$$R_g = (\overline{R^2})^{\frac{1}{2}} = \left(\frac{\sum_i M_i r_i^2}{\sum_i M_i}\right)^{\frac{1}{2}}$$

The radius of gyration can be related to the dimensions of the molecular model.

For a spherical molecule $R_g^2 = \frac{3D^2}{20}$,

a rod-shaped molecule $R_g^2 = \frac{L^2}{12}$

and a coil molecule $R_g^2 = \frac{r^2}{6}$

where D is the diameter of the sphere, L is the length of the rod and r is the root mean square end-to-end distance of the coil.

Light-scattering of Large Particles

So far only point scatterers of light have been considered. In many light-scattering experiments the particles scattering the light have dimensions which are greater than $\frac{\lambda}{20}$.

For dimensions greater than this, several incident rays are liable to strike the particle. Each of these gives a source of scattered light. The light produced by these different sources are likely to interfere with each other and thus cause a diminution of the intensity of the scattered light at the various angles (Figure 3).

The incident rays which are in phase at plane O strike the particle at points P_i and P_j. The difference between the dis: :tances OP_iA and OP_jA is greater than the difference between the distances OP_iB and OP_jB. Therefore the light scattered by P_i and P_j are more out of phase in plane A than in plane B.

This results in a greater destructive interference of the scattered light at plane A than at plane B and so the scattered light will have a lower intensity at the angle Θ to the incident beam than at the angle Θ_1.

When $\Theta = 0$, however, it will be seen that the path lengths of the incident light and the light scattered from the points P_i and P_j are the same. At this angle no destructive interference at all occurs. It is impossible, however, to measure the scattered light at this angle due to the overwhelming intensity of the incident light.

The effect of the size of the scattering particles in reducing the intensity of the scattered light can be said to be a function of $P(\theta)$ when

$$P(\theta) = \frac{\text{Intensity of scattered light in presence of internal interference}}{\text{Intensity of scattered light in absence of internal interference}}$$

or, alternatively

$$P(\theta) = \frac{i_\theta}{i_0}$$

where i_0 is the intensity of light scattered at $\theta = 0$.

$P(\theta)$ is unity for small particles but becomes less than unity when the size of the scattering particle is greater than $\frac{\lambda}{20}$.

In a particle in which destructive interference occurs the intensity of the scattered light is no longer symmetrical but varies with θ, the angle of observation.

The path length, Δ_i, the distance travelled by the light-ray to the observer, has a definite value for each scattering point and the differences between the distances gives rise to path differences between the rays which gives internal interference.

Equation 5 gave the relationship for the field strength of the scattered radiation E_s

$$E_s = \frac{4\pi^2 . v^2 . K E_o . \sin\phi_1}{c^2 . r} \cos 2\pi (\nu t - \frac{x}{\lambda}) \quad \ldots\ldots(5)$$

and $x = \Delta i$

$$E_s = \frac{4\pi^2 . v^2 . K . E_o . \sin \phi_1}{c^2 . r} \cos 2 (\nu t - \frac{\Delta_i}{\lambda}) \quad \ldots\ldots (57).$$

If it is assumed that the particle has σ scattering points

and if the contribution from each scattering point is summated then

$$E_s = \sum_{i=1}^{\sigma} Es_i$$

$$= \frac{4\pi^2 . v^2 . \kappa E_o \sin\phi_1}{c^2 . r} \sum_{i=1}^{\sigma} \cos 2\pi(\nu t - \frac{\Delta_i}{\lambda}) \quad \ldots\ldots(58)$$

If r_{ij} is the distance between the i^{th} and the j^{th} scattering points then it can be shown that

$$P(\theta) = \frac{1}{\sigma^2} \sum_{i=1}^{\sigma} \sum_{j=1}^{\sigma} \frac{\sin \mu r_{ij}}{\mu r_{ij}} \quad \ldots\ldots(57)$$

where $\mu = \frac{4\pi}{\lambda} . \sin \frac{\theta}{2}$ $\qquad (\lambda' = \lambda/n)$

Equation 57 gives an expression for $P(\theta)$ in terms of the number of scattering points and in terms of the distance between each scattering point. Therefore $P(\theta)$ is a function of molecular shape.

By expanding $\frac{\sin . \mu r_{ij}}{\mu r_{ij}}$ and only considering the first two terms of the expansion equation 57 becomes

$$\lim_{\theta \to 0} P(\theta) = 1 - \frac{\mu^2}{3!\sigma^2} \sum_{i=1}^{\sigma} \sum_{j=1}^{\sigma} r_{ij}^2 \quad \ldots\ldots\ldots(58)$$

It is necessary to relate the value of $P(\theta)$ with the radius of gyration, Rg, of the molecule.

If the molecule is considered to be composed of mass elements each of mass, M_i and a distance r_i from the centre of mass of the particle then

$$Rg = \left(\frac{\sum \overline{m_i r_i^2}}{\sum m_i}\right)^{\frac{1}{2}} \quad \ldots\ldots(59).$$

It can be shown that

$$Rg^2 = \frac{1}{2\sigma^2} \sum_{i=1}^{\sigma} \sum_{j=1}^{\sigma} \overline{r_{ij}^2} \quad \ldots\ldots(60).$$

By introducing this relationship into (58)

$$\lim_{\theta \to 0} P(\theta) = 1 - \frac{\mu^2 R^2 g}{3} \qquad \ldots\ldots(61)$$

$$\lim_{\theta \to 0} P(\theta) = 1 - \frac{16\pi^2}{3\lambda^2} R_g^2 . \sin^2 \frac{\theta}{2} \qquad \ldots (62).$$

This equation only holds at small values of $\sin^2 \frac{\theta}{2}$ as it is a limiting expression. It is not only essential to extrapolate to zero angle, it is also necessary to extrapolate to zero concentration to avoid intermolecular interactions affecting the value of Rg.

This extrapolation is effected by Zimm's method[204, 205], by plotting $\frac{Hc}{\tau}$ against $(\sin^2 \frac{\theta}{2} + kc)$ where k is a constant.

The final equation becomes

$$\lim_{c=0} \frac{Hc}{\tau} = \frac{1}{MP(\theta)}$$

$$= \frac{1}{M}\left(1 + \frac{16\pi^2}{3\lambda^2} R_g^2 . \sin^2 \frac{\theta}{2} \ldots\right) \qquad \ldots\ldots (63).$$

The Zimm method consists of plotting the experimental values of $\frac{Hc}{\tau}$ against $(\sin^2 \frac{2\theta}{2} + kc)$ at different concentrations. The constant in the term $(\sin^2 \frac{\theta}{2} + kc)$ is an arbitrary constant chosen so that there is a good plot of the points on the graph.

By extrapolating the concentration lines to zero angle and the angular lines to zero concentration, two limiting lines are obtained; one corresponding to the plot at zero concentration and one to zero angle.

The equation for the zero concentration line is (63),

and the zero angle line is

$$\left(\frac{Hc}{T}\right)_{\theta=0} = \frac{1}{M} + 2Bc + 3Cc^2 \ldots.$$

When these two lines are extrapolated they should have the same intercept on the $\frac{Hc}{T}$ axis and provide information on the scattering substance at zero concentration and at zero angle.

The particle scattering factor, $P(\theta)$, can be evaluated in terms of molecular shape and in fact provides an invaluable instrument in molecular shape determination.

The simplest derivation for $P(\theta)$ was for a rod-like molecule and it was found to be [206, 207]

$$P(\theta) = \frac{1}{x}\int_0^{2x} \frac{\sin w}{w}\,dw - \left(\frac{\sin x}{x}\right)^2 \qquad \ldots.(64)$$

where $x = \frac{2}{\lambda}.\sin.\frac{\theta}{2}.L$ and L = length of the rod.

This integral has a known solution, and by expanding the sine to the second term, a limiting expression is obtained

$$P(\theta) = 1 - \frac{x^2}{9} \qquad \ldots..(65)$$

So for small rod-like particles[205,208]

$$\left(\frac{Hc}{T}\right)_{\substack{c=0 \\ x \text{ small}}} = \frac{1}{M_w}\left[1 + \frac{x^2}{9}\right] \qquad \ldots..(66)$$

If the particles were large[208,209]

$$P(\theta) = \frac{2x_w}{\pi}\left[1 + \frac{1}{x_N} + \frac{1}{\pi^2 x_N^2} + \ldots\right] \qquad \ldots(67)$$

and as $\frac{x_w}{x_n} = \frac{M_w}{M_n}$

$$\left(\frac{Hc}{T}\right)_{\substack{c=0 \\ x \text{ large}}} = \frac{1}{M_N}\left[\frac{2x_N}{\pi} + \frac{2}{\pi^2} + \frac{2}{\pi^3 x_N} \ldots.\right] \qquad \ldots\ldots(68).$$

From this the number average molecular properties are obtained.

The simplest result for flexible coiled molecules was obtained by Debye[199,210] who assumed that the separation between each segment formed a Gaussian distribution

$$P(\theta) = \left(\frac{2}{W}\right)\left(e^{-W} + W - 1\right) \quad \ldots\ldots(69)$$

where $W = \mu^2 Rg^2$ and $\mu = \frac{4\pi}{\lambda} \sin\frac{\theta}{2}$.

Similar treatments for coiled molecules yielded[205,213] when W was large

$$\frac{Hc}{\tau} = \frac{1}{M_n}\left(\frac{1}{2} + \mu^2 Rg_n^2\right) \quad \ldots\ldots (70)$$

Again number average properties are obtained. These treatments give an idea of the effects of polydispersivity of the samples on the zero concentration line of the Zimm plot. At very low angles, weight average molecular weights and Z-average radii of gyration are obtained, while at high angles, the scattering is more due to the smaller molecules.

The asymptote to the limiting line is governed by equations 68 and 70 for rods and coils. Hence a great deal of information is obtainable from Zimm plots.

Holtzer, Benoit and Doty[211,212] gave an idea of where the various equations should apply. For light of a wavelength of 3,200 Å equation 66 held up to a value of the root mean squared end-to-end distance of 800 Å and equation 68 when this value excessed 3,000 Å.

Peterlin[214,215] extended this relationship to include stiff

coils and Benoit[213] considered the effects of branching of the coils on the equation for $P(\theta)$ and showed that values of $P(\theta)$ fell between those for rods and coils of the same radius of gyration.

Dissymmetry Method

In the previous measurements of light-scattering it was essential that the intensity of light scattered at various values of θ were obtained to provide accurate extrapolation to zero angle.

Measuring the intensities of the scattered light at 45° and 135° to the incident beam gives a ratio which is called the dissymmetry, Z ,

$$Z = \frac{i_{45^\circ}}{i_{135^\circ}} = \frac{R_{45^\circ}}{R_{135^\circ}}$$

If no internal interference is present , the intensities of the scattered light at 45° and 135° would be the same and the dissymmetry would be unity.

However , in the presence of internal interference the dissymmetry is

$$Z = \frac{P_{45^\circ}}{P_{135^\circ}}$$

The dissymmetry can be measured at various concentrations and , by extrapolation , a value for zero concentration obtained.

The value of the dissymmetry gives some indication of the shape of the molecule as tables of $P(\theta)$, Z and the characteristic dimensions of the particle are available. Also the value of $P\ 90^{\circ}$ may be obtained from Z to enable the 90° scattering to be corrected for internal interference and the molecular weight to be calculated.

The dissymmetry method, however, is more limited than those which employ measurement of the scattered light at various values of θ since a model for the molecular shape must be chosen. With the Zimm method such a choice is not required.

SECTION 2.

LIGHT SCATTERING AND VISCOSITY STUDIES ON GHATTI GUM FRACTIONS.

LIGHT-SCATTERING AND VISCOSITY STUDIES ON GHATTI GUM FRACTIONS

Fractionation

While ghatti gum has been considered a water-soluble gum there has always been a certain percentage, from 10% to 25%, which was not soluble in water. The insoluble portion on contact with water swelled up into large opaque masses. It may be that these insoluble nodules of gum were adulterants and not gum from Anogeissus latifolia. It is possible that they were produced by Terminalia sp. which produce insoluble gum and which are found under the same climatic and geographic conditions as A.latifolia.

The ghatti gum was supplied by Evans Medical Ltd., Liverpool 24 and authenticated by Dr. Fish, Royal College of Science and Technology, by comparison with a genuine sample supplied by Professor Bole, St. Xavier's College, Calcutta.

It was found that the best method for dissolving the gum was to mix the whole tears of gum with water and to stir this mixture slowly at 20° for twenty-four hours.

Under these conditions the soluble nodules dissolved and the insoluble nodules swelled up and most of them could be removed quite easily. The slow agitation prevented the masses of insoluble gum from breaking up and made their removal much easier.

The resultant solution was filtered through Whatman No. 54 filter paper to remove any remaining insoluble gum, pieces of bark and insoluble foreign material.

The crude gum was the calcium salt of an acidic polysaccharide and it was necessary to convert it to the free acid form. This transformation was carried out by either addition of a mineral acid to the solution of the gum or by passing the solution down a column of a strong cation exchanger. The conversion of calcium salt to free acid was readily and conveniently followed by infra-red spectroscopy.

When the gum was in the form of the metallic salt there was a single peak at 1600 cm.$^{-1}$ on the infra-red spectrograph. However when the gum was in the free-acid form this became a double peak. The part of this double peak at 1740 corresponded exactly to the absorption peak of lactones.

It was assumed therefore that the gum acid was present in the lactone form. The infra-red spectra corresponding to the crude gum and the free acid form of the acidic polysaccharide, ghattic acid, are shown in Figures 4 and 5.

Two methods of fractionation were used in the purification of crude ghatti gum.

In the first process the solution of the crude ghatti gum was acidified by the addition of hydrochloric acid to convert the calcium salt into the free acid. Sufficient acid was added to make the gum solution approximately 0.1 N.

The ghatti gum was then precipitated by the addition of absolute alcohol. The resulting white precipitate was filtered, washed with more absolute alcohol and redissolved in water.

This solution was then put in dialysis tubing and dialysed against tap water for twenty-four hours to remove any inorganic impurities.

After dialysis this solution was reduced in volume on the rotary evaporator and precipitated with absolute alcohol.

This precipitation process was then repeated for a third time. The final washed precipitate of ghattic acid was redissolved in water and the solution neutralised with sodium hydroxide solution to give the sodium salt of the ghattic acid. The pH of the neutralisation point was previously determined from a small portion of the dried sample.

This solution was then concentrated and finally dried in a vacuum oven at 35° over phosphorus pentoxide. This material was known as Fraction 1.

A chromatographic fractionation of the crude gum was also attempted.

The solution of ghatti gum was passed down a column of a strong cation exchange resin (Zeo-Carb 225) to convert it to the free acid form. This solution of the ghattic acid was then dialysed and evaporated to dryness as before.

The ghattic acid obtained from this process (16.5g) was dissolved in 175 mls. of water. When it was completely dis: :solved, 350 mls. of methyl alcohol were added to the solution.

This solution of ghattic acid in a 1 : 2 water/methanol solvent was then passed down a column containing 450 g. of silica gel.

Elution of this column with more of the water/methanol solvent gave 8g of material (Fraction 2).

The water content of the solvent was gradually increased and the column was finally eluted with 1 l. of water. This process gave, after evaporation to dryness, 3.5g material (Fraction 3). The remainder of the material on the column could not be eluted with water.

The progress of both these chromatographic processes was followed by reading the refractive index of the effluent material on an Abbe refractometer.

Both fractions 2 and 3 were evaporated to small volume in the rotary evaporator. The concentrated solution was then neutra-:lised with sodium hydroxide to give the sodium salt of the ghattic acid. The end-point of the titration of the acid with the sodium hydroxide was determined by drying a small portion of each fraction and finding the titration curve from it.

Finally the solutions of Fractions 2 and 3 were dried in a vacuum oven at 35° over phosphorus pentoxide.

From the potentiometric titrations the equivalent weights of the fractions 1, 2 and 3 were found to be 1750, 1800 and 2040 respectively and the values of the pKa 3.90, 4.15 and 4.28 respectively.

Materials

Water

All water used in the experiments was double distilled from glass apparatus. The second distillation was from a dilute potassium permanganate solution.

Glass-Ware

All glass ware was thoroughly washed with Teepol and water and then soaked in chromic acid. It was then thoroughly rinsed with water and finally dried with dry acetone.

Chemicals

All chemicals used in the various experiments were AnalaR reagent quality.

Light-scattering Apparatus and Cell

An apparatus for light scattering had been constructed in the department after the design of Parreira and Ottewill[216] and Robinson[217] (Figures 6 and 7 and Plate 1).

The light source in the apparatus was a 250 w. mercury vapour lamp (Osram type ME/D) and the power supply to this lamp was stabilised by a constant voltage transformer (advance 250 w. type CUH).

The light from the lamp was made parallel by using a system of lenses and slits and the green line (5461 Å) was isolated by using an interference filter. The last traces of the sodium light were removed by passing the light through a neodymium glass filter.

The parallel beam of light was then passed through two slits 2 mm. broad and 32 mm. high set 32 cm. apart to define the beam. The final beam which passed through the cell was 2 mm broad and 26 mm. deep.

The light scattered by the solution was detected by an eleven stage photomultiplier (EMI Tube type 6097B) whose voltage supply was obtained from two Siemens-Ediswan power packs, type R.1184, operated in series. The area of the solution viewed by the photomultiplier was defined by two slits 8 x 12 mm. set 8 cms. apart. One of these slits was close to the curved cell window and the other was immediately in front of the photo: :multiplier end window.

The photomultiplier was mounted horizontally in a can on a broad Tufnol arm which was pivoted immediately beneath the centre of the cell. This arm lay on the Tufnol sheet base of the light-scattering apparatus and could be rotated smoothly and quickly about the cell axis, to give readings of between 30° and 135° to the incident beam.

The signal from the photomultiplier was recorded by a d'Arsonval galvanometer and read on a 50 cm. scale mounted above the light-scattering apparatus.

To minimise fluctuations in signal the glass wall of the photomultiplier tube was coated with silver paint, raised to cathode potential and bound with parafilm.

Part of the incident beam inside the apparatus was lead to a photocell (EMI type Z5110) and fluctuations in the intensity of the light could be detected. A light-proof box surrounded most of the apparatus and is shown as a dotted line in Figure 6.

A new type of cell was developed from earlier designs[218]. The previous cells which allowed light-scattering measurements from 45° to 135° were used to find the disaymmetries of various solutions. However it was important in this case for the complete envelope to be read so that Zimm plots could be construct: :ed. It was necessary therefore to have a cell which would allow readings of the scattered light down to low angles. With this modified cell it was possible to obtain readings from the scattered light from 30° to 135° to the incident beam.

The cell was made from a cylinder of brass 66 mm. high and 50 mm. in diameter. In order to provide a long entrance channel for the light the cell was made as shown in Figure 8.

Three circular light traps 10 mm., 8 mm. and 6 mm. in diameter were cut in the back wall of the cell. This reduced internal reflection and cut down the stray light which would affect the readings on the photomultiplier.

The exit and entrance windows of the cell were 4 mm. wide and 38 mm. deep. The scattering windowwas larger than in the previous designs to allow readings at lower angles.

There was a long entrance channel so that the entrance window could not be seen directly from the position at which the readings were taken, i.e. through the curved window. This was necessary to prevent reflection of light from the entrance window entering the photomultiplier and giving anomalous results.

To remove internal reflections and stray light the whole cell was blackened by the Relanol process.

The entrance window was cut from a microscope slide 1 mm. thick and the large curved window, which covered both the scatter: :ing window and the exit window, from a glass tube 2 mm. thick. The glass tubing had the same internal diameter as the diameter of the cell. The latter window was made from thicker glass because it had to be fairly robust.

The black surface formed in the Relanol process was removed from the edges of the slits, and the windows were attached to

the cell by Araldite epoxy resin. The cell was then cured for twenty-four hours at 37°. This low temperature was used to prevent any excessive strain on the glass windows. The Araldite joints formed in this way were very firm and completely water-tight.

There was a small hole bored between the top of the cell and the entrance slit to prevent any air bubbles being trapped in the cell during filling. For the same reason the roof of the exit slit was slanted upwards towards the centre of the cell.

In the light-scattering apparatus the cell fitted into a hole cut into a Tufnol stand. It was important that the cell windows should be exactly at right angles to the incident beam. Part of the incident light was reflected from the entrance window and this reflection could be seen on one of the brass plates in which the slits had been cut to define the beam. The cell was revolved until the main beam of light and the reflected beam coincided.

In this position the entrance and therefore the exit windows were perpendicular to the beam of light and the cell was in the correct position. This method of positioning the cell was quick, easy and reproducible.

Readings of turbidity of the various solutions were made in comparison with a Perspex block, by interchanging block and cell in cell holder mount. The block had been previously calibrated by McIntosh[219] and MacFarlane[220] using Ludox solutions. Immediately after this calibration the turbidity of benzene was found

to be 27.2 $\pm$ 0.4 x 10^{-5}cm.$^{-1}$. Eighteen months later four repeat measurements on benzene gave 27.3 $\pm$ 0.3 x 10^{-5}cm^{-1}. This agreement indicated that there was no change, within experimental error, over the time period in which the light-scattering results were made.

Tests on the light-scattering cell with dilute Ludox solutions showed that normalisable envelopes were obtained down to 30° to the incident beam after the solvent reading had been subtracted.

Clarification of Light-scattering Solutions

It was most important that the light-scattering solutions should be completely free of dust. The presence of dust would have greatly affected the intensity of the scattered light and given anomalous results for the values of the molecular weights and the other properties derived from the light-scattering experiments.

Each solution was made from double-distilled water and was filtered through a No. 5 sintered glass gas filter until it was clear.

Each solution was checked by placing the light-scattering cell in position in the light-scattering apparatus and inspecting the solution through the viewing window at a small angle to the incident beam. Under these conditions any particles of dust showed up as bright scattering points and this provided an easy and convenient method for determining the clarity of the solution.

The sintered glass filter was cleaned between each solution by potassium permanganate and concentrated sulphuric acid followed by hydrogen peroxide and concentrated sulphuric acid. The filter was then rinsed very thoroughly with dust-free double-distilled water. Before the next solution was filtered the sintered glass was finally rinsed with a little of the solution.

The light-scattering cell was cleaned with Teepol and water. It was then thoroughly rinsed with water and finally dried with hot acetone vapour. The cell was also rinsed with a little of

the filtered solution before the bulk of the solution was filtered into it.

The solution was filtered directly into the light-scattering cell which was always kept covered during the filtration process and during the actual reading with a circular brass plate. This cover had, like the inside of the cell, been treated by the Relanol process to avoid any internal reflections.

Some solutions were checked for loss in concentration before and after filtration by the Hilger-Rayleigh interferometer. No loss of material was evident from these readings.

Depolarization

The depolarization ratios for the various solutions were measured by inserting a polaroid disc between the photo-multiplier tube and the cell and measuring the intensities of the horizontal and vertical components separately.

Since the Cabanne's factor[202] was so close to unity and would have made very little difference to the final results the correction due to depolarization has not been applied. However the depolarization ratios of the various systems are quoted in Table 2.

Refractive Index Increments

When light-scattering studies are carried out on polyelectrolytes in salt solutions, some account must be taken of the interaction of the simple electrolyte molecules with the polyelectrolyte molecules.

When a polyelectrolyte is surrounded by a binary system there may be selective adsorption of one of the components. Such adsorption would affect the polarisability of the molecule and therefore the intensity of the scattered light.

When the subscripts 1, 2 and 3 refer to solvent, polyelectrolyte and simple electrolyte it can be shown that

$$\left(\frac{\delta n}{\delta c_2}\right)_{\mu_3} = \left(\frac{\delta n}{\delta c_2}\right)_{c_3} + \left(\frac{\delta n}{\delta c_3}\right)\left(\frac{\delta c_3}{\delta c_2}\right)_{\mu_3}$$

Strauss and Ander[221] measured the quantity $\left(\frac{\delta c_3}{\delta c_2}\right)_{\mu_3}$ from membrane equilibrium results.

In most cases however it is possible to measure the refractive index increment directly if the solvent and the solution are at constant chemical potential[106]. This can be achieved by dialyzing the solution of the polyelectrolyte in salt against the corresponding salt solution until equilibrium has been reached.

The various fractions of ghatti were made up in the corresponding salt concentration and put into small sections of dialysis tubing (Visking Dialysis tubing $^{36}/_{32}$"). The tubing

was then sealed and immersed in the appropriate salt solution for twenty-four hours with occasional agitation. At the end of this time the solution of polyelectrolyte and the sodium chloride solution were at constant chemical potential, i.e. there was no change in the values of dn/dc on further dialysis.

The refractive index increments were read on a Hilger-:Rayleigh interference refractometer using the green light of mean wave-length 5461 $\overset{o}{A}$.

In this instrument two intersecting light beams from the source produce a system of interference bands. When solvent is placed in both sides of the cell there is no displacement of these bands compared with reference set of fringes, given by rays not passing through solvent and solution. However when one side contains the solvent, in this case salt solution, and the other the solution there is a displacement of the interference bands which can be measured.

From this reading the refractive index increment was calculated from

$$\frac{dn}{dc} = \frac{n.\lambda}{c} \qquad \text{(for the 1 cm. cells used)}$$

where n = number of bands displaced
λ = wavelength of the light
c = concentration of the polyelectrolyte in gms./ml.

n was determined by Bauer's et al[222] method by obtaining the zero setting with solvent in both sides of the cell. Then with solvent in one side and the solution to be measured in the

other the balance points were located using white light. A filter was then inserted which transmitted light with a wave-length of 5461 Å and the number of bands crossing the field between this setting and the zero setting of the instrument was counted.

For each system the dn/dc of three concentrations up to 0.15% was calculated.

The dn/dc readings are shown below

TABLE 1

	H_2O	0.005 NNaCl.	0.05 NNaCl.	0.5 NNaCl.
Fraction 1	0.149		0.139	0.137
" 2	0.148	0.143	0.138	0.136
" 3	0.141			0.130

Description of Couette Viscometer

A Couette viscometer was constructed after the design of Ogston and Stanier[223] (Plate 2).

A Hanovia constant speed motor (Engelhart Hanovia type SD 6/00763) was fitted with two pulleys 2¾" and 2" in diameter. These were connected by a polythene belt to a corresponding system of three pulleys on the viscometer. The diameters of the pulley wheels on the viscometer were 1 7/16" , 2" and 2¾" respectively (Fig. 9a).

The power to the motor was supplied by a constant voltage transformer (Advance Components Ltd., Type M.T.267A) to the motor stabilising unit (Hanovia); the speed of the motor being varied by a 50,000 ohm Fox helical precision potentiometer (Type PX4/H10).

By these means, the speed of revolution of the viscometer pot could be accurately adjusted from 0 to 116 revolutions per minute. It was also very constant at any particular setting of the potentiometer. This gave a maximum shear rate for the apparatus of 76 sec^{-1}.

The viscometer framework consisted of a brass plate (b) ½" thick which was supported on three 6" long brass legs. Two of these legs had adjustable feet so that the whole apparatus could be accurately levelled.

Above the plate were two 12" long vertical brass rods which supported the viscometer head (c).

In the centre of the plate there was a hole 2⅞" in diameter. Attached to the plate and concentric with this hole there was a brass cylinder 2⅞" in diameter and 4" long.

Inside this cylinder were two sets of ball races (d) into which the cylinder holder fitted.

The outer cylinder holder was a tube of brass which push-fitted into the bearing assembly. It was $2\frac{7}{8}$" in external diameter and at the top it carried the three pulleys just clear of the top of the brass plate.

The outer cylinder or 'pot' was a brass cylinder $5\frac{1}{2}$" long, $\frac{3}{4}$" internal diameter and 1" external diameter. The closed end of the pot was recessed and had a "Perspex" base so that the inner cylinder could be accurately centred. The inside of the pot was carefully ground with emery cloth until it was very smooth.

The whole apparatus beneath the plate was surrounded by a water jacket 4" deep and 6" in diameter through which water could be circulated

The viscometer head (c) which fitted on to the vertical rods from the base plate was so designed that the inner cylinder could be removed from the pot and swung clear.

The viscometer head was composed of two horizontal brass plates joined by vertical plates.

Holes were bored at one end of the brass plates to fit over one of the uprights. At the other end two U-shaped cuts were made so that the other upright would fit into it and could be held firmly in that position by two grub screws.

There was an adjustable stop-ring on one of the uprights which held the viscometer head in any position required.

The suspension wire to the bob ran through a $\frac{1}{8}$" diameter brass cylinder on the viscometer head. The wire was connected to a torsion head (g). The circular top of the torsion head rested on top of this cylinder.

Since it was imperative that the bob hung centrally in the outer cylinder the position of the torsion head could be adjusted by three screws set at 120° to each other. These screws ran through the viscometer head cylinder and clamped the torsion head in position. By adjusting these screws it was possible to move the position of the inner cylinder very precisely.

The torsion wire used was Mallory 73 Beryllium copper with a diameter of 0.0045". Both ends of the wire were attached to small brass rods $\frac{3}{32}$" in diameter. These rods fitted into the torsion head and the inner cylinder and were clamped tightly in position by small grub screws. On the lower rod a small mirror was attached so that the deflection of the inner cylinder could be measured optically by the reflection of an image projected by a Cambridge spot galvanometer outfit.

The inner cylinder of 'bob' (h) was made from brass and was $5\frac{3}{8}$" long. The lower $3\frac{1}{8}$" of the cylinder was $\frac{5}{8}$" in diameter and the upper portion was $\frac{1}{4}$" in diameter. At the top of the cylinder there was a vertical hole $\frac{1}{8}$" in diameter to hold the lower end of the torsion wire. The lower end of the bob was concave. This trapped an air bubble when it was immersed in the solution and so reduced the end-effect.

The deflection of the bob was measured by focusing an image reflected by a mirror on the lower end of the torsion wire on to a

circular scale. This had a radius of 50 cm. and an effective length of 150 cms.

The speed of revolution of the outer cylinder was counted automatically. On the bank of pulleys on the pot holder was an upright brass rod $1\frac{3}{8}$" high and $\frac{3}{8}$" in diameter. Attached by clamps to the brass plate were an automatic counter and a light source (Counting Instruments Ltd. type 500). When the brass rod cut the light-beam the revolution was registered on the counter.

To determine the viscosity of a solution the pot was filled with 25 mls. of the liquid and the bob lowered until the level of the liquid was just above the top of the bob.

The deflection of the bob was then measured at a series of speeds of revolution of the inner cylinder and the results plotted to give straight lines as in Figures 21 - 24.

The relative viscosity of a solution was obtained from the ratio of the deflection of the bob in the solution to the deflection of the bob in solvent alone.

Light-scattering Results and Discussion

Light-scattering measurements were made on all three fractions of ghatti gum in 0.5N sodium chloride; on fraction 1 in 0.05N sodium chloride and fraction 2 in 0.05N and 0.005N sodium chloride and in water. All the light-scattering experiments were carried out at a temperature of $20^{\circ} \pm 1$.

The intensity of the scattered light was measured from 30° to 135° to the incident beam. Zimm plots were constructed for every system and these are shown in Figures 10 - 16. In the Zimm plots C is the concentration of sodium ghattatein g/ml. and Sθ is the intensity of the light scattered from the solute at an angle θ to the incident beam.

Zimm plots are useful because the various results are extra-:polated to zero concentration and to zero angle. From the two lines obtained from these extrapolations various physical charac:teristics of the solute can be determined.

The equation of the zero angle line is given by equation 62 and the equation of the zero concentration line is given by equation 63.

The values of (dn/dc) were made at constant chemical potential as described by Vrij and Overbeek[106].

The intercept of this line is also $\frac{1}{M_w}$ and from the ratio of the slope of the line to the intercept the Z-average radius of gyration can be calculated from the equation

$$\frac{\text{Slope}}{\text{Intercept}} = \frac{16\pi^2}{3} R_{g_z}^2 . \left(\frac{n}{\lambda_o}\right)^2$$

TABLE 2.

DATA FROM LIGHT-SCATTERING MEASUREMENTS

Fraction	Solvent	dn/dc	10^6 Mw	R_{g_z} (Å)	10^{-5} B	L(Å)	P
1	0.5N NaCl	0.137	2.1	727	4	2520	0.017
1	0.05N NaCl	0.139	2.1	821	10	2840	0.016
2	0.5N NaCl	0.136	2.2	768	4	2660	0.027
2	0.05N NaCl	0.138	3.3	873	10	3030	0.027
2*	0.005N NaCl	0.143	2.7	1005	41	3460	0.020
2	Water	0.148	2.7	1061	260	3680	0.048
3	0.5N NaCl	0.130	2.6	740	2	2560	0.033

* - by dissymmetry method P - depolarization.

The fraction prepared by alcoholic precipitation has the lowest molecular weight of all the fractions.

For fraction 2 there is considerable variation in the molecular weights as determined in various solvents. It is possible that this variation in Mw may be due to certain inaccuracies inherent in the Zimm plot method for determining molecular weight. Several authors[211,224,225] have shown that the errors in the determination of Mw can be as high as ±10% and these estimates have been based on a study of equation 55 when particles small enough for $P(\theta)$ to be taken as unity have been used.

In the Zimm plot method the angular values of $\left(\frac{HC}{\tau}\right)_\theta$ must be extrapolated to $\theta = 0$ and the points thus obtained must again be extrapolated to $C = 0$ to obtain a value of Mw. This double extrapolation procedure may increase the potential percentage error appreciably.

As the concentration of salt decreases the radius of gyra:
:tion increases and this is normal polyelectrolyte behaviour [42,52,54,55]. This means that as the salt concentration is decreased the molecule expands and the radius of gyration increases until a maximum value is reached in water. At this point each molecule is fully ex:
:panded because of the electrostatic repulsion between each of the polar groups.

On addition of electrolyte the repulsive forces between the charged groups on the macromolecule are decreased and the macro:
:molecule contracts with a corresponding decrease in the radius of gyration.

The radii of gyration obtained for all the fractions are reasonably consistent and it may be that the values obtained for the radii of gyration have lower limits of error than the values obtained for the molecular weights of the various fractions, since the radii of gyration are obtained from the ratios of the limiting slopes to the intercepts. It may be that in such a calculation where experimental or graphical errors affect both parts of the ratio some cancellation of error occurs.

For fraction 1 in 0.5N sodium chloride and fraction 2 in 0.5N sodium chloride and in water the molecular model which fitted the limiting zero concentration line was calculated. Using the observed Rg values calculation of the particle scattering factors for monodisperse rods and coils and for coils with a molecular weight distribution $M_z : M_w : M_n$ of 3 : 2 : 1 were made.

The particle scattering factor, $P(\theta)$, of a solution is given in the introduction, equations 64 - 70 were used.

Since the radius of gyration is known for each system the particle scattering factor at each angle θ can be calculated and from this the theoretical value of $\left(\frac{HC}{\tau}\right)_\theta$ from

$$\mathcal{L}\left(\frac{HC}{\tau}\right)_{C=0} = \frac{1}{M\,P(\theta)}$$

This then gives the theoretical zero concentration line for a monodisperse rod, i.e. $M_z = M_w = M_n$, with the observed radius of gyration.

For monodisperse rods

$$x = \frac{2 \sin \frac{\theta}{2} \cdot L}{\lambda'}$$

where L is the length of the rod which can be calculated from $Rg^2 = \frac{L^2}{12}$. From this, $P(\theta)$ and therefore the theoretical scattering at each angle θ can be calculated to give the zero concentration line for a system of monodisperse rods with the observed length.

The line for the monodisperse rods gave the closest fit to the experimental line for all the models investigated. However there was not a perfect agreement between the experimental line and the calculated line for monodisperse rods and so the effect of polydispersity of the molecular weights was investigated by using Reichmann's treatment[226].

The equation for $P(\theta)$ for rigid rods is given in equation 64.

Where x is small $1/P(\theta)$ can be expressed as

$$\frac{1}{P(\theta)} = 1 + \frac{x_z^2}{9}$$

and therefore

$$\left(\frac{HC}{\tau}\right)_{C=0} = \frac{1}{M_w}\left(1 + \frac{x_z^2}{9}\right) \quad \ldots\ldots (66)$$

This equation holds up to a value of $x_z = 1.5$.

For the upper part of the limiting line approaching the asymptote where smaller molecules make a significant contribution to the scattered light and if $\frac{x_w}{x_n} = \frac{M_w}{M_n}$ then

$$\left(\frac{HC}{\tau}\right)_{C=0} = \frac{1}{M_n}\left(\frac{2}{\pi^2} + \frac{2x_n}{\pi}\right)$$

This equation gives suitable results for values of x_n down to $x_n = 2$.

However its usefulness can be increased if the series is expanded and the higher terms are included.

$$\left(\frac{HC}{\tau}\right)_{C=0} = \frac{1}{M_n}\left(\frac{2x_n}{\pi} + \frac{2}{\pi^2} + \frac{2}{\pi^3 x_n} + \frac{2}{\pi^4 x_n^2} + \frac{2}{\pi^5 x_n^3}\right) \ldots (71)$$

Tests showed that this equation was valid down to the values of $x_n = 1.5$.

Since M_w and R_{g_z} and therefore L_z and x_z were directly determinable from the Zimm plots equation 66 was applied to the results up to a value of $x_z = 1.5$.

As light-scattering measurements could not be made at high enough angles to indicate the asymptote to the limiting of the Zimm plot, equation 71 was used by successive approximation.

From the Zimm plots the M_w and L_z values of the molecular weight and the length of the rod were known. Therefore by assuming a certain ratio for the molecular weight distribution $M_z : M_w : M_n$ and therefore $L_z : L_w : L_n$ the other related molecular weight values and lengths could be calculated.

In this way by starting from the monodisperse case where $M_z = M_w = M_n$ and $L_z = L_w = L_n$, cases of increasing polydispersity were considered until the theoretical zero concentration line for polydisperse rods which most closely approached the experimental line was obtained.

TABLE 3.

DISTRIBUTION GIVING BEST FIT TO LIMITING LINE OF ZIMM PLOT

Fraction	Solvent	$L_z : L_w : L_n$
1	0.5N NaCl	1.2 : 1.1 : 1.0
2	0.5N NaCl	1.2 : 1.1 : 1.0
2	Water	3.0 : 2.0 : 1.0

From these calculations it was clearly shown that a rod-like molecule gave the best fit for the experimental results, Figure 17. This indicated that a rod model was the most probable shape for the macromolecule although some deviation from a perfect rod shape could be present.

The deviations between the best theoretical line and the experimental line may be due to various other characteristics of the macromolecule other than polydispersity. The effects of branching of the molecule or a certain degree of polydispersity

in the thickness of the macromolecules may account for the fact that the fit is not perfect.

The rod-like shape suggested by the method above for the macromolecules was maintained when the solvent was changed from 0.5N sodium chloride to water although an apparent change in the degree of polydispersity of the molecules has occurred.

In 0.5N sodium chloride both fractions 1 and 2 had a surprisingly narrow molecular weight distribution $M_w : M_n$ of 1.1 : 1.0. However in water this distribution appeared to be 2.0 : 1.0.

This phenomenon of a change in polydispersity may be connected with the contraction of the molecule on addition of simple electrolyte. In water the macromolecule is fully expanded. However in concentrated salt solution the molecule becomes contracted. Possibly the larger differences in the various molecular lengths in water are masked and minimised in concentrated salt solution to give an apparently narrower distribution.

Viscosity Results and Discussion

Viscosity experiments were carried out on all three fractions of sodium ghattate with the suspended level dilution viscometer and the Couette viscometer. The viscosity experiments were carried out at a temperature of $20^{\circ} \pm 0.01$.

In the former, fraction 1 was studied in 0.005N, 0.05N, 0.5N, 2.0N, in iso-ionic dilution and in water; fraction 2 in 0.005N, 0.05N, 0.5N, in iso-ionic dilution and in water, and fraction 3 in water. The graphs corresponding to these are shown in Figures 18 - 20.

In the Couette viscometer fraction 1 was studied in 0.005N, 0.5N, in iso-ionic dilution and in water and fraction 2 in 0.005N and 0.5N sodium chloride. The results obtained from these systems are shown in Figures 21 - 24. The reduced viscosity was calcu:lated from the Couette results and the values obtained are shown in the various graphs. Good agreement between the values of the reduced viscosity from the suspended level and the Couette visco:meter was obtained.

Both fractions exhibited Newtonian flow in the range of con:centrations examined in the Couette viscometer up to the maximum velocity gradient obtainable in the instrument of 76 $sec.^{-1}$. Since the capillary viscometer was the more precise instrument it was used for the remaining experiments. The average velocity gradient for the capillary viscometer used was 1310 $sec.^{-1}$.

Since the reduced viscosities of the solutions agreed from the Couette and the suspended level dilution viscometer results then it is evident that the solutions exhibited Newtonian flow over the range of velocity gradients studied.

The viscosity of the various fractions of sodium ghattate decreased with increased simple electrolyte concentration. This has been shown to be normal polyelectrolyte behaviour[42,52,54,55,121]. According to Fuoss the peculiar physico-chemical properties of poly-:electrolytes arise from the high-charge density and the flexibi:-:lity of the macromolecular chain structure. Since the viscosity of any solution depends on the dimensions of the molecule, any decrease in size, as happens on the addition of simple electrolyte to a polyelectrolyte solution, has the effect of reducing the viscosity.

The $\frac{\eta_{sp}}{c}$ against concentration graphs for the fractions in water all showed a distinct rise at low concentrations. This phenomenon has been shown in general for polyelectrolytes and in particular[179] for sodium arabate solutions[121].

The reason for this particular result is that when no simple electrolyte is present in solutions of polyelectrolyte the only mobile ions present are the counter-ions of the macromolecule. As the concentration of the polyelectrolyte decreases so the concentration of the counter-ions and the ionic strength falls. This decrease in the ionic strength causes an increase in the size of the polyelectrolyte.

As well as a decrease in the ionic strength having an effect on the viscosity of dilute polyelectrolyte solutions it may be that in such solutions the macromolecules are so expanded that the concentration of the macromolecules may have an effect on the configuration.

Schneider and Doty[188] plotted the viscosity intercept $[\eta]$ against $1/N^{\frac{1}{2}}$ where N was the normality of the added salt. The straight line graphs obtained by this procedure could be extra: :polated to infinite ionic strength i.e. where $1/N^{\frac{1}{2}} = 0$. At this point the molecule could be treated as being completely uncharged.

From Figure 25 the viscosity intercepts at infinite ionic strength were 112 and 94 cc/g for fractions 1 and 2 respectively.

The high values of these intercepts indicated that the macro: :molecule was either highly asymmetric, highly solvated or both.

Water-vapour absorption studies have been used[227] to deter: :mine the hydration of macromolecules. The water-vapour adsorption studies on these two fractions of sodium ghattate indicated that the hydration in g.water/g. sodium ghattate were 0.20 g/g and 0.14 g/g respectively for fractions 1 and 2.(see Section 3).

Simha's shape factor was calculated for two conditions, when w_1 was zero and for the values of w_1 determined by the water-vapour absorption studies.

It was apparent that with this level of hydration the

deviation of the viscosity intercepts from the Einstein[76,77] value of 2.5 was due to the asymmetry of the macromolecule. Since, from the light-scattering experiments the most probable shape for the sodium ghattate molecules was a rod, the viscosity results were interpreted on this basis.

Mehl, Oncley and Simha[80] showed that, for prolate ellipsoids, v, the shape factor could be calculated and tables of these shape factors were published. Since the light-scattering results gave L, the length of the rod, it was necessary to convert the ratio, a/b, used by Mehl, Oncley and Simha, into the ratio L/d where d was the diameter of the rod.

This was done by the procedure adopted by Tanford[228]. Since $L = 2a$ and $\frac{4\pi ab^2}{3} = \frac{\pi Ld^2}{4}$ by solving these two equations for a and b, it could be shown that

$$\frac{a}{b} = (0.6666)^{\frac{1}{3}} \frac{L}{d}.$$

Since the molecular weights were known from the light-scattering data, the densities and the values of hydration of both fractions had been measured (See Section 3), it was possible to determine the volume of the molecules.

From these results and the viscosity experiments it was possible to obtain the molecular dimensions from Simha's relationship. (p. 32)

TABLE 4.

MOLECULAR DIMENSIONS CALCULATED FROM VISCOSITY INTERCEPTS AT INFINITE IONIC STRENGTH

Fraction	Solute density P	$W_1 = 0$			$W_1 = 0.20$ (fraction 1) $W_1 = 0.19$ (fraction 2)		
		a/b	L	d	a/b	l	d
1	1.52	49.0	2190	37	43.4	2160	41
2	1.54	44.5	2220	41	38.5	2190	47

The lengths and diameters are given in Angstroms.

The densities of the two fractions were determined by displacement in dry benzene.

The lengths of the macromolecules obtained by the light-scattering experiments for the various salt concentrations were graphed against $1/N^{\frac{1}{2}}$ where N was the normality of the added salt. The values of the lengths of the rods at infinite ionic strength were found by extrapolating the graph to $1/N^{\frac{1}{2}} = 0$. The lengths of the macromolecules for fractions 1 and 2 were 2500Å and 2580Å respectively.

The lengths of the macromolecules as obtained from the light-scattering and the viscosity results show remarkably fair agreement with each other.

Expansion of the Molecule

In water the graph of $\frac{\eta sp}{c}$ against concentration curved upwards as the concentration decreased. This is typical polyelectrolyte behaviour and has been observed for other polyelectrolytes in water. The intercept of the graph can be determined[52] by plotting $\frac{c}{\eta sp}$ against $c^{\frac{1}{2}}$. This was done for two fractions of sodium ghattate and the intercepts for fractions 1 and 2 were found to be 2600 and 2350 ml/g respectively.

As has been shown from the light scattering results , Rg increased with decreased salt concentration. The increase of Rg and $[\eta]$ with decreased salt concentration can be taken as a measure of the expansion of the molecule.

Pals and Herman[179,184,185], using the sodium salts of pectin and carboxymethylcellulose in aqueous sodium chloride solutions showed that the expansion factor, α, was related to the intrinsic viscosity as $\frac{[\eta]}{[\eta]_o} = \alpha^2$ where $[\eta]_o$ was the value obtained by extrapolation to infinite ionic strength.

Schneider and Doty[188] studied sodium carboxymethylcellulose by light scattering and viscosity methods in various salt solutions and showed from the light scattering that

$$\alpha^2 = \frac{Rg^2}{Rg_o^2}$$

where Rg_o was the radius of gyration at infinite ionic strength.

The expansion factor , α , was calculated for the various fractions of sodium ghattate from the viscosity and light scattering results by the methods described above.

TABLE 5.

EXPANSION FACTOR, α, AT VARIOUS SALT CONCENTRATIONS

Normality, NaCl.	2.0	2.5	0.05	0.005	0.0017
Fraction 1 (Viscosity)	1.01	1.04	1.18	1.46	1.69
1 (Light-scattering)		1.04	1.17		
2 (Viscosity)		1.04	1.18	1.47	
2 (Light-scattering)		1.03	1.17	1.34	

There is, in general, excellent agreement between the expansion factors calculated for each fraction from the light-scattering and the viscosity results.

Although fraction 1 has a higher charge density than fraction 2 the expansion factor is very similar for both fractions.

Schneider and Doty found α for sodium carboxymethylcellulose from their light-scattering and viscosity experiments but the values obtained by the two different methods did not agree. The value of α in 0.01 M sodium chloride from the viscosity results was 1.73 but from the light-scattering α was found to be 1.335. Schneider and Doty suggested that this discrepancy in the results was due to the fact that the frictional constant depended on the state of expansion and that the equation relating the radius of gyration, intrinsic viscosity and expansion factor implied that the frictional constant remained constant throughout the range of expansion studied.

For a rod-shaped molecule Rg^2 is proportional to L^2 and to h_{av}^2 for a coil where h_{av} is the average end-to-end distance of the coil. Therefore a comparison of results at low ionic strength

should lead to a measure of α^2 for the rod-shaped molecule. However, for a coiled-up molecule, like sodium carboxymethyl-cellulose, $[\eta]$ is proportional to α^3, so that the ratio of $\frac{[\eta]}{[\eta]_o}$ should yield α^3 for this type of molecule. (p. 32).

A recalculation of Schneider and Doty's results showed that $\sqrt[3]{\frac{[\eta]}{[\eta]_o}}$ gave a value of α in fair agreement with that obtained from their light-scattering data.

However, for rod-like particles, Simha's relationship between the shape factor v and the axial ratio a/b can be generalised in the range of axial ratios of interest here to[229]

$$v = \text{CONSTANT.} \left(\frac{a}{b}\right)^{1.8}$$

where a is the major and b the minor semi-axis.

Since $[\eta]$ is directly proportional to v, it was expected that $\alpha^{1.8}$ would be obtained from the $\frac{[\eta]}{[\eta]_o}$ ratio, if the molecule were rod-like. However, within the limits of experimental error, α^2 was obtained.

This discrepancy between the indices can be explained if $\alpha^{1.8}$ is considered to be the lower limit for a rod-like molecule. It would be expected that during a molecular expansion process the length, L, would increase but that the diameter would, correspondingly, decrease. It was assumed, however, in the above discussion that when L increased, d, the diameter, remained constant. The expansion, therefore, should lead to a higher value than $\alpha^{1.8}$. In fact α^2 was obtained and this agreed with the light-scattering data.

It would be stretching the results too far to attempt a calculation of the degree of thining of the molecule. This, of course, may not be the only factor affecting such a ratio. It may be that the charged groups present on the side chains cause the side chains to swing out during ionisation.

It was shown by the light-scattering results that the sodium ghattate molecules were rod-shaped both in sodium chloride solutions and in water. There was a considerable increase in the length of the sodium ghattate molecules from infinite ionic strength to water. The length of the molecules in fraction 2 at infinite ionic strength was 2580 Å and in water 3680 Å. It would appear from this that a certain amount of flexibility is present in the structure of the sodium ghattate molecules.

It is possible that this rod-like molecular shape is maintained when the molecule is fully extended by electrical forces and that the unionised side chains aid this electrical effect by causing a stiffening of the galactose framework.

As was shown by Veis and Eggenberger the contraction of the gum arabic molecules is hindered by the size of the monosaccharide units in the molecules. Carrageenin was suggested to have an extended branched structure which was flexible in its major axis.

It seems obvious that the hindering effect of the monosaccharide units on contraction will be the same for ghatti gum molecules as it is for gum arabic.

However the ghatti gum molecules also have a branched structure similar to that suggested for carrageenin. Thus, while a rod-shaped molecule fits the experimental facts, at high salt concentration the main framework of the macromolecules must be highly kinked. Possibly under these conditions the side chains bunch together and help to stiffen the molecule.

On decreased salt concentration the molecule expands and the increase of electrostatic interactions will stiffen the structure of the molecule and so the rod model for the macromolecules will apply.

Second Virial Coefficient

The value of the second virial coefficient, B, was obtained at infinite ionic strength by graphing the values of the second virial coefficients obtained at the various salt concentrations against $1/_{N}{}^{0.73}$ where N = normality of the sodium chloride. This gave a convenient straight line plot.

At infinite ionic strength the counterions should be held close to the main part of the molecule and the charge, Z, does not contribute to intermolecular interactions. Under these conditions the second virial coefficient is a function of molecular shape and size only.

The equation for the excluded volume of rod-like particles has been determined by Zimm[230] and from this the equation of the second virial coefficient was found[231] to be

$$B = \frac{L\bar{V}_2}{dM} = \frac{LV}{dM^2} \qquad \text{.....(72)}$$

where V is the molecular volume. The lengths of the macromolecules as determined by the light-scattering experiments were used in the calculations.

TABLE 6

CALCULATED AND OBSERVED SECOND VIRIAL COEFFICIENTS

Normality	Fraction 1			Fraction 2		
	$10^5 B$			$10^5 B$		
	(i)	(ii)	(iii)	(1)	(ii)	(iii)
Infinite	3	2*		3	2*	
0.5N NaCl	4		15	4		16
0.05N NaCl	10		154	10		163
0.005N NaCl.			1540	41		

(i) = experimental

(ii) = calculated from equation (72)

(iii) = calculated from equation (73)

* calculated for unhydrated molecules.

It can be seen that in the uncharged state the values obtained for B agree reasonably well with the values obtained for a rod-like molecule with the dimension determined by the light-scattering experiments. This is particularly true since there are large errors in the experimental determination of small values of B.

As the ionic strength decreased from infinite ionic strength the values of the second virial coefficient increased. When the ionic strength is decreased the shielding effect of the simple electrolyte in the solution of the polyelectrolyte also decreased and this would result in mutual repulsion of the macromolecules.

Donnan-like conditions should be approached where the counter-ions are distributed between the ionic atmosphere of the macro-molecules and the solution. An equation for the second virial

coefficient for such conditions is given by Tanford[232]

$$B = \frac{1000Z^2V_1^o}{4M^2M_3} \quad \ldots\ldots\ (73)$$

where M_3 is the molality of the sodium chloride and Z is the charge.

The Donnan terms were calculated for the various fractions of sodium ghattate (Table 6) and were found to be considerably larger than the observed second virial coefficients.

This was also noticed for sodium carboxymethylcellulose[188] where the Donnan term was found to be 2 or 3 times greater than the observed values of the second virial coefficients. For sodium ghattate however the Donnan term was 4 to 40 times greater.

This greater difference between the Donnan term and the observed value for sodium ghattate and for sodium carboxymethyl-:cellulose may be due to the much lower charge density of sodium ghattate than that of sodium carboxymethylcellulose. It probably indicates that a fair amount of ion-binding occurs even in dilute salt solutions.

The result of this ion binding would be to neutralise some of the macromolecular charge to the other large ions. However, as was already shown by light-scattering the molecule expands as the ionic strength decreases and so local shielding of one part of the macromolecule from another cannot be complete.

Sodium carboxymethylcellulose, which is a coiled molecule, will occupy a much larger spatial volume in solution than the

fairly compact rod-like sodium ghattate molecule, although sodium ghattate have a molecular weight about five times greater.

From this it would be expected that much smaller interferences would be expected and this is reflected in the second virial coefficient of sodium ghattate being approximately $^{1}/_{30}$ that of sodium carboxymethylcellulose.

SECTION 3.

WATER VAPOUR SORPTION.

WATER-VAPOUR SORPTION

Introduction

233-238

The adsorption of water-vapour has been studied for proteins and for Lecithin and related phosphatides[217,239]. For proteins it was suggested that there were two types of hydrophilic groups capable of binding water through hydrogen bond formation[240]. These were the polar side-chains and the oxygen and nitrogen atoms associa: :ted with the peptide linkages. For lecithin and the related phos: :phatides, lysolecithin and cephalin, it was suggested that the polar head groups of the phosphatides were principally responsible for the adsorption of the water molecules.

It is possible from the graphs of the amount of water sorbed against the vapour pressure of the system to obtain the value of the amount of water adsorbed in a monolayer and some measure of the thermodynamics of adsorption. It is also possible from the adsorption isotherms to obtain some idea of the type of adsorption which takes place.

Brunauer classified the five main types of adsorption iso: :therms. The two main ones were the Langmuir and the Brunauer, Emmett and Teller adsorption isotherms[241].

The Langmuir isotherm was characterized by a gradual increase in the amount of water adsorbed with increased water vapour pressure until a maximum was reached. At the maximum it was assumed that a monolayer of water molecules had been adsorbed and that no further adsorption took place.

The Brunauer, Emmett and Teller (B.E.T.) isotherm[241] was, at low partial pressures, essentially similar to the Langmuir adsorption isotherm, in that a monolayer was formed. However, in the B.E.T., the adsorption proceeded further than monolayer adsorption and subsequent layers of sorbate had to be considered.

In the derivation of the Langmuir adsorption isotherm the rates of adsorption and desorption of the sorbate on the sorbent are balanced and this same approach is used for the B.E.T. except that a balance between the various layers is considered. Since, in the B.E.T. isotherm, several layers are adsorbed it is possible to consider each adsorbed layer as in the Langmuir adsorption derivation.

The final equation for the B.E.T. isotherm is

$$\frac{x}{a(1-x)} = \frac{1}{C.a_1} + \frac{(C-1)\,x}{C.a_1}$$

in which $x = \frac{P}{po}$ = relative vapour pressure

C = B.E.T. constant

and a_1 = monolayer capacity.

From the graph of $\frac{P}{a(p-po)}$ where a was the amount of water adsorbed it was possible to obtain $\frac{1}{C.a_1}$ from the intercept and $\frac{C-1}{C.a_1}$ from the slope. From these two relationships the value of a_1 and C were derived.

Apparatus

The apparatus previously described for the adsorption of water-vapour by phosphatides[227,239] was modified.

Approximately 0.4 g. of the three fractions of sodium ghattate were placed in three sample tubes of known weight which fitted into wells cut into a thick brass plate. This plate rested on a glass support 3 cms. high at the bottom of a wide-mouthed glass bottle (Figure 26). A 2 cms. layer of the sulphuric acid solution was placed in the bottom of this bottle.

The bottle was connected to a three-way tap which allowed a vacuum to be applied gently to the samples.

The sulphuric acid solution and the sodium ghattate samples were outgassed at a pressure of 0.01 mm. for two hours. During this process the bottle was cooled in a carbon dioxide/acetone mixture and occasionally allowed to regain room temperature.

Adsorption experiments were started with samples which had been dried in a vacuum oven and outgassed and the desorption experiments with samples which had been outgassed and placed in contact with saturated water vapour for forty-eight hours.

The whole apparatus was placed in a thermostated water-bath. The adsorption and desorption runs were carried out on all fractions at 25° and 40° ($\pm$ 0.01°).

The change in relative vapour pressure during the adsorption and desorption runs was effected by changing the concentration of the sulphuric acid solution in the flask.

The samples were weighed three times every week until their weights were constant. The concentration of the sulphuric acid solutions was determined by titration with sodium hydroxide solution after equilibrium had been reached. The concentration of the solutions was converted to relative vapour pressure for the 25° experiments from Stokes and Robinson[242] and for the 40° experiments from International Critical Tables[243].

Results and Discussion

The adsorption and desorption isotherms of the number of grammes of water sorbed per 100 grammes of material (a) against the relative vapour pressure of the system (x) were drawn for all three fractions at 25° and 40° (Figures 27 a, b and c). No hysteresis loops were observed for any of the samples at either temperature.

It was noticed that each sample of sodium ghattate adsorbed more water at lower relative vapour pressure at 25° than at 40° but at higher vapour pressures more water was sorbed at 40° than 25°.

Good B.E.T. plots were obtained for each sample at both temperatures below a value of 0.4 for x. The B.E.T. plots were obtained by plotting $\frac{p}{a(p_o - p)}$ against x. These are shown in Figures 28 a, b and c.

From the slopes and the intercepts of the various B.E.T. graphs at the different temperatures the values of C and a_1 were calculated for each sample (Table 7). C was the B.E.T. constant and a_1 the amount of water adsorbed in the first monolayer.

The values of a_2 and a_s, the amounts of water adsorbed in the second layer and at saturation respectively, were determined for both temperatures by plotting the values of $\frac{a}{x}$ against x (Figures 29 a, b, c). The values of a_2 were determined from the minima of the curves and the values of a_s from the intercepts

on the $a/_x$ axes at x = 1.0. The values of a_2 and a_s for all fractions at both temperatures are shown in Table 7.

TABLE 7

WATER VAPOUR SORPTION

		a_1	a_2	a_s	C	a, moles/polar group
Fraction 1	25°	7.69	15.35	19.70	13.0	7.13
	40°	6.58	8.99	36.75	4.75	
Fraction 2	25°	7.66	15.44	18.75	12.32	7.80
	40°	7.35	10.08	39.30	4.39	
Fraction 3	25°	7.50	13.77	18.00	11.80	7.73
	40°	7.95	9.00	45.00	5.09	

At 25° the value of a_2 for all fractions was approximately twice the value of a_1 and the value of a_s was approximately 2½ times the value of a_1 .

The values for the number of moles of water adsorbed per polar group of sodium ghattate were calculated and are shown in Table 7.

In general there is little difference between the three fractions in the amounts of water adsorbed in the first layer, although fraction 1 has the lowest equivalent weight. By analogy with the sorption of water vapour by proteins and phos:phatides, it could be expected that the polar groups would be responsible for adsorption, and there is also the possibility of interaction with the hydroxyl groups of the sugar residues in the macromolecules. The thermodynamics of adsorption gives some aid in the differentiation of these effects.

The differential heats and entropies of adsorption were calculated from the various isotherms. In the calculation it was assumed that the value of $\Delta\bar{H}$, the differential heat of adsorption, varied linearly over the temperature range $25^{\circ} - 40^{\circ}$.

The thermodynamic quantities were calculated for each fraction from

$$\Delta\bar{H} = \bar{H}_s - \tilde{H}_1 = R\left\{ \frac{\partial \ln\left(\frac{p}{p_o}\right)}{\partial\left(\frac{1}{T}\right)} \right\}_{p, N_1, N_2}$$

and $$\Delta\bar{S} = \bar{S}_s - \tilde{S}_1 = \frac{1}{T}\left[\Delta\bar{H} - RT\ln\left(\frac{p}{p_o}\right)\right]$$

where $\bar{H}_s$ and $\bar{S}_s$ were the partial molar enthalpies and entropies of the sorbate, $\tilde{H}_1$ and $\tilde{S}_1$ were the molar enthalpies and entropies of liquid water and N_1 and N_2 were the number of moles of sorbate and sorbent respectively.

The values of $\Delta\bar{H}$ and $\Delta\bar{S}$ were plotted against a for each fraction (Figures 30, a, b, c and Figures 31 a, b, c).

It was noticed from these graphs of $\Delta\bar{H}$ against a that the adsorption of water by the various fractions was an exothermic reaction at low values of a and endothermic at higher values.

Similarly the entropies for all three fractions at lower values of a were negative but positive at higher values. This implied that, during the initial stages of water adsorption, there was a distinct ordering of the water molecules on the sodium ghattate molecules compared to their state in liquid water.

This may be a result of sorption on to the polar groups and

counterions of the macromolecules. Further sorption caused the values of $\Delta \bar{S}$ to become more positive. The sorption was probably a result of two processes , the first being sorption on the polar groups and the second sorption concerned with the hydroxyl groups.

If this second process were more akin to a mixing process than to any specific ordering of water molecules around specific sites, it would yield positive values of $\Delta \bar{S}$. The observed $\Delta \bar{S}$ values would be a resultant of both processes and presumably at higher relative vapour pressure the mixing process predominated over the sorption on to the polar groups.

At a_1 , the values of $\Delta \bar{H}$ and $\Delta \bar{S}$ were calculated and are shown in Table 8.

TABLE 8.

	$\Delta \bar{H}$	$\Delta \bar{S}$
Fraction 1	-8.7 kcals $mole^{-1}$	-22.9 cals $mole^{-1}$ $degree^{-1}$
Fraction 2	-6.8 kcals $mole^{-1}$	-18.3 cals $mole^{-1}$ $degree^{-1}$
Fraction 3	-5.4 kcals $mole^{-1}$	-16.4 cals $mole^{-1}$ $degree^{-1}$

It was noticed that the lowest point in Figures 30 and 31 occurred below monolayer coverage, which indicated that the mixing process commenced before the adsorption on to the polar groups was complete. Table 7 showed that 7-8 water molecules were sorbed

for each polar group depending on the fraction of sodium ghattate. This was more than required for the solvation of Na^+ and $-COO^-$ ions in aqueous solutions. (It can be calculated from Stokes and Robinson[242] that five water molecules are required for Na^+ and COO^- ions. This is probably an upper limit of hydration. Other estimates[245] give a total of three water molecules for COO^- and Na^+). This, again, indicated that several processes were responsible for the sorption.

As was mentioned, the sorption isotherms crossed each other as x was increased. This may have been due to polar groups, which were attached to the side chains in the macromolecule being easily available to the water vapour at low x values and controlling the sorption.

If, at higher temperatures, the molecular structure were more expanded, this would allow more interaction between the water vapour and the hydroxyl groups and would provide greater sorption at higher temperatures if the sorption of water on to the hydroxyl groups were the controlling factor.

In previous work[227,244] water vapour sorption studies have been used to obtain an idea of particle hydration. This method consisted of extrapolating the graph of $\frac{a}{x}$ against x to $x = 1.0$ and using the values of a_g obtained by this procedure as a measure of hydration.

This method is an empirical one but in the systems so far studied, good agreement between the hydration determined from the

sorption isotherms and from intrinsic viscosities (of spherical particles) has been obtained.

The results obtained at 25° for the fractions of sodium ghattate were tentatively used in Section 2 as a rough measure of the hydration of the macromolecules. Any change in s_s between 25° and 20°, the temperature of the viscosity experiments, was ignored.

SECTION 4.

SURFACE TENSION.

SURFACE TENSION

Introduction

The surface tensions of sodium ghattate solutions in various concentrations of sodium chloride and in water were studied by the sessile drop method. This technique has been used for gum arabic[96, 97] and has certain advantages over the other forms of surface tension apparatus.

The main advantage of the sessile drop method was that each measurement could be made without disturbing the surface of the solution. The solution was thus able to age without any mechanical interference at the surface.

It was stated by Shotton that the sessile drop method was particularly suited for measuring the surface tension of solutions of large molecules where a comparatively long time was required for the interface to reach equilibrium.

Originally the Wilhelmy plate was used for the measurement of the surface tension of the solutions but the results obtained by this method were uncertain and unreliable. It was felt that the repeated stress of the plate on the surface layer caused anomalous results and hindered the natural formation of the surface. There was also the possibility that the solute was adsorbed on the platinum plate and affected the contact angle.

The other advantages of measuring the surface tension by some static means like the sessile drop were outlined by Andreas and others[246].

The sessile drop method was sufficiently simple for a complete mathematical analysis and the results obtained were independent of the angle of contact. The results were not complicated by any viscosity effects and it was possible, even with small quantities of material, to measure a wide range of surface or interfacial tensions.

Theory of Surface Tension

There is a relationship between the surface tension of a liquid and the pressure difference across the curved interface of that liquid. The pressure on the concave side of the liquid surface is greater than that on the convex side by an amount which directly depends on the surface tension of the liquid and the curvature of the surface.

The displacement of a curved surface gives an increase in area of that surface as it moves towards the convex side. The work required by the system to effect this displacement and subsequent increase in area is supplied by the pressure difference moving the surface.

In Diag. 32a a rectangle of curved surface ABCD displaced a distance Sn towards its convex side to A'B'C'D' . The normals from A and B meet at O_1 thus giving the radius of curvature of AB at R_1 and the normals from B and C meet at O_2 giving the radius of curvature of BC at R_2.

The area of the surface after displacement is

$$\left(AB + \frac{AB}{R_1}.\ Sn\right)\left(BC + \frac{BC}{R_2}.\ Sn\right)$$

$$= ABCD\left(1 + \frac{Sn}{R_1} + \frac{Sn}{R_2}\right)$$

The work done in this expansion from ABCD to A'B'C'D' against the free energy on the surface tension is

$$\gamma\ ABCD.Sn\left(\frac{1}{R_1} + \frac{1}{R_2}\right)$$

If the pressure on the concave side is p_1 and on the convex side p_2 then the work done by the pressure difference

$$(p_1 - p_2).\delta n.ABCD$$

These two relationships must be equal since the surface is at equilibrium at the position A'B'C'D'

$$P_1 - P_2 = \gamma.\left(\frac{1}{R_1} + \frac{1}{R_2}\right) \quad \ldots\ldots\ldots (74)$$

This is the Young and Laplace equation.

If the two radii of curvature are equal then

$$P_1 - P_2 = \frac{2\gamma}{R}$$

Equation 74 can be modified by considering the densities of the liquid and the medium. If D_1 is the density of the liquid and D_2 the density of the medium and $p_1 - p_2 = c$ then

equation 1 becomes (Figure 32b)

$$c + gz(D_1 - D_2) = \gamma\left(\frac{1}{R_1} + \frac{1}{R_2}\right) \quad \ldots\ldots\ldots (75)$$

If the sessile drop is considered (Figure 33a) then if PC is the radius of curvature of the drop and the radius of curvature perpendicular to the diagram is p then equation (75) can be modified to give

$$\gamma\left(\frac{1}{\rho} + \frac{\sin.\phi}{x}\right) = \frac{2\gamma}{b} + gz\,(D_1 - D_2) \quad \ldots(76)$$

where b is the radius of curvature at O and $C = \frac{2\gamma}{b}$.

From equation 76 it can be shown that if

$$\beta = \frac{gb^2}{\gamma}(D_1 - D_2) = \frac{zb^2}{a^2}$$

where the capillary constant $a^2 = \frac{2\gamma}{g(D_1 - D_2)}$

then $$\frac{1}{x/b} + \frac{\sin\phi}{x/b} = 2 + \beta \cdot \frac{z}{b}$$

Bashforth and Adams' tables give the values of x/b, z/b and v/b^3 where v is the volume included between the horizontal plane at a height z and the apex of the drop.

It is possible to describe the radius of curvature of a drop in terms of a rectangular co-ordinated system. In Figure 33b if R_1 is the radius of curvature in the plane of the diagram and R_2 perpendicular to the diagram then it can be shown that

$$\frac{1}{R_1} = \frac{d^2y/dx^2}{\left[1 + (dy/dx)^2\right]^{3/2}}$$

It can also be shown that

$$\frac{y^2}{a^2} - \frac{h^2}{a^2} = \frac{-1}{\left[1 + \left(\frac{dy}{dx}\right)^2\right]^{\frac{1}{2}}}$$

Porter[247] used Bashforth and Adams' tables to give

$$\frac{h^2}{2r^2} - \frac{a^2}{2r^2} = 0.3047\,\frac{h^3}{r^3}\left(1 - \frac{4h^2}{r^2}\right)$$

This gives a means of finding 'a' from the measurement of h and r of the drop.

Wheeler[248] showed that the readings for h either by the photographic method or by using a comparator gave incorrect values

and showed that more accurate results could be obtained by using

$$\frac{a^2}{2r^2} = 0.4353 \frac{h^2}{r^2} - 0.223 \frac{h^4}{r^4} + 1.675 \frac{h^6}{r^6}$$

$$\text{for } 0.065 < \frac{h^2}{r^2} < 0.300$$

and $$\frac{a^2}{2r^2} = 0.4543 \frac{h^2}{r^2} - 0.860 \frac{h^4}{r^4}$$

$$\text{for } 0 < \frac{h^2}{r^2} < 0.065$$

Description of Apparatus

Ferguson[249] and Worthington[250] studied the surface tension of liquids by the pendant drop method. However, according to Andreas and others[246] the calculations used by them were tedious and rather imprecise and the photographic apparatus not satisfactory.

Andreas and others[246] however studied the surface tension of liquids by the pendant drop method. The apparatus used simply consisted of a thermostated tank containing the drop which was illuminated by a mercury arc lamp. The image eventually was photographed.

This type of apparatus has been used often for the determination of surface tension by the sessile bubble, [248,251], pendant drop [252-254] and the sessile drop method[96,97].

The apparatus used is shown in Figure 34. The sessile drop was surrounded by a thermostated water-jacket which controlled the temperature in the box to $\pm$ 0.1°C. The drop itself was placed on a piece of glass which had been previously coated with a thin layer of hard paraffin to make the surface hydrophobic. The glass was dipped quickly into an ethereal solution of hard paraffin and when this coating had dried it was soaked in distilled water for two hours to remove any water-soluble impurities.

The drop was illuminated by a sodium vapour lamp (Mazda 80/H, 250 volt). The light passed through a condensing lens and the area of illumination was limited by an aperture in front of the cell.

The illuminated drop was viewed through the cathetometer through two neutral density filters (Kodak colour compensating filters). The cathetometer allowed measurements of the height and width of the

drop to be taken at any time and calculations of the surface tension to be carried out quickly and easily.

The measurements on the cathetometer were taken in the vertical plane from the readings on the Vernier scale. However, the horizontal readings were taken by comparison with an ebonite rod hanging directly above the centre of the drop in the cell. The width of this rod was known accurately and the width of the drop could be accurately computed from a scale placed inside the optical system of the cathetometer.

The drop was viewed through the body of a half-plate camera. The cathetometer could be removed, the lens system replaced in the camera and photographs of the drop taken. The size of the drop on the photographic plates was measured on a Cambridge Universal Measuring machine which was graduated down to 0.001 cm. Estimation of 0.0002 cm. could be made with reasonable accuracy (Plate 3).

To prevent any evaporation from the surface of the drop during the time taken for ageing, two small tubes filled with water were placed inside the cell to saturate the atmosphere.

The apparatus was tested by measuring the surface tension of water. The readings for this at 20°C and 25°C were found to be 72.9 dynes/cm. (72.75 dynes/cm.) and 72.0 dynes/cm. (71.97 dynes/cm.) respectively. The correct results[255] are given in parenthesis.

Results and Discussion

The surface tension of the second fraction of ghatti gum was studied in water and in 0.5N and 0.05N sodium chloride solutions.

Approximately 0.9 ml. of the solution was placed on the glass plate for the determination of surface tension. The surface tension was calculated regularly from the cathetometer readings and the system was left until there was no further change of surface tension with time.

It was found (Figure 35) that generally between 24 and 36 hours were required for equilibrium. It was possible that this delay was due to the slow diffusion of the solute to the surface layer and to the fact that considerable orientation of the macromolecules was necessary in the surface layer. In salt solutions equilibrium was generally reached sooner than for aqueous solutions. This was possibly due to the fact that in salt solutions the molecules were contracted and could possibly diffuse and orientate quicker.

It will be seen from the graphs of surface tension with concentration (Figure 36) that the surface tension decreased sharply with increased concentration until a stable value was obtained.

The effect of sodium chloride was to reduce the surface tension at any particular concentration. The surface tension of a 2.5% solution fell from 50.6 dynes/cm. in aqueous solution to 43.0 dynes/cm. in 0.005N and 37.2 dynes/cm. in 0.5N sodium chloride solution.

Strauss[94] has studied the surface tension of polyelectrolytes

and stated that for the coil molecule polyelectrolyte studied there was no significant surface activity. As shown here sodium ghattate is considerably surface active, while similar behaviour has been reported for sodium arabate[96,97]. The depression of the surface tension as shown in Figure 36 is quite considerable. It is significant that both ghatti gum and gum acacia have fairly stiff structures containing side chains on which the ionized groups are believed to be present. It may be that the surface activity is due to the stiffened type of structure.

Adsorption of a detergent at an air/water interface gives a film structure in which the hydrocarbon chain is repelled by the water and the hydrophilic groups are present in the water. An explanation of the surface activity of sodium ghattate may lie in the fact that the molecule could arrange itself in two regions. The flexible side chains containing the polar groups would remain largely in the water and the main part of the molecule in the air.

This type of arrangement is difficult to visualise for the coiled type of molecule as solvent can permeate through it and as the energy required to straighten the molecule and to orientate it in the surface would be considerable.

Such an orientation process of sodium ghattate may involve denaturation of the molecule; if the polar side-chains are held in the water surface while other parts are forced above it, irreversible changes may occur in the molecular structure. The behaviour of potassium arabate at benzene/water or oil/water

interface seems to agree with this hypothesis. At such inter: :faces it appears that denatured films form. It was shown that under such conditions potassium arabate solutions formed a solid film which exhibited certain mechanical properties. The evidence for the presence of such a film between sodium ghattate solutions and benzene was demonstrated. A drop of sodium ghattate solution was placed in contact with benzene and it was seen that a coherent film was formed which could be manipulated.

The addition of salt had a very striking effect in consider: :ably enhancing the surface activity. It has been shown that an increase in the ionic strength causes the molecules to contract. This contraction of the molecules may cause a more closely packed film to be formed at the surface. Under these conditions the polar groups may be screened from each other thus allowing closer packing within each molecule. The surface tension decreased sharply with increased sodium ghattate concentration and then became roughly constant indicating that few more molecules were adsorbed in the surface layer above concentrations of 1.0 - 1.5%.

It was felt that it would be impossible to apply the Gibb's equation to the results at the present time, as a suitable form for multivalent electrolytes has not been developed.

In any application of the Gibb's isotherm there would be doubts as to the reversibility of the adsorption and to the validity of applying activity coefficients.

REFERENCES

1. CHOPRA, "Indigenous Drugs of India", U.N. Dhur & Sons Private Ltd., Calcutta, 1958.
2. HOOPER, "Edible Gums; Rept. Labor. Ind. Mus.", 1904-5, 23.
3. WATT, "The Commercial Products of India", John Murray, London, 1908, 70.
4. PREBLE, Pharm. J., 1888, 19, 1.
5. MANDER, Pharm. J., 1888, 19, 876.
6. RIDEAL & YOULE, Year Book of Pharmacy, 1891, 405.
7. MANDER, Pharm. J., 1891, 22, 224.
8. RIDEAL & YOULE, J. Soc. Chem. Ind., 1891, 10, 610.
9. RIDEAL, J. Soc. Chem. Ind., 1892, 11, 403.
10. RIDEAL, Pharm. J., 1892, 23, 1073.
11. Bull. Imp. Inst., 1908, 6, 29.
12. BIRDWOOD, "Bombay Products", 1845, 265.
13. HENRY, Pharm. J., 1890, 20, 781.
14. BRITISH PHARMACOPOEIA, 1898; Eastern & Colonial Addendum, 1900, General Medical Council, London, 1900.
15. BRITISH PHARMACOPOEIA, 1914, General Medical Council, London, 1914, 169.
16. SQUIRE'S COMPANION TO THE BRITISH PHARMACOPOEIA, 8th Ed., J.A. Churchill, London, 1908, 588.
17. BRITISH PHARMACEUTICAL CODEX, 1907; The Pharmaceutical Press, London, 1907.
18. WHISTLER, "Industrial Gums", Academic Press, New York & London, 1959.
19. BLUNT, "Gum Arabic, with Special Reference to its Production in the Sudan", Oxford University Press, London, 1926.
20. WALLIS, "Textbook of Pharmacognosy", J. & A. Churchill, London, 1955.
21. THAYSEN & BUNKER, "The Microbiology of Cellulose, Hemi-cellulose, Pectin & Gums", Oxford University Press, London, 1927.
22. JONES & SMITH, "Advances in Carbohydrate Chemistry", 1949, 4, 243.
23. HANNA, McREYNOLDS & SHAW, Jr., Proc. S. Dak. Acad. Sci., 1939, 19, 130.
24. HANNA & SHAW, Jr., Proc. S. Dak. Acad. Sci., 1941, 21, 78.
25. ASPINALL, HIRST & WICKSTRØM, J. Chem. Soc., 1955, 1160.
26. HIRST & JONES, J. Chem. Soc., 1938, 1174.
27. JONES, J. Chem. Soc., 1939, 558.

28. JONES, J. Chem. Soc., 1949, 3141.
29. HOTCHKISS & GORSEL, J. Biol. Chem., 1937, 121, 195.
30. SMITH, J. Chem. Soc., 1940, 1035.
31. CARHART & SHAW Jr., Proc. S. Dak. Acad. Sci., 1935, 15, 46.
32. CARHART & SHAW Jr., Proc. S. Dak. Acad. Sci., 1936, 16, 34.
33. SHAW Jr., Proc. S. Dak. Acad. Sci., 1937, 17, 27.
34. FOLIN, J. Biol. Chem., 1929, 81, 231.
35. YOUNGBURG & YOUNGBURG Jr., J. Lab. Clin. Med., 1930, 16, 158.
36. KOCH & McMEEKIN, J. Amer. Chem. Soc., 1924, 46, 2066.
37. LEWIS & SMITH, J. Amer. Chem. Soc., 1957, 79, 3929.
38. KULSHRESTHA, J. Polymer Sci., 1962, 58, 791.
39. GRAY, Bull. Agr. Mech. Coll. Texas; Texas Eng. Expt. Sta. Bull., 1946, 96, 63.
40. TCHILLINGARIAN & BEESON, Petrol. Eng., 1952, 24, B.45.
41. DAVIDSON & RIGBY, U.S. Patent 2,680,068.
42. FUOSS, Science, 1948, 108, 545.
43. KIMBALL, CUTLER & SAMELSON, J. Phys. Chem., 1952, 56, 57.
44 FLORY, J. Chem. Phys.,1952,20, 192.
45. KUHN, KUNZLE & KATCHALSKY, Helv. Chim. Acta, 1948, 31, 1994.
46. KATCHALSKY, KUNZLE & KUHN, J. Polymer Sci., 1952, 5, 283.
47. HARRIS & RICE, J. Phys. Chem., 1954, 58, 725.
48. HARRIS & RICE, J. Phys. Chem., 1954, 58, 733.
49. HERMANS & OVERBEEK, Rec. Trav. Chim., 1948, 67, 761.
50. KUNZLE, Rec. Trav. Chim., 1949, 68, 699.
51. ARNOLD & OVERBEEK, Rec. Trav. Chim., 1950, 69, 192.
52. FUOSS & STRAUSS, J. Polymer Sci., 1948, 3, 246.
53. FUOSS & STRAUSS, J. Polymer Sci., 1948, 3, 602.
54. FUOSS, J. Polymer Sci., 1948, 3, 603.
55. FUOSS & CATHERS, J. Polymer Sci., 1949, 4, 97.
56. PALS & HERMANS, J. Polymer Sci., 1948, 3, 897.
57. MACLAY & FUOSS, J. Polymer Sci., 1951, 6, 511.
58. PALS & HERMANS, J. Polymer Sci., 1950, 5, 733.
59. STRAUSS, GERSHFIELD & CROOK, J. Phys. Chem., 1956, 60, 577.
60, CONWAY, J. Polymer Sci., 1955, 18, 257.

61. SCHURZ, Makromol. Chem., 1953, 10, 194.
62. FLORY & OSPENHELD, J. Phys. Chem., 1954, 58, 653.
63. TERAYAMA & WALL, J. Polymer Sci., 1955, 16, 357.
64. JORDAN, MATHIESON & PORTER, J. Polymer Sci., 1956, 21, 463, 473, 483, 495.
65. CONTOIS, J. Polymer Sci., 1955, 18, 479.
66. BUTLER, ROBINS & SHOOTER, Proc. Roy. Soc., 1957, A241, 299.
67. TERAYAMA, J. Polymer Sci., 1956, 19, 181.
68. MATHIESON & McLAREN, J. Chem. Soc., 1960, 3581.
69. EISENBERG & POUYET, J. Polymer Sci., 1954, 13, 85.
70. ROSEN, KAMATH & EIRICH, Discuss. Faraday Soc., 1951, 11, 135.
71. DOTY & STEINER, J. Chem. Phys., 1952, 20, 85.
72. HUIZENGA, GRIEGER & WALL, J. Amer. Chem. Soc., 1950, 72, 2636.
73. HUIZENGA, GRIEGER & WALL, J. Amer. Chem. Soc., 1950, 72, 4228.
74. WALL & DOREMUS, J. Amer. Chem. Soc., 1954, 76, 868.
75. WALL & DOREMUS, J. Amer. Chem. Soc., 1954, 76, 1557.
76. EINSTEIN, Ann. Physik., 1906, 19, 289.
77. EINSTEIN, Ann. Physik., 1911, 34, 591.
78. ONSAGER, Phys. Rev., 1932, 40, 1028.
79. SIMHA, J. Phys. Chem., 1940, 44, 25.
80. MEHL, ONCLEY & SIMHA, Science, 1940, 92, 132.
81. EISENBERG, J. Polymer Sci., 1958, 30, 47.
82. LONGWORTH & HERMANS, J. Polymer Sci., 1957, 26, 47.
83. HERMANS, J. Polymer Sci., 1955, 18, 527.
84. EIGEN & SCHWARZ, J. Colloid Sci., 1957, 12, 181.
85. FUOSS, J. Polymer Sci., 1954, 12, 185.
86. FITZGERALD & FUOSS, J. Polymer Sci., 1954, 14, 329.
87. EDELSON & FUOSS, J. Amer. Chem. Soc., 1950, 72, 306.
88. BRIGGS, J. Phys. Chem., 1934, 38, 867.
89. KULSHRESTHA, J. Polymer Sci., 1962, 58, 809.
90. WALL, STENT & ONDREJCIN, J. Phys, Colloid Chem., 1950, 54, 979.
91. ALLGÉN & ROSWALL, J. Polymer Sci., 1957, 23, 635.
92. NAGASAWA, SODA & KAGAWA, J. Polymer Sci., 1958, 31, 439.

93. MARJUS & HERMANS, J. Colloid Sci., 1959, 14, 252.
94. JORGENSEN & STRAUSS, J. Phys. Chem., 1961, 65, 1873.
95. RAMERJI, J. Indian Chem. Soc., 1952, 29, 270.
96. SHOTTON, J. Pharm. Pharmacol., 1955, 7, 990.
97. SHOTTON & WIKBERLEY, J. Pharm. Pharmacol., 1959, 11, 120T.
98. SHOTTON & WIKBERLEY, J. Pharm. Pharmacol., 1960, 12, 105T.
99. OTH & DOTY, J. Phys. Chem., 1952, 56, 43.
100. WALL, DRENAN, HATFIELD & PAINTER, J. Chem. Phys., 1951, 19, 585.
101. CASSIN, J. Colloid Sci., 1951, 6, 271.
102. FUOSS & EDELSON, J. Polymer Sci., 1951, 6, 145.
103. DOTY & STEINER, J. Chem. Phys., 1949, 17, 743.
104. MUKHERJEE & DEB, J. Indian Chem. Soc., 1962, 39, 823.
105. VEIS & ANGEMBERGER, J. Amer. Chem. Soc., 1954, 76, 1560.
106. VRIJ & OVERBEEK, J. Colloid Sci., 1962, 17, 570.
107. HEIDELBERGER, ADAMS & DISCHE, J. Amer. Chem. Soc., 1956, 78, 2853.
108. ANDERSON & HEHRICH, J. Chem. Soc., 1963, 1.
109. O'SULLIVAN, J. Chem. Soc., 1884, 45, 41.
110. BUTLER & CRETCHER, J. Amer. Chem. Soc., 1929, 51, 1519.
111. HIRST & PERLIN, J. Chem. Soc., 1954, 2622.
112. HOKMAN, Biochem. J., 1929, 23, 524.
113. HIRST, J. Chem. Soc., 1942, 70.
114. ASPINALL, CHARLSTON, HIRST & YOUNG, J. Chem. Soc., 1963, 1696.
115. HEIDELBERGER & KENDALL, J. Biol. Chem., 1929, 84, 639.
116. CHALLINOR, HAWORTH, & HIRST, J. Chem. Soc., 1931, 258.
117. HIRST & JONES, Research, 1951, 4, 411.
118. PERCIVAL, "Structural Carbohydrate Chemistry", Muller, London, 1950.
119. SMITH & MONTGOMERY, "The Chemistry of Plant Gums & Mucilages", Rheinhold, New York, 1959.
120. OAKLEY, Trans. Faraday Soc., 1937, 33, 372.
121. BASU, DASGUPTA & SIRCAR, J. Colloid Sci., 1951, 6, 539.
122. TIEBACKX, Pharm. Weekblad., 1922, 59, 574.
123. THOMAS & MURRAY, J. Phys. Chem., 1928, 32, 676.
124. MOORJANI & NARWANI, J. Indian Chem. Soc., 1948, 25, 503.

125. MUKHERJEE & GHOSH, J. Indian Chem. Soc., 1949, 26, 277.
126. SÄVEHBORN, "The Svedburg Memorial Volume", 1944, 508.
127. OAKLEY, Trans. Faraday Soc., 1935, 31, 136.
128. OAKLEY, Trans. Faraday Soc., 1936, 32, 1360.
129. VAN BEEK, J. Polymer Sci., 1958, 33, 463.
130. SCHLEIF, HIGUCHI & BUSSE, J. Amer. Chem. Soc., 1951, 40, 221.
131. VEIS, J. Phys. Chem., 1953, 57, 189.
132. MUKHERJEE & BHOWMIK, J. Indian Chem. Soc., 1949, 26, 151.
133. MUKHERJEE & BHOWMIK, J. Indian Chem. Soc., 1949, 26, 313.
134. GHOSH & GYANI, J. Indian Chem. Soc., 1951, 30, 349.
135. TENDELOO, Rec. Trav. Chim., 1929, 48, 23.
136. CLARK & MANN, J. Biol. Chem., 1922, 52, 157.
137. BRIGGS, J. Phys. Chem., 1934, 38, 1145.
138. BRIGGS, J. Phys. Chem., 1948, 52, 76.
139. BANERJI, J. Indian Chem. Soc., 1952, 29, 270.
140. MATTHEWS, Trans. Faraday Soc., 1939, 35, 1113.
141. SHOTTON, Pharm. Weekblad., 1962, 97, 629.
142. SHOTTON & WHITE, J. Pharm. Pharmacol., 1960, 12, 108T.
143. WIRSEHLEY, J. Pharm. Pharmacol., 1960, 14, 87T.
144. O'SULLIVAN, J. Chem. Soc., 1901, 79, 1164.
145. JAMES & SMITH, J. Chem. Soc., 1945, 739.
146. JAMES & SMITH, J. Chem. Soc., 1945, 749.
147. ROWSON, Quart. J. Pharm., 1937, 10, 161.
148. BASU & SIRCAR, J. Colloid Sci., 1953, 10, 263.
149. ASPINALL & BAILLIE, J. Chem. Soc., 1963, 1702.
150. ASPINALL & BAILLIE, J. Chem. Soc., 1963, 1714.
151. GRALEN & KARRHOLM, J. Colloid Sci., 1950, 5, 21.
152. TSENG, Science, 1945, 101, 597.
153. DEWAR & PERCIVAL, J. Chem. Soc., 1947, 1622.
154. BUCHANAN, PERCIVAL & PERCIVAL, J. Chem. Soc., 1943, 51.
155. RUSSEL-WELLS, Biochem. J., 1922, 16, 578.
156. O'NEILL, J. Amer. Chem. Soc., 1955, 77, 2837.
157. O'NEILL, J. Amer. Chem. Soc., 1955, 77, 6324.

158. YOUNG & RICE, J. Biol. Chem., 1946, 164, 35.

159. JOHNSTON & PERCIVAL, J. Chem. Soc., 1950, 1994.

160. HAAS, Biochem. J., 1921, 15, 469.

161. HAAS & RUSSELL-WELLS, Biochem. J., 1929, 23, 425.

162. COOK, ROSE & COLVIN, Biochim. Biophys. Acta, 1952, 8, 595.

163. SMITH & COOK, Arch. Biochem. Biophys., 1953, 45, 232.

164. SMITH, COOK, & NEAL, Arch. Biochem. Biophys., 1954, 53, 192.

165. SMITH, O'NEILL & PERLIN, Canad. J. Chem., 1955, 33, 1352.

166. MASSON & GORING, Canad. J. Chem., 1955, 33, 895.

167. MASSON & CAINES, Canad. J. Chem., 1954, 32, 51.

168. COOK, ROSE & COLVIN, Biochim. Biophys. Acta, 1951, 7, 601.

169. GORING & GORDON, Canad. J. Chem., 1955, 33, 480.

170. GORING, Canad. J. Chem., 1953, 31, 1078.

171. GORING & CHEPESWICK, J. Colloid Sci., 1955, 10, 440.

172. SITARAMAIAH & GORING, J. Polymer Sci., 1962, 58, 1107.

173. WHISTLER & CORBETT in "The Carbohydrates", Editor. Pigman, Academic Press Inc., New York, 1957.

174. WHISTLER, "Methods in Carbohydrate Chemistry" Volume III, Academic Press Inc., New York, 1963.

175. BASU & DASGUPTA, J. Colloid Sci., 1952, 7, 53.

176. FUJITA & HOMMA, J. Colloid Sci., 1954, 9, 591.

177. EISENBERG, J. Polymer Sci., 1957, 23, 579.

178. AKKERMAN, PALS & HERMANS, Rec. Trav. Chim., 1952, 71, 56.

179. PALS & HERMANS, Rec. Trav. Chim., 1952, 71, 433.

180. INAGAKI, J. Colloid Sci., 1956, 11, 226.

181. FUJITA & HOMMA, J. Polymer Sci., 1955, 15, 277.

182. INDUE, J. Chem. Soc. Japan, 1956, 77, 441.

183. INAGAKI, SAKURAI & SASAKI, Bull. Inst. Chem. Res. Kyoto Univ., 1956, 34, 74; Chem. Abs., 1957, 51, 4798.

184. PALS & HERMANS, Rec. Trav. Chim., 1952, 71, 458.

185. PALS & HERMANS, Rec. Trav. Chim., 1952, 71, 513.

186. TRAP & HERMANS, J. Phys. Chem., 1954, 58, 757.

187. REZANOWICH & GORING, J. Colloid Sci., 1960, 15, 452.

188. SCHNEIDER & DOTY, J. Phys. Chem., 1954, 58, 762.

189. HUQUE, GORING & MASON, Canad. J. Chem., 1958, 36, 952.

190. GORING, SEMEZ, MELANSEN & HUQUE, J. Colloid Sci., 1957, 12, 12.

191. GORING & TIMELL, J. Phys. Chem., 1960, 64, 1426.

192. GORING & JOHNSON, J. Chem. Soc., 1952, 33.

193. BECKER, Amer. Prof. Pharm., 1954, 20, 939, 987.

194. RAYLEIGH, Phil. Mag., 1871, 41, 447.

195. RICHTER, Uber Die Neuern Gegenstande Der Chemie, 1802, 11, 81.

196. TYNDALL, Phil. Mag., 1869, 37, 384.

197. SCHMOLUCHOWSKI, Bull. Int. Acad. Sci. Cracovie, 1907, 1057.

198. EINSTEIN, Ann. Physik, 1910, 33, 1275.

199. DEBYE, J. Appl. Phys., 1944, 15, 338.

200. MOELWYN-HUGHES, "Physical Chemistry", Pergamon Press, London, 1961, 389.

201. TANFORD, "Physical Chemistry of Macromolecules", John Wiley & Sons Inc., New York, 1961, 308.

202. CABANNES, "La Diffusion Moléculaire De La Lumière", Presses Universitaires de France, Paris, 1929.

203. GEIDUSCHEK, J. Polymer Sci., 1954, 13, 408.

204. ZIMM, J. Chem. Phys., 1948, 16, 1093.

205. ZIMM, J. Chem. Phys., 1948, 16, 1099.

206. NEUGEBAUER, Ann. Physik., 1943, 42, 509.

207. ZIMM, STEIN & DOTY, Polymer Bull., 1945, 1, 90.

208. GOLDSTEIN, J. Chem. Phys., 1953, 21, 255.

209. HOLTZER, J. Polymer Sci., 1955, 17, 432.

210. DEBYE, J. Phys. & Colloid Chem., 1947, 51, 18.

211. HOLTZER, BENOIT & DOTY, J. Phys. Chem., 1954, 58, 635.

212. HOLTZER, BENOIT & DOTY, J. Phys. Chem., 1954, 59, 624.

213. BENOIT, J. Polymer Sci., 1953, 11, 507.

214. PETERLIN, Makromol. Chem., 1952, 9, 244.

215. PETERLIN, J. Polymer Sci., 1953, 10, 425.

216. OTTEWILL & PARREIRA, J. Phys. Chem., 1958, 62, 912.

217. ROBINSON, Ph.D. Thesis, London, 1959.

218. ELWORTHY & McINTOSH, J. Pharm. Pharmacol., 1960, 12, 260T.

219. McINTOSH, Ph.D. Thesis Submission, Glasgow, 1963.

220. MACFARLANE, Ph.D. Thesis Submission, Glasgow, 1963.

221. STRAUSS & ANDER, J. Amer. Chem. Soc., 1958, 80, 6494.

222. BAUER, FAJANS & LEWIN, in WEISSBURGER "Physical Methods of Organic Chemistry, 3rd Ed., Vol. 1, Part 2, 1960, 1139.

223. OGSTON & STANIER, Biochem. J., 1953, 53, 4.

224. ROBINSON & SAUNDERS, J. Pharm. Pharmacol., 1959, 11, 115T.

225. ELWORTHY & MACFARLANE, J. Chem. Soc., 1962, 537.

226. REICHMANN, Canad. J. Chem., 1959, 37, 489.

227. ELWORTHY, J. Chem. Soc., 1961, 5385.

228. Ref. 201, p. 342.

229. Ref. 201, p.336.

230. ZIMM, J. Chem. Phys., 1946, 14, 64.

231. Ref. 201, p.196.

232. Ref. 201, p.229.

233. ALTMAN & BENSON, J. Phys. Chem., 1960, 64, 851.

234. MELLON, HORN & HOOVER, J. Amer. Chem. Soc., 1947, 69, 827.

235. MELLON, HORN & HOOVER, J. Amer. Chem. Soc., 1948, 70, 1144, 3040.

236. MELLON, HORN & HOOVER, J. Amer. Chem. Soc., 1949, 71, 2761.

237. DOLE & McLAREN, J. Amer. Chem. Soc., 1947, 69, 651.

238. BULL, J. Amer. Chem. Soc., 1944, 66, 1499.

239. ELWORTHY, J. Chem. Soc., 1962, 4897.

240. SPONSLER, BATH & ELLIS, J. Phys. Chem., 1940, 44, 996.

241. BRUNAUER, EMMETT & TELLER, J. Amer. Chem. Soc., 1938, 60, 309.

242. STOKES & ROBINSON, "Electrolyte Solutions", Butterworth's Scientific Publications, London, 1959, 457.

243. INTERNATIONAL CRITICAL TABLES, 3, 303.

244. ELWORTHY & MACFARLANE, J. Chem. Soc., In The Press.

245. ELWORTHY, J. Chem. Soc., 1963, 388.

246. ANDREAS, HAUSER & TUCKER, J. Phys. Chem., 1938, 42, 1001.

247. PORTER, Phil. Mag., 1933, 15, 163.

248. WHEELER, TARTAR & LINGAFELTER, J. Amer. Chem. Soc., 1945, 67, 2115.

249. FERGUSON, Phil. Mag., 1912, 6 23, 417.

250. WORTHINGTON, Proc. Roy. Soc., 1881, 32, 362.

251. TARTAR, SIVERTZ & HEITMEIER, J. Amer. Chem. Soc., 1940, 62, 2375.

252. MACK, DAVIS & BARTELL, J. Phys. Chem., 1941, 45, 846.

253. SMITH & SORG, J. Phys. Chem., 1941, 45, 671.

254. SMITH, J. Phys. Chem., 1944, 48, 168.

255. "HANDBOOK OF CHEMISTRY & PHYSICS", 39th Ed., Chemical Rubber Publishing Co., Cleveland, Ohio, 1958, 2022.

256. REF. 201. p. 391.

LIGHT SCATTERING APPARATUS

PLATE 1.

PLATE 2.

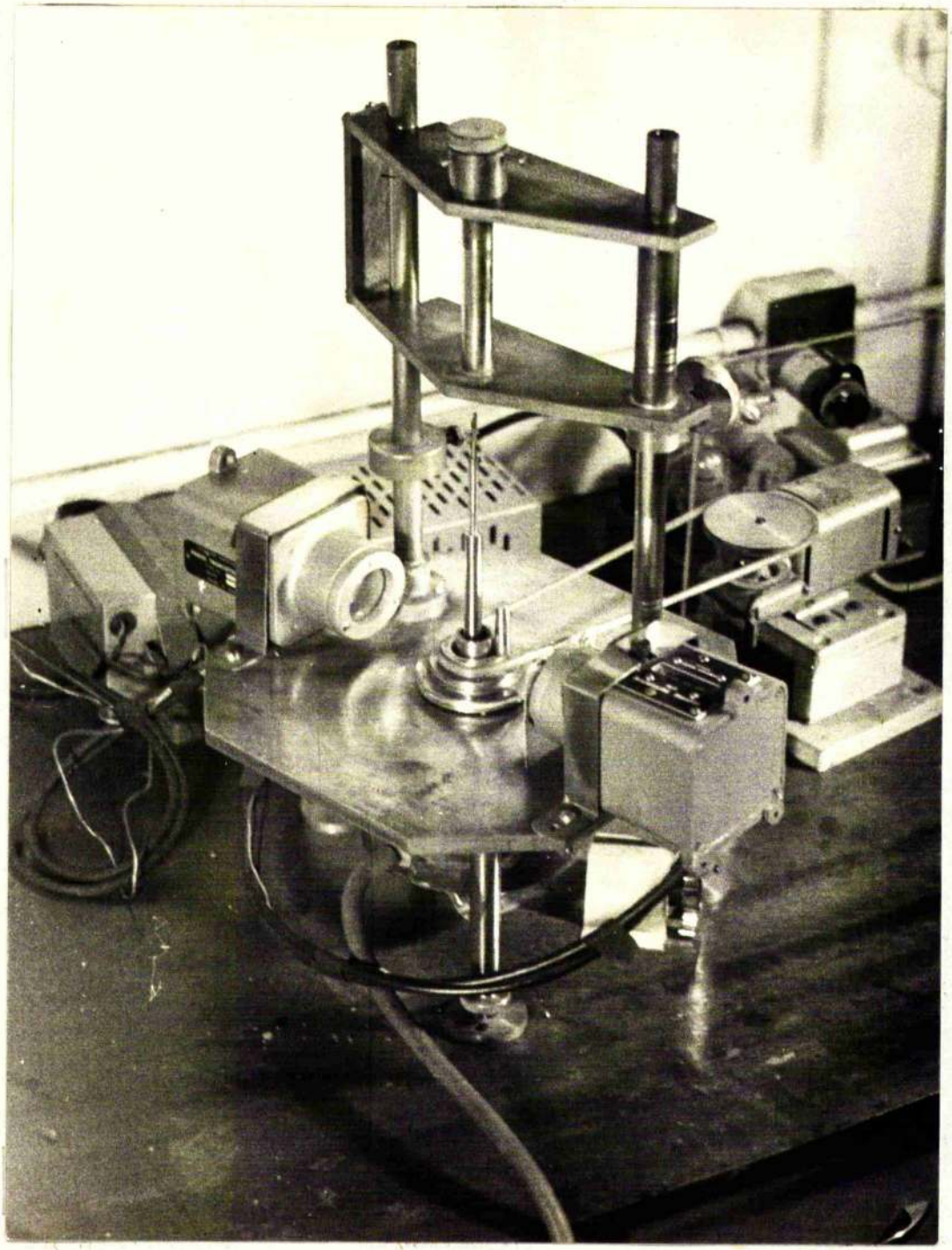

COUETTE VISCOMETER.

PLATE 3.

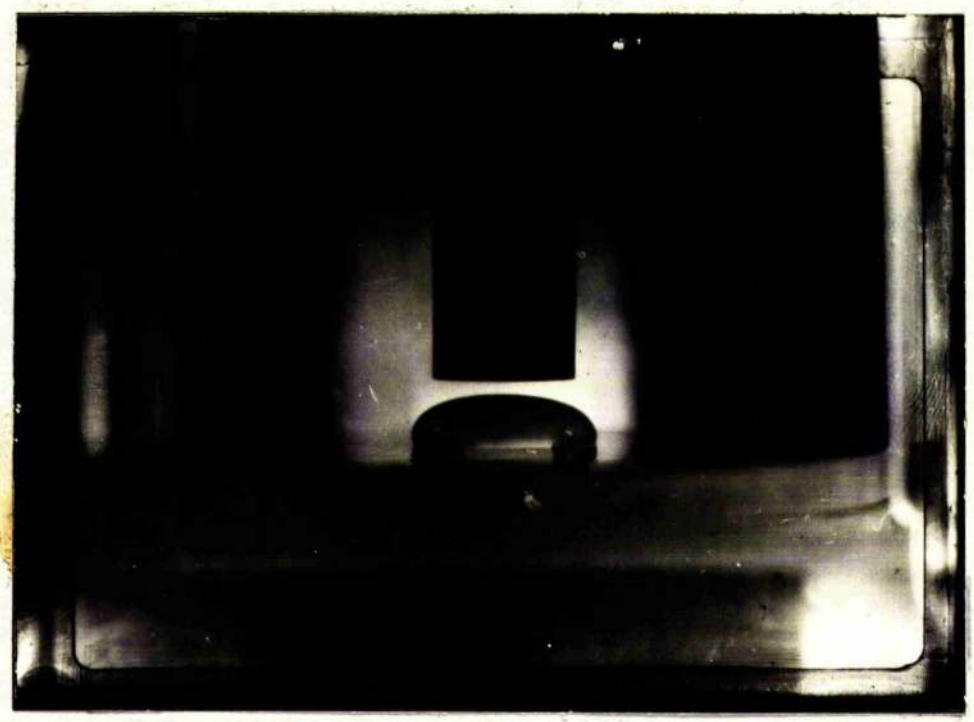

PLATE 4.

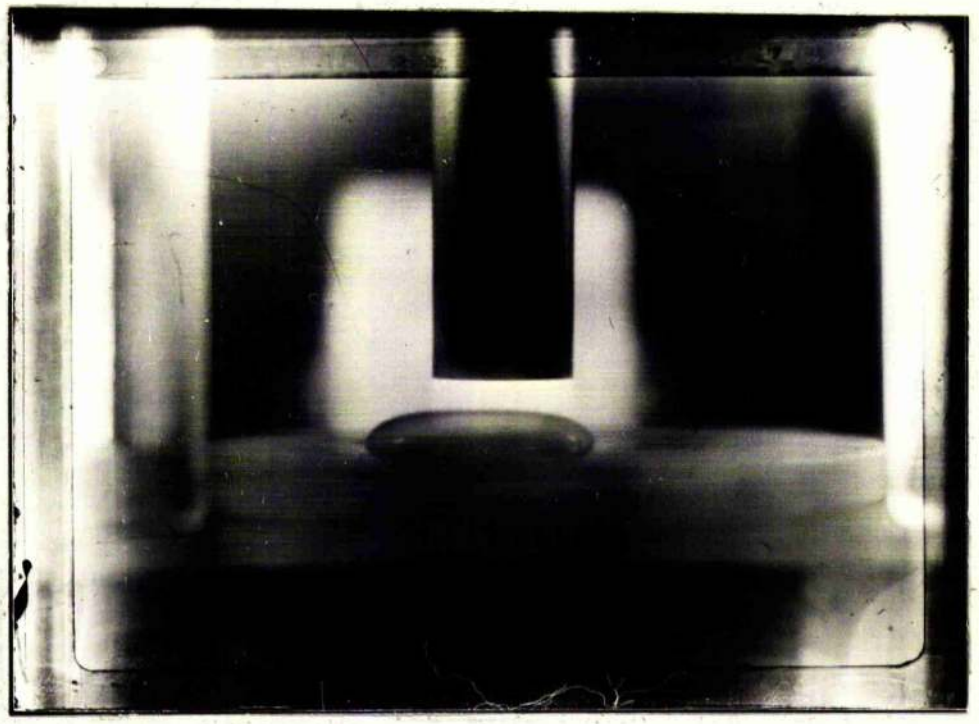

SESSILE DROPS.

FIGURE 1

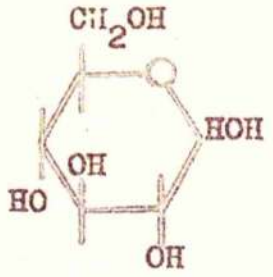

D-glucose

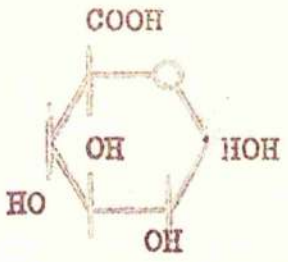

D-glucuronic acid

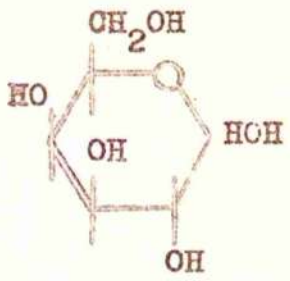

D-galactose

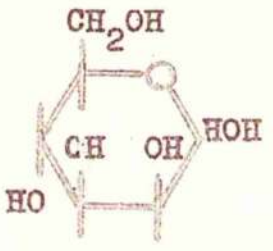

D-mannose

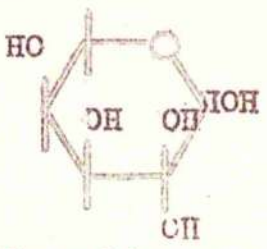

L-arabinose

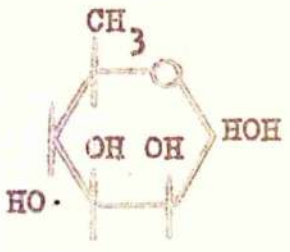

D-rhamnose

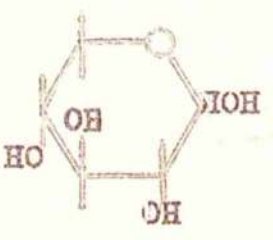

D-xylose

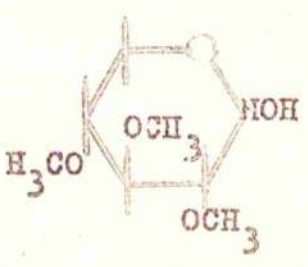

2,3,4,-tri-O-methylxylose

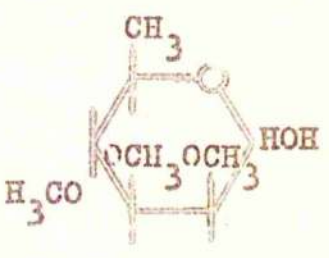

2,3,4,-tri-O-methyl rhamnose.

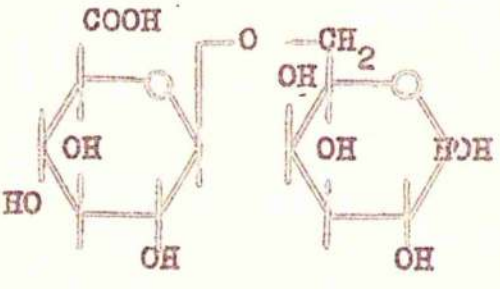

6,0 D glucopyranosyluronic acid D-galactose

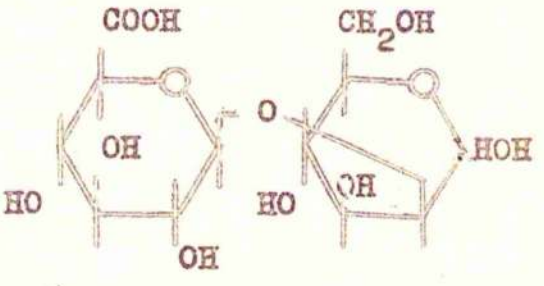

2,0 D-glucopyranosyluronic acid D-mannose

FIGURE 2.

Angular dependence of scatter
for polarized light.

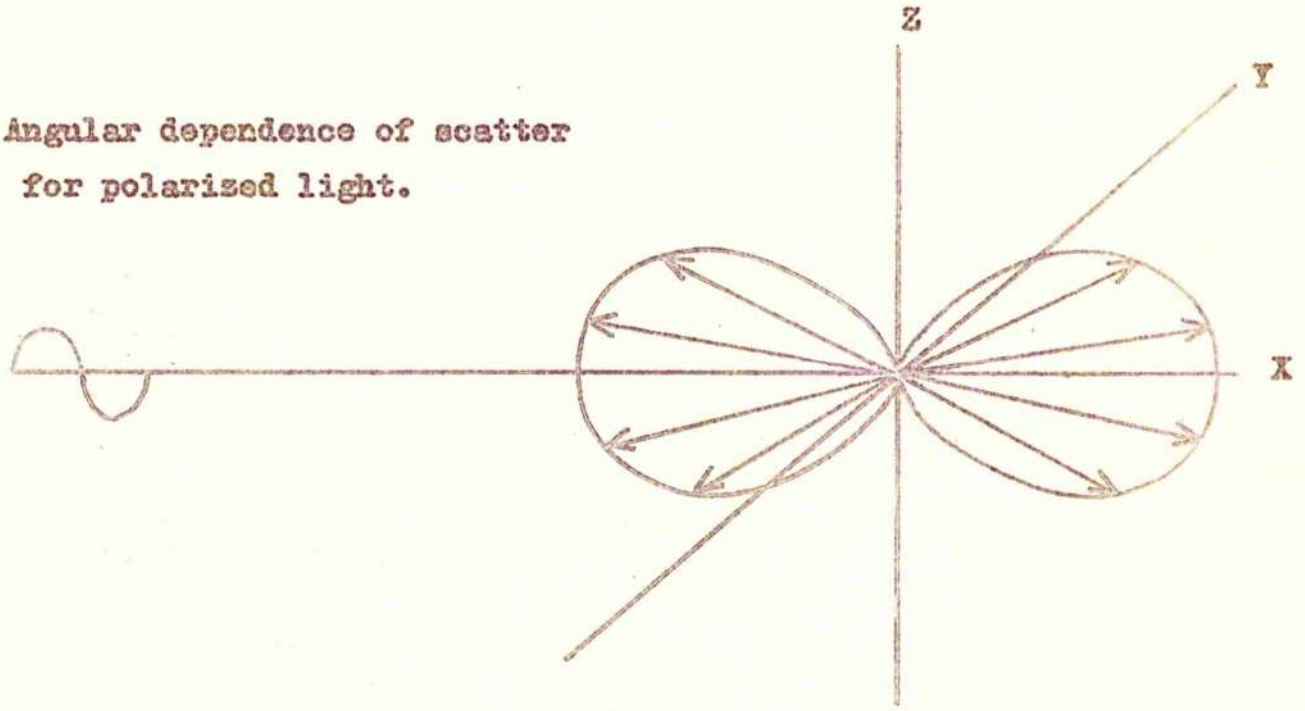

Angular dependence of scatter
for unpolarized light.

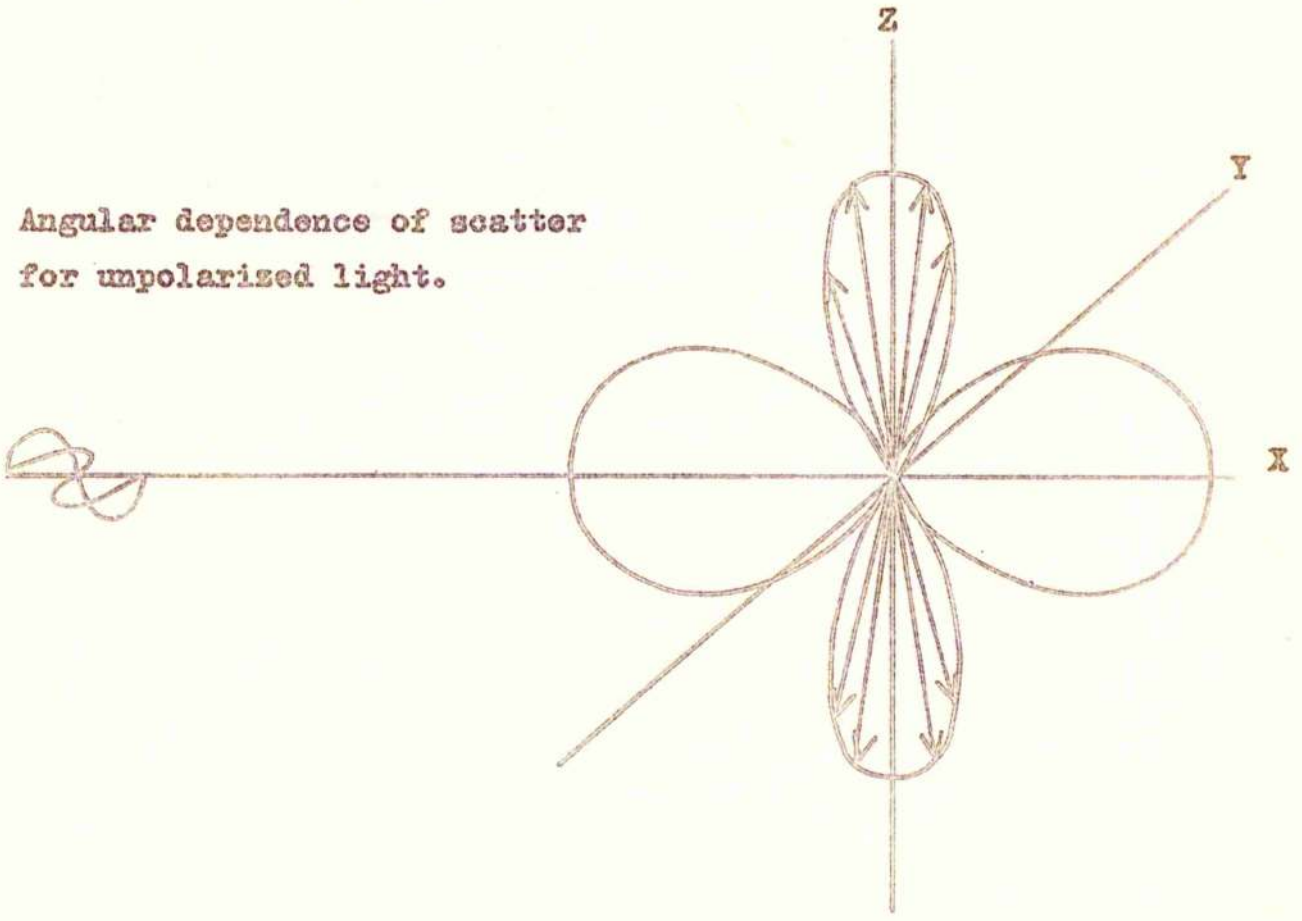

FIGURE 3.

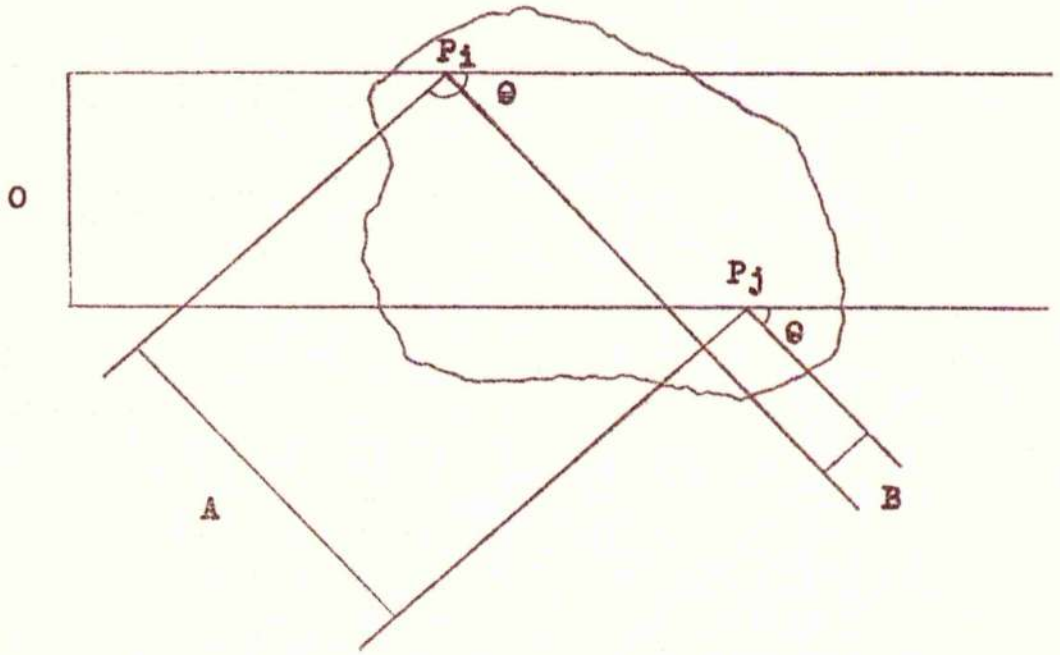

FIGURE 4.

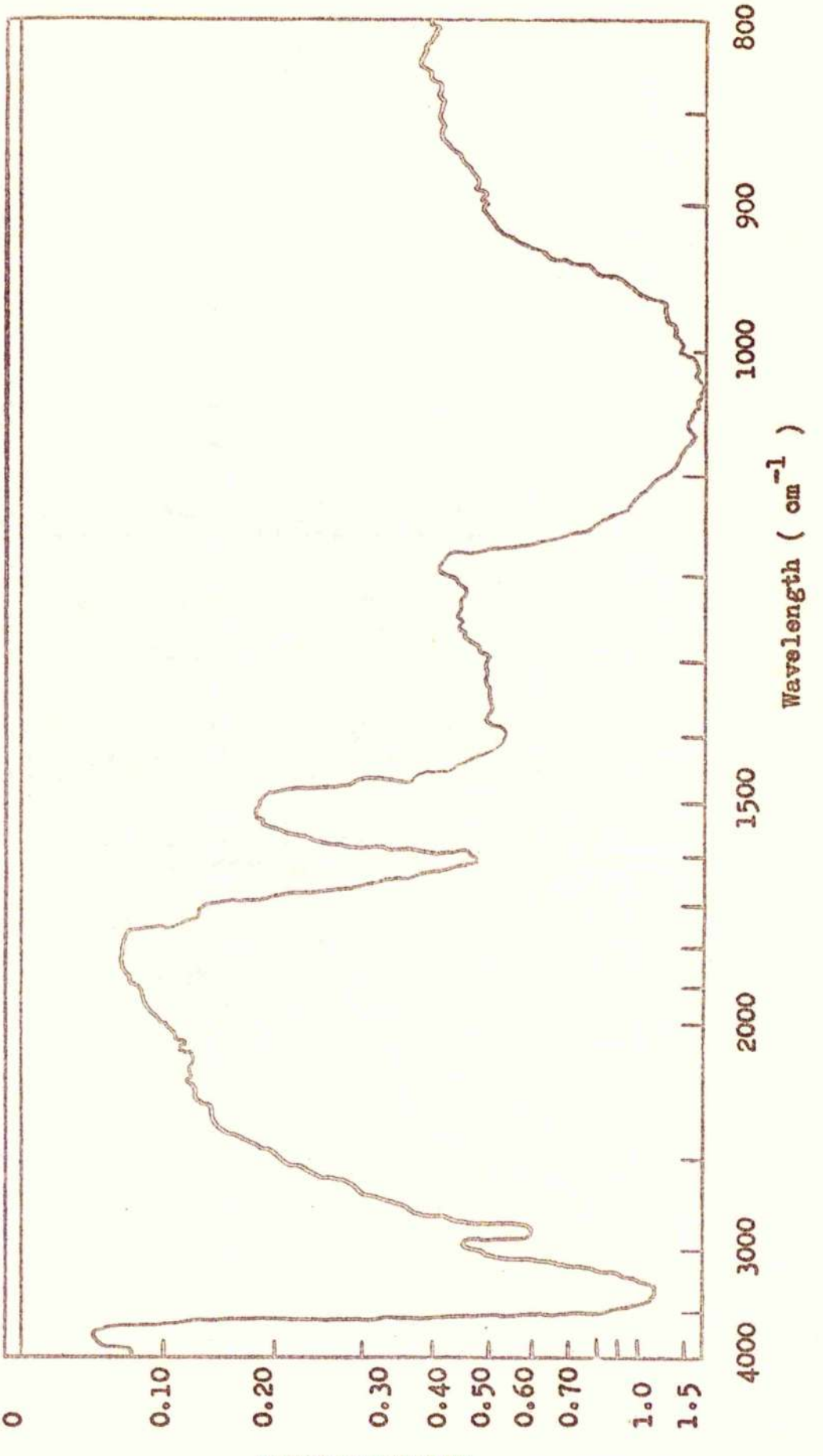
Transmittance.
0
0.10
0.20
0.30
0.40
0.50
0.60
0.70
1.0
1.5
4000
3000
2000
1500
1000
900
800
Wavelength (cm^{-1})

FIGURE 5.

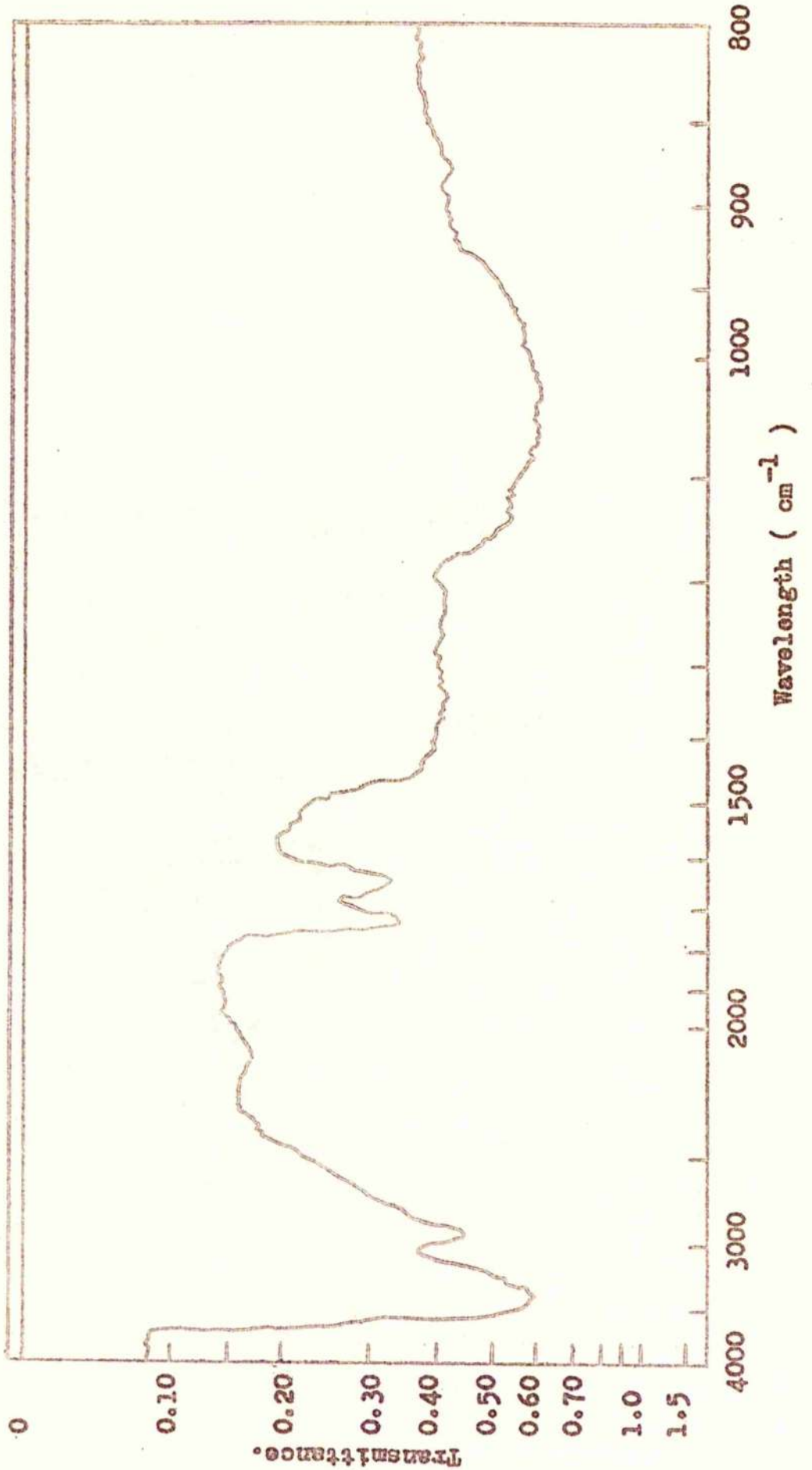
Transmittance.
0
0.10
0.20
0.30
0.40
0.50
0.60
0.70
1.0
1.5
4000
3000
2000
1500
1000
900
800
Wavelength (cm^{-1})

FIGURE 6.

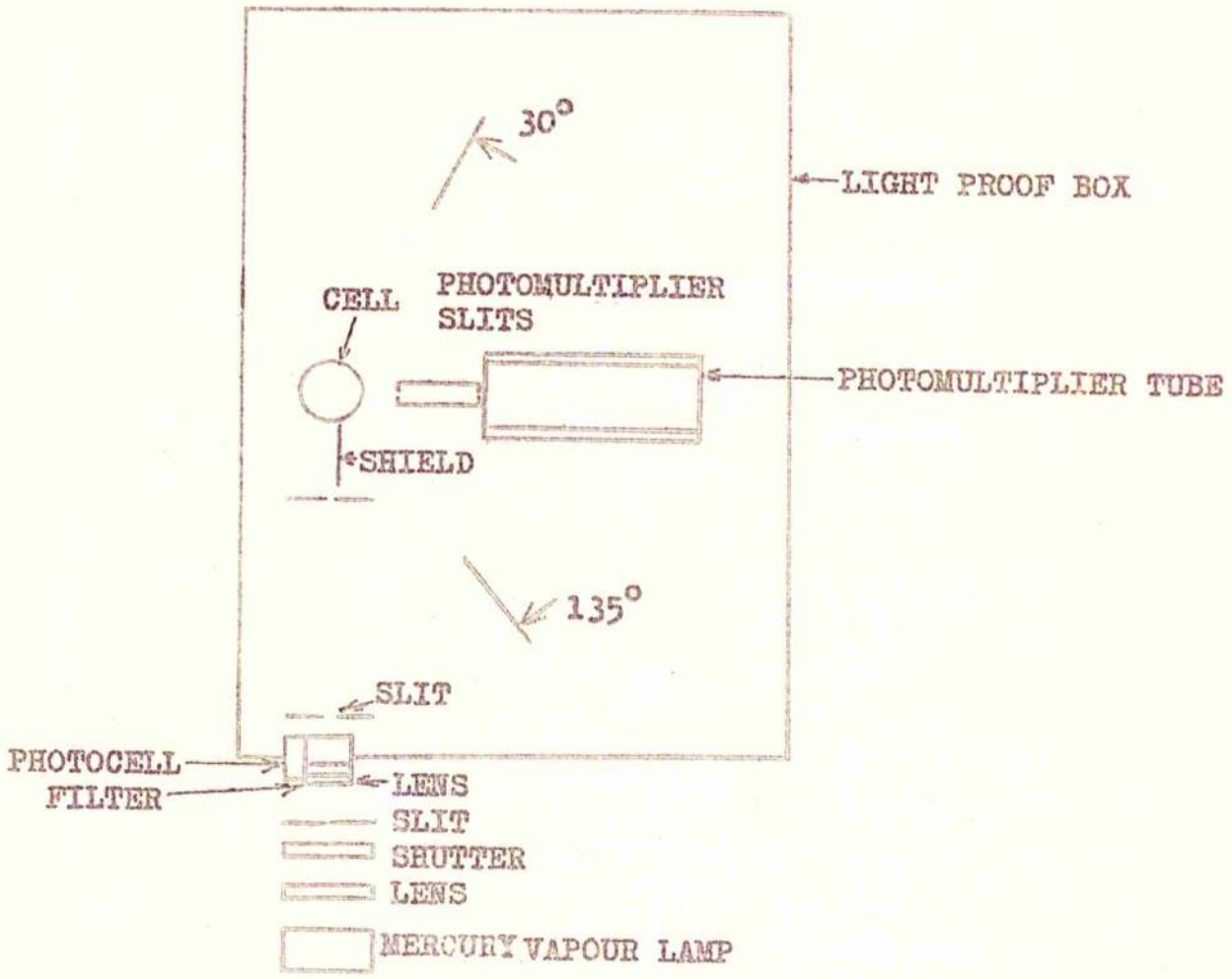
30°
LIGHT PROOF BOX
CELL
PHOTOMULTIPLIER SLITS
PHOTOMULTIPLIER TUBE
SHIELD
135°
SLIT
PHOTOCELL
FILTER
LENS
SLIT
SHUTTER
LENS
MERCURY VAPOUR LAMP

FIGURE 7.

Wiring Diagram

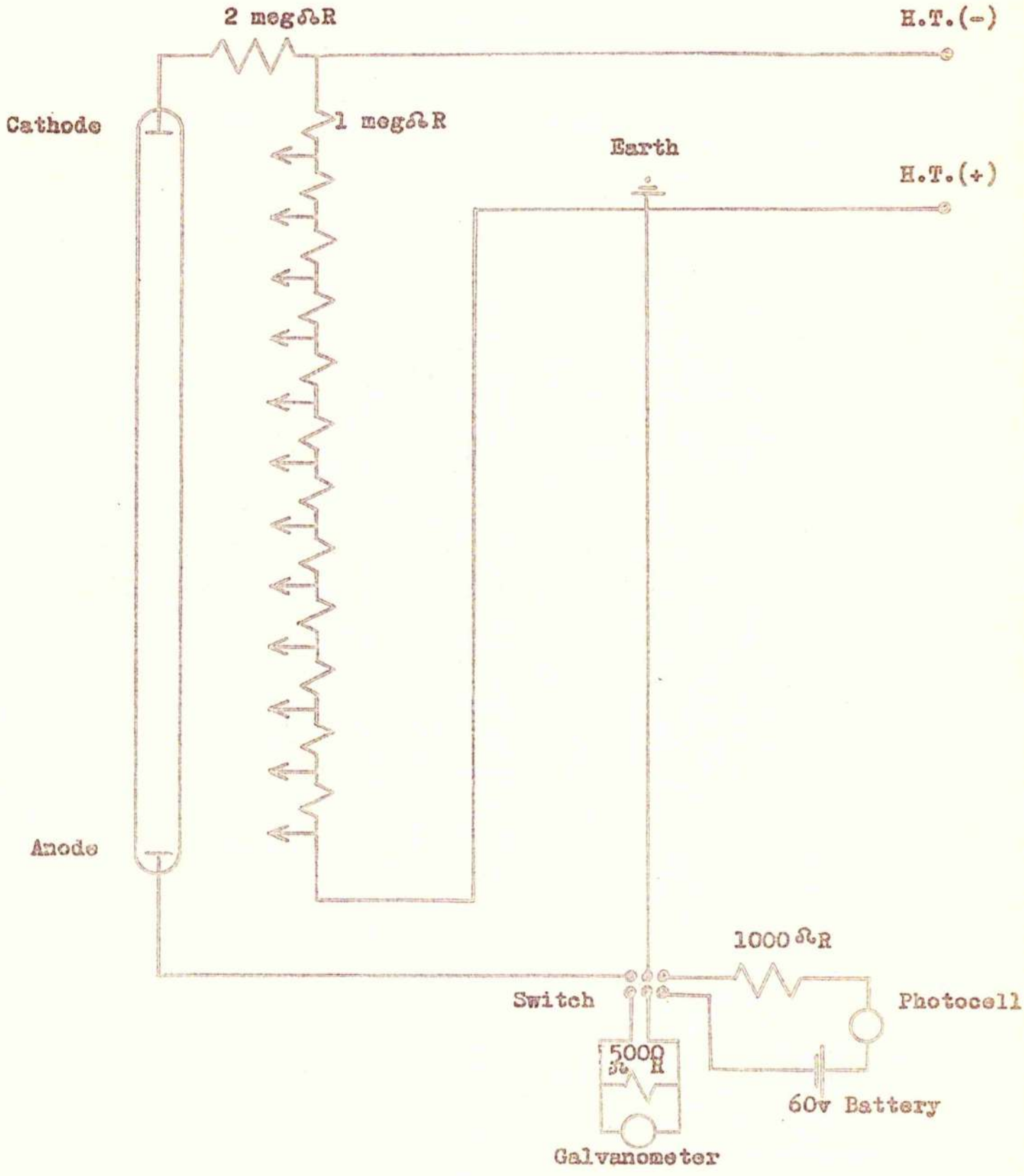

FIGURE 8.

LIGHT SCATTERING CELL.

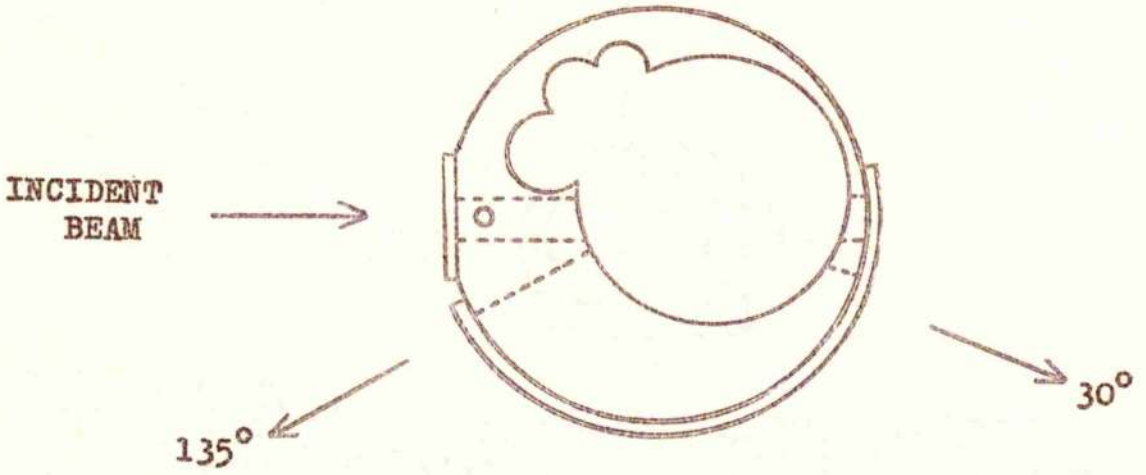

Plan

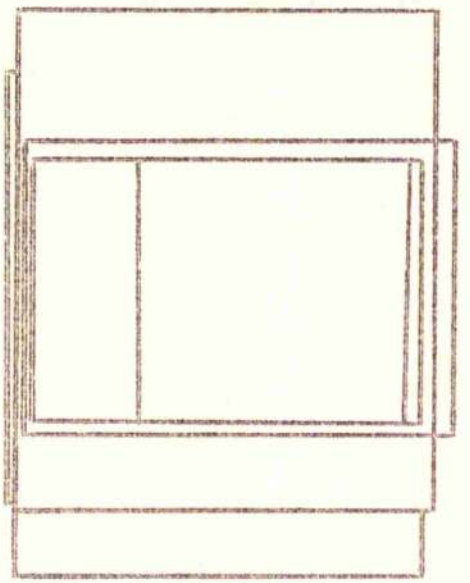

Side-view

FIGURE 9.

Donatta Viscometer

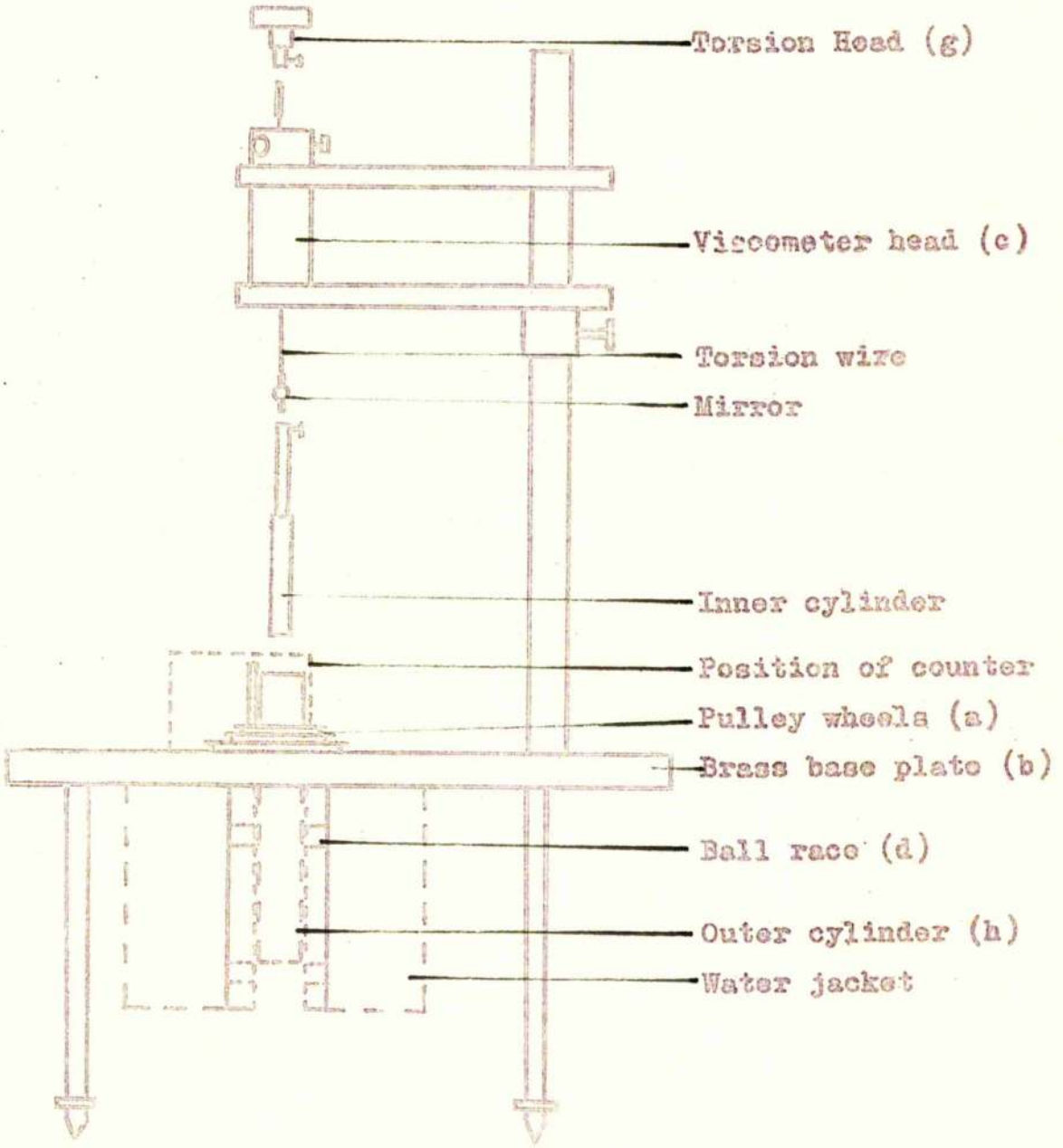

FIGURE 10.

Fraction 1 / 0.5N NaCl.

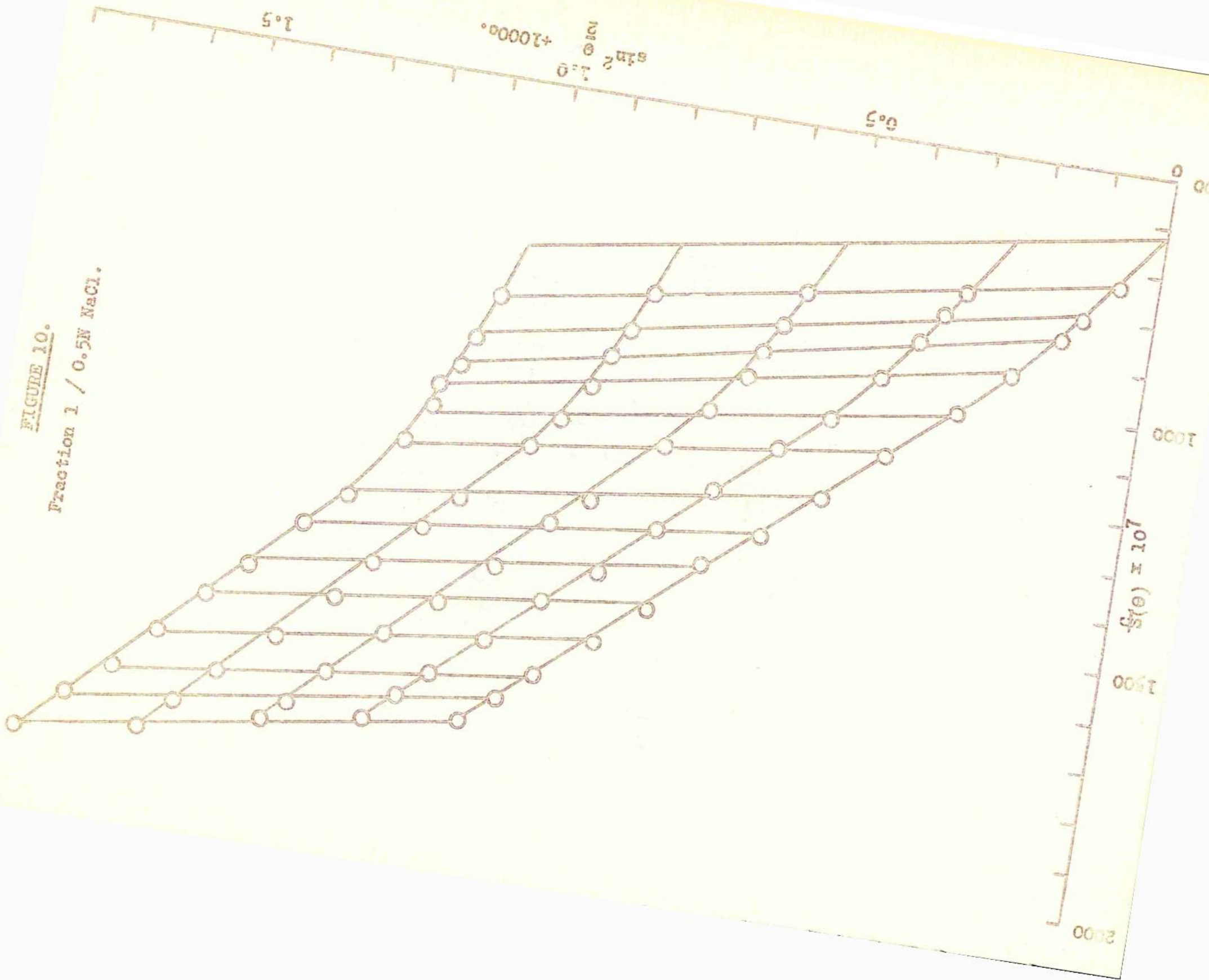

FIGURE 11.

Fraction 1 / 0.05N NaCl.

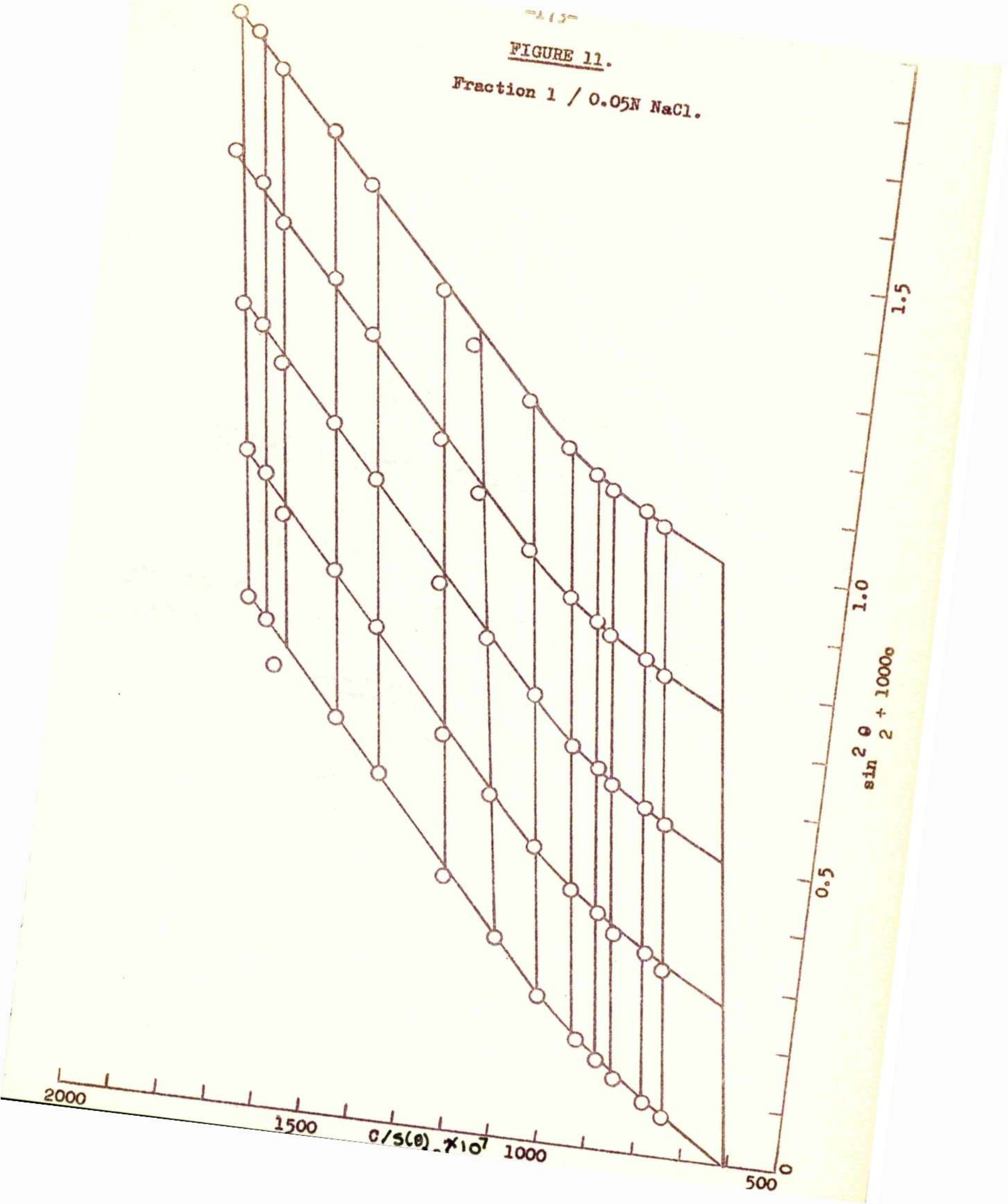

FIGURE 12.

Fraction 2 / 0.5N NaCl.

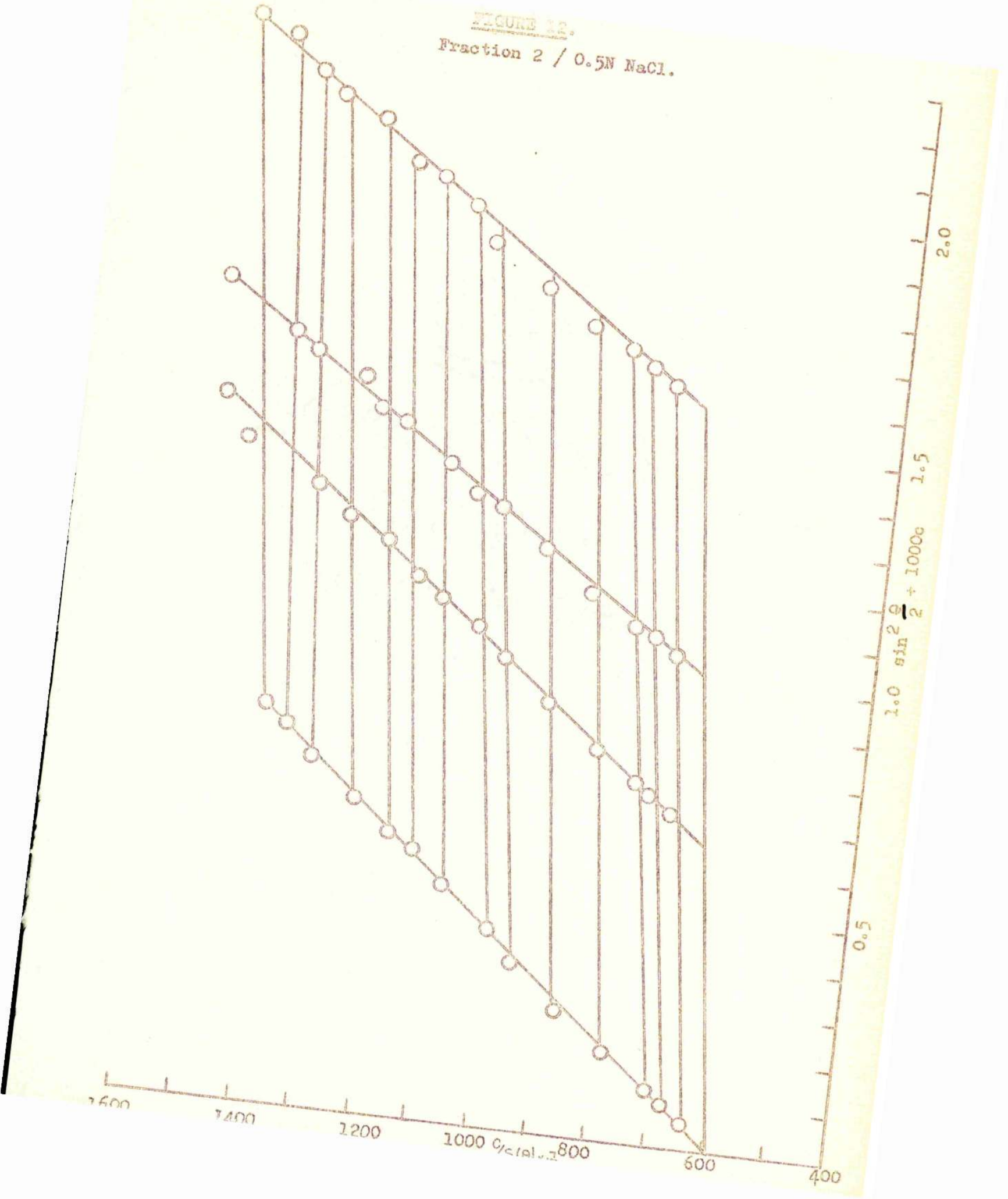

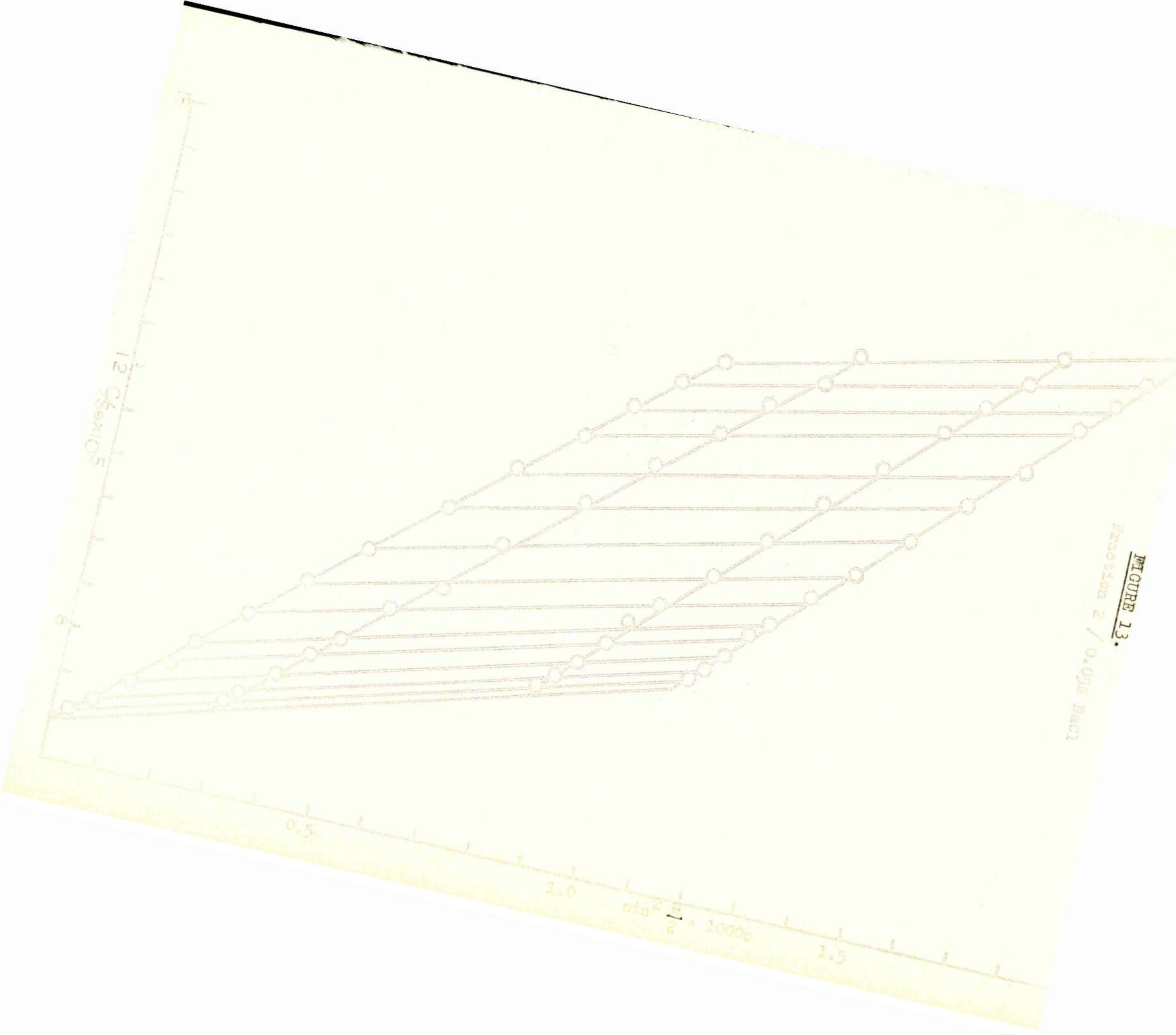

FIGURE 13.

FIGURE 14.

Fraction 2 / 0.005N NaCl

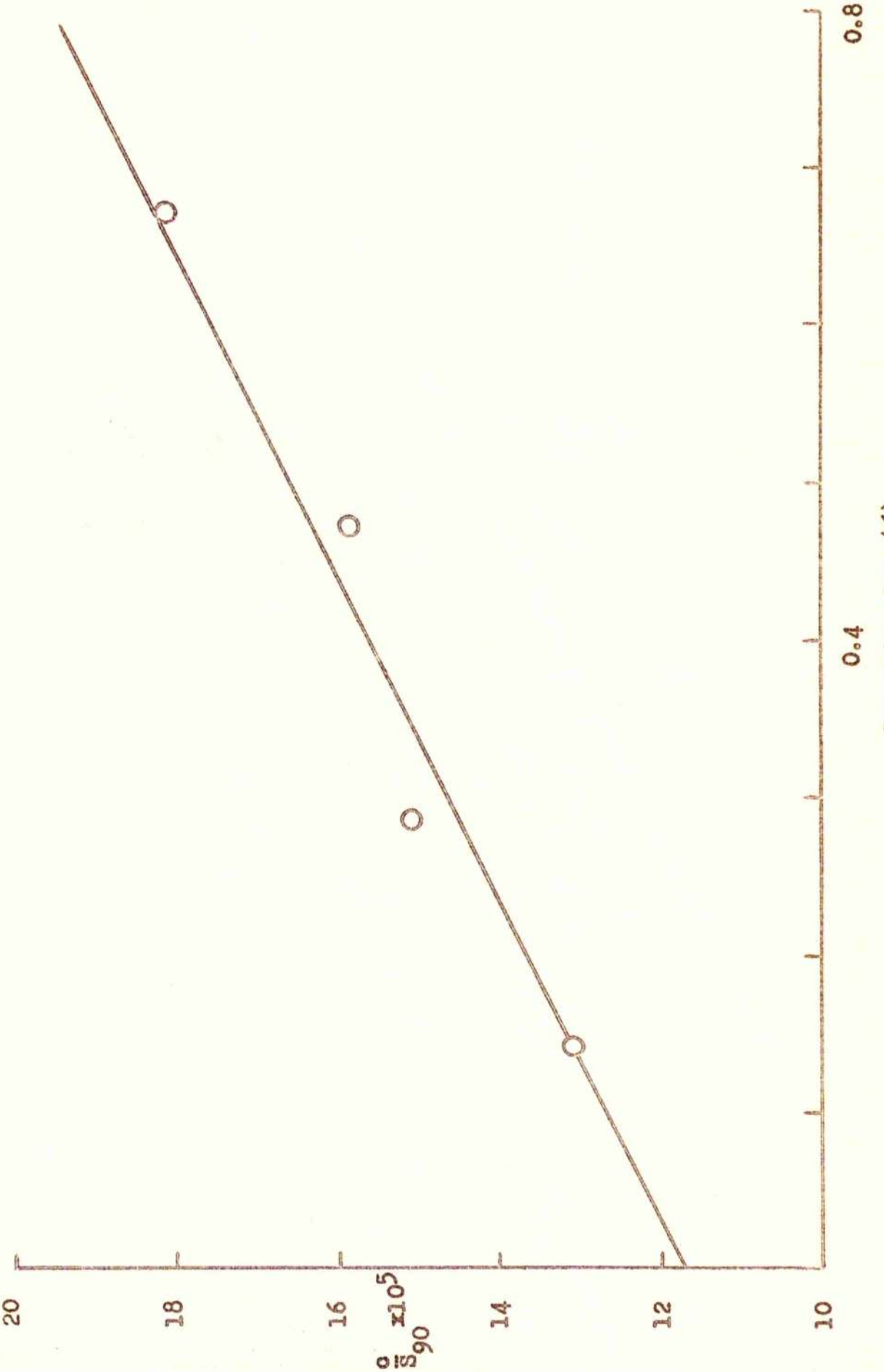

FIGURE 1[illegible].

Fraction 2 / H_2O.

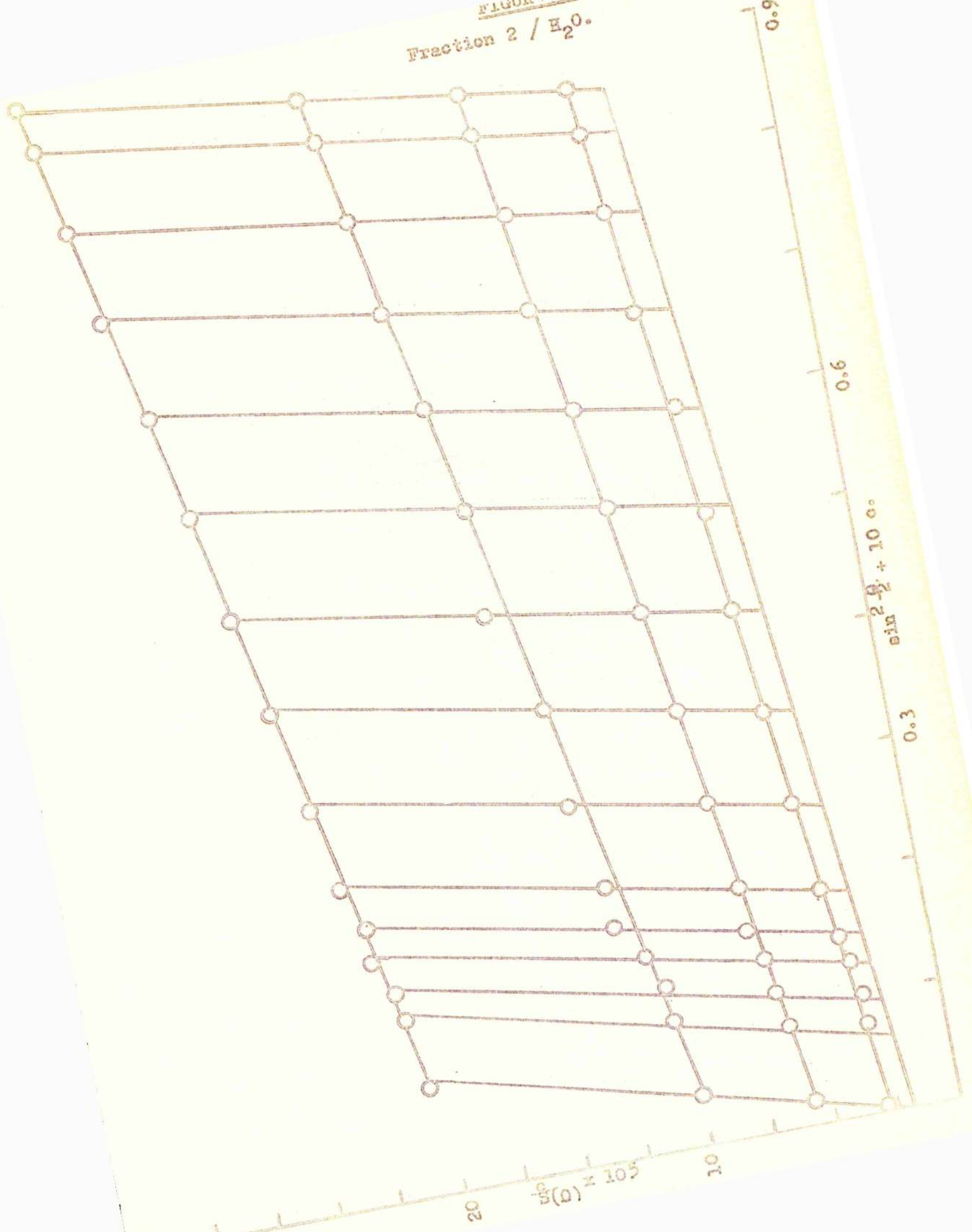

FIGURE 16.

Fraction 3 / 0.5N NaCl.

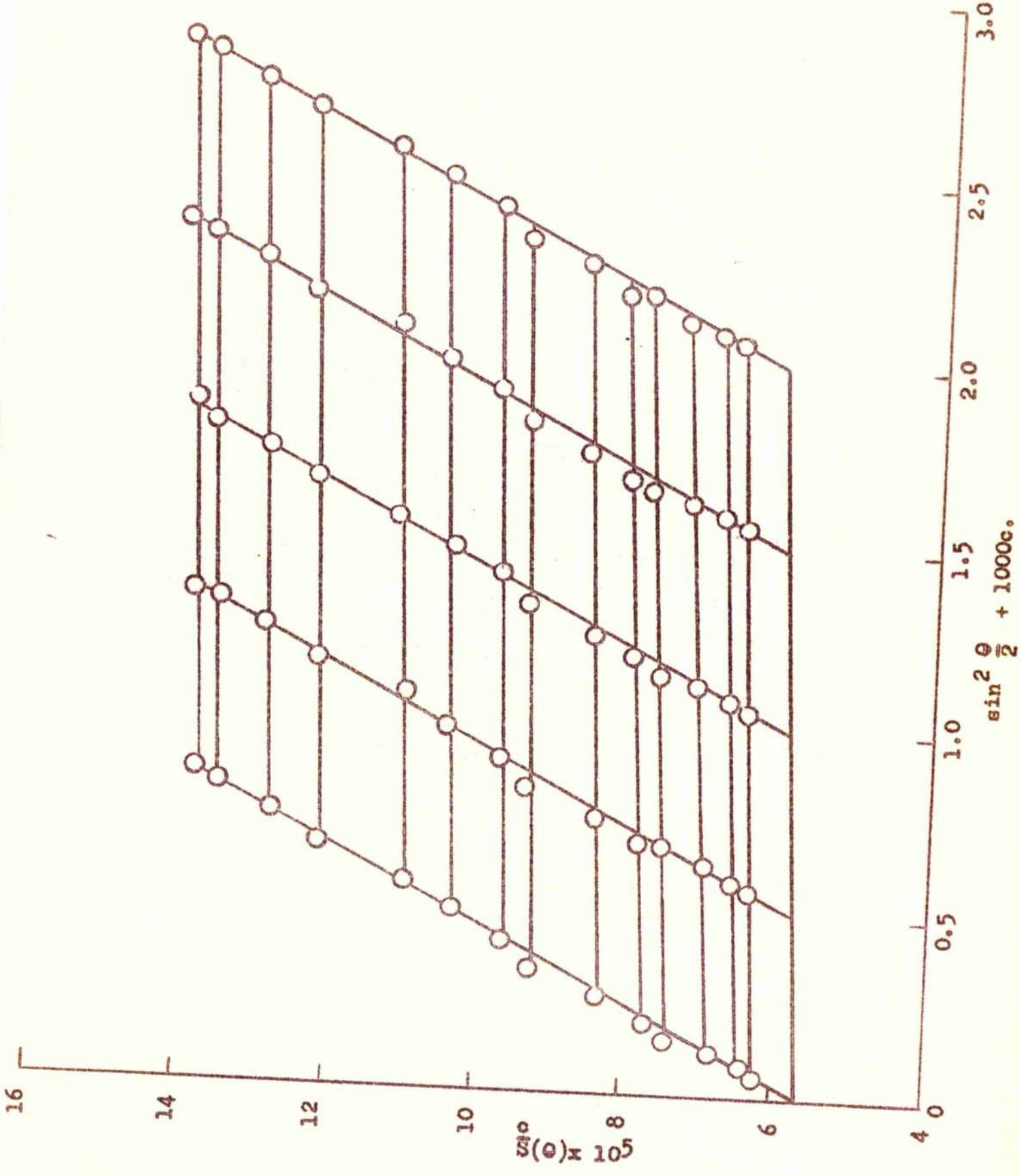

FIGURE 17.

(a) Coils with $M_w:M_n$ =2:1 (c) Monodisperse rods

(b) Monodisperse coils (d) Best fit

○ Experimental points.

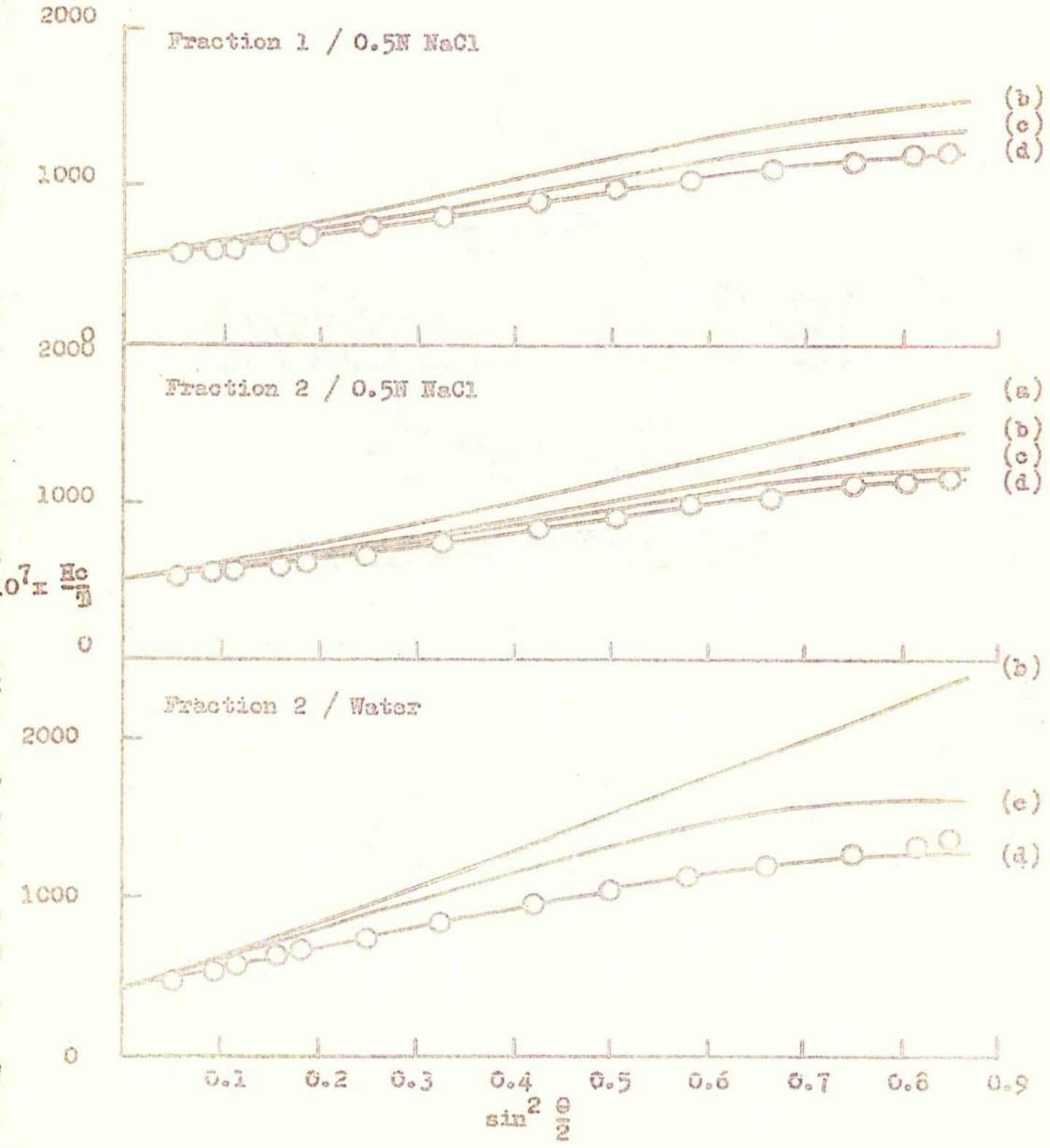

FIGURE 18.

Fraction 1.

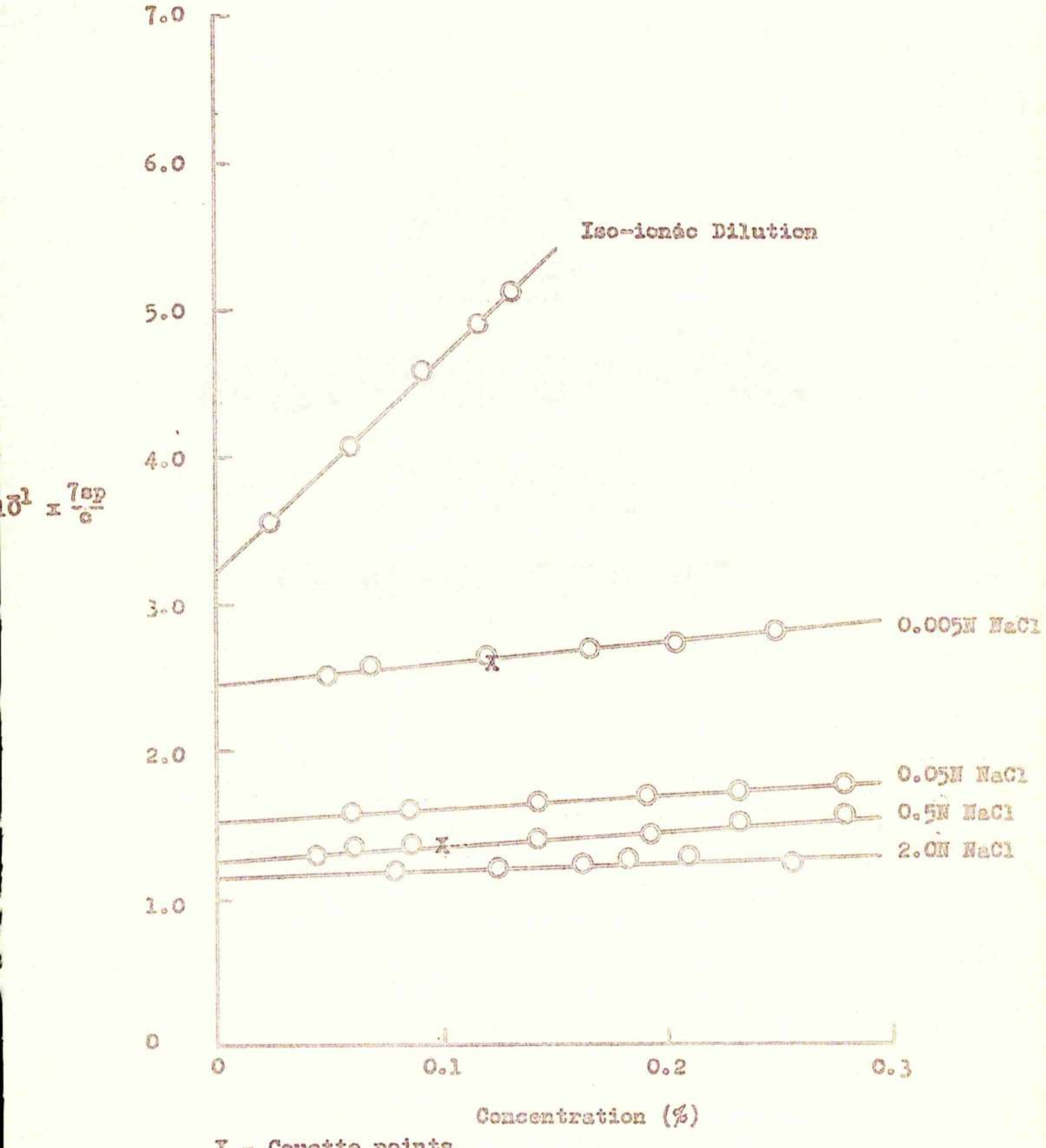

X = Couette points

FIGURE 19.

Fraction 2

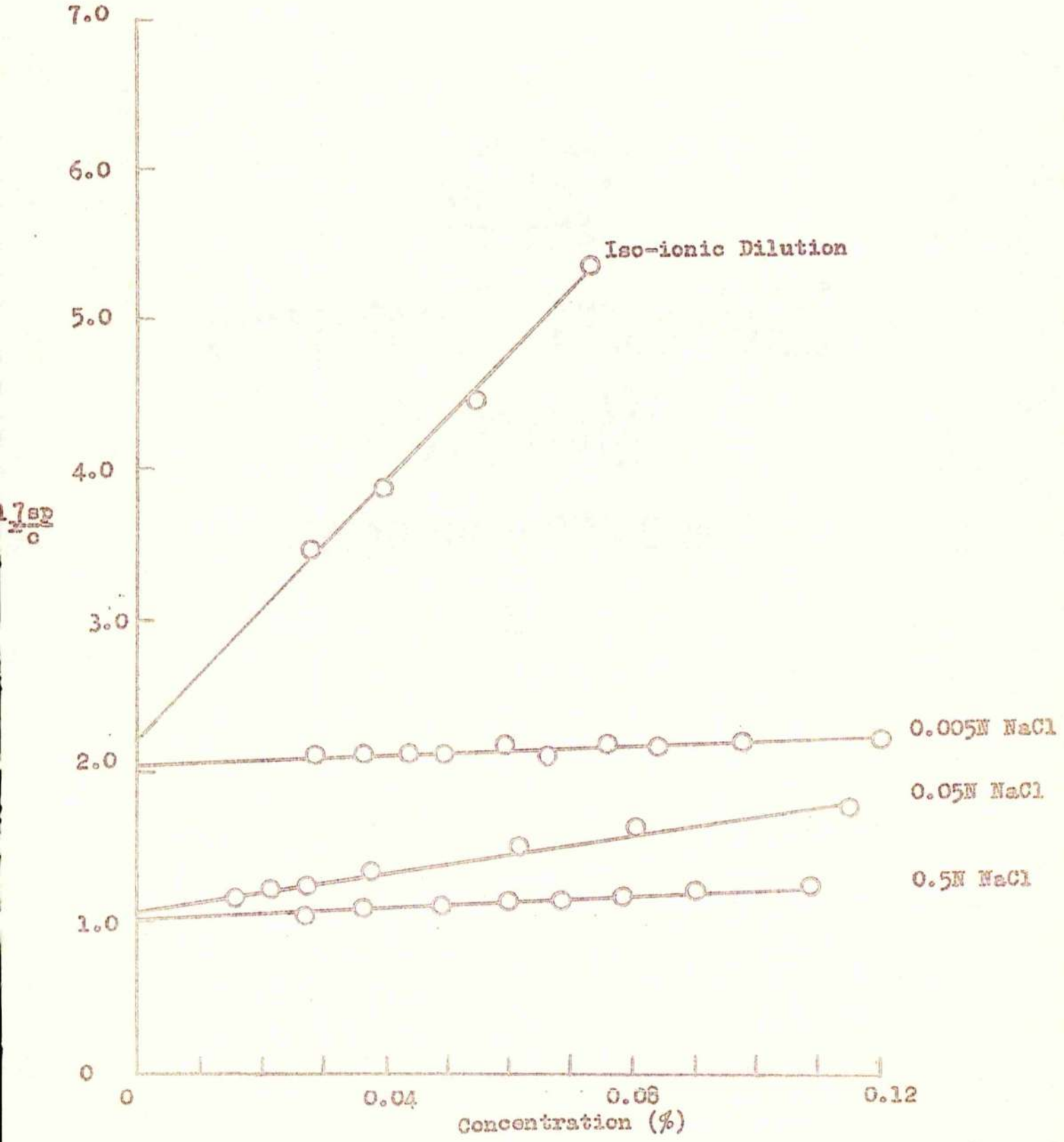

FIGURE 20.

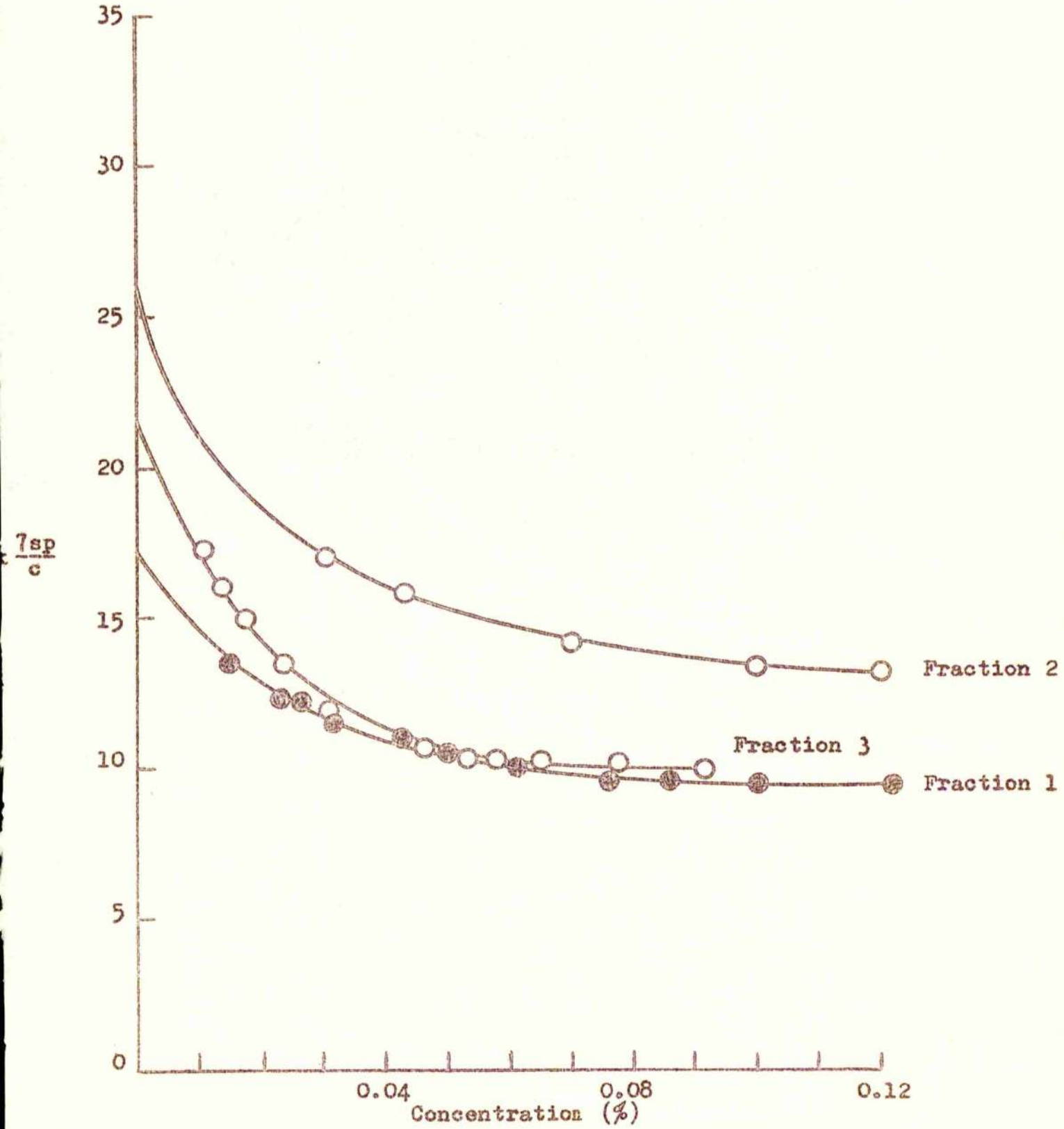
35
30
25
20
15
10
5
0
$\frac{\eta sp}{c}$
0.04
0.08
0.12
Concentration (%)
Fraction 2
Fraction 3
Fraction 1

FIGURE 21

Fraction 1 / 0.5M NaCl.

FIGURE 22

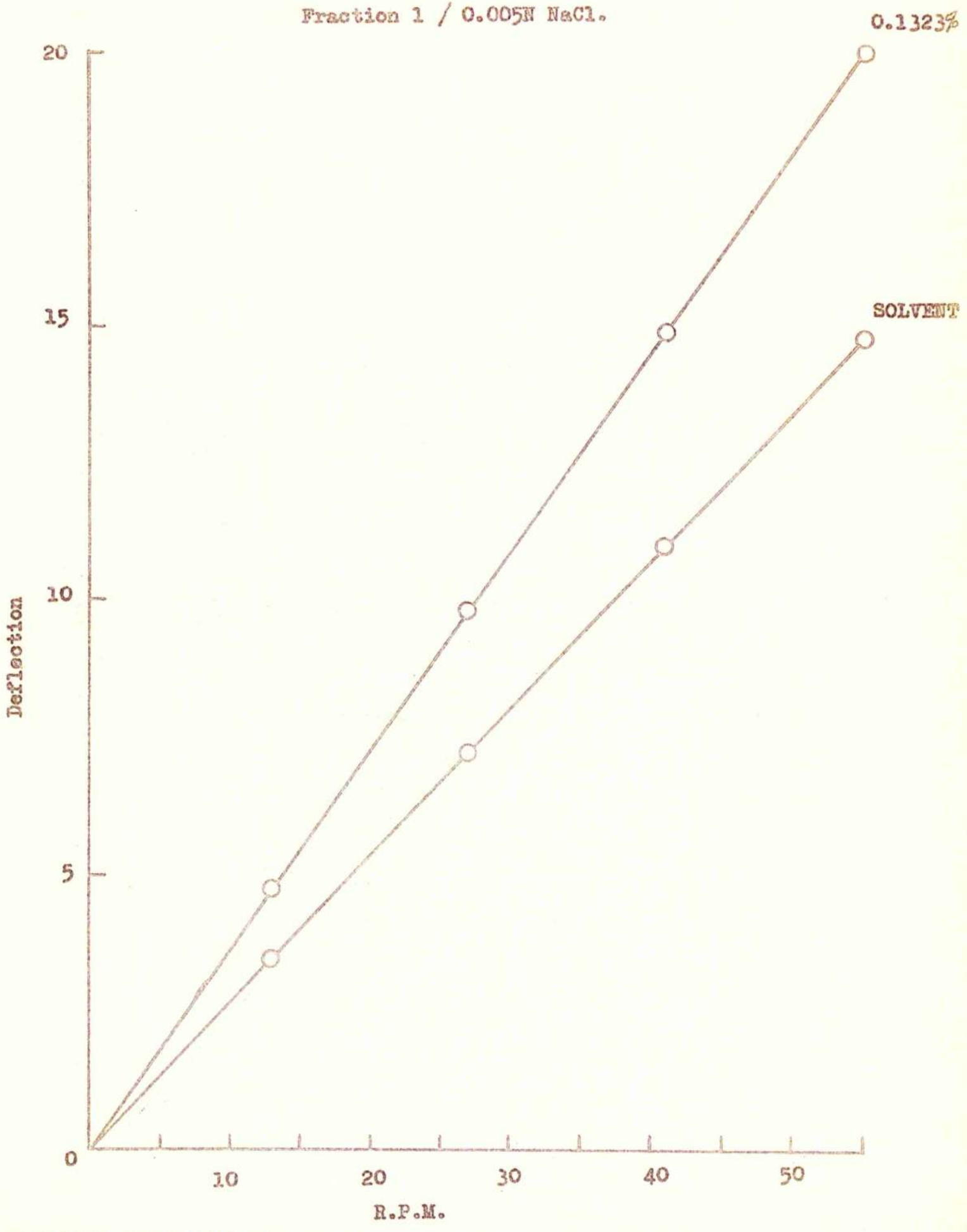
Fraction 1 / 0.005N NaCl.
0.1323%
SOLVENT
Deflection
20
15
10
5
0
10
20
30
40
50
R.P.M.

FIGURE 23.

Fraction 2 / 0.5N NaCl.

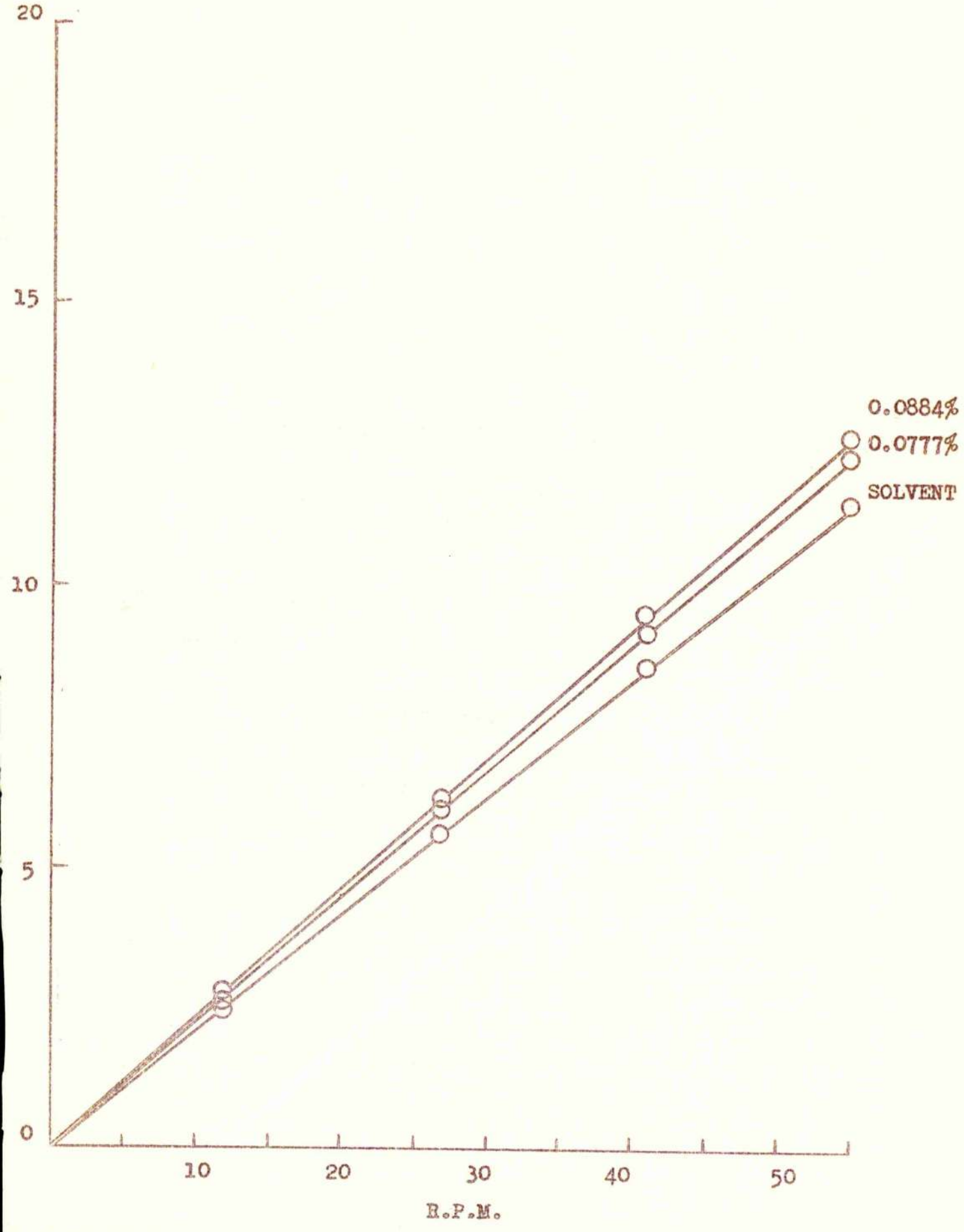

FIGURE 24.

Fraction 2 / 0.005N NaCl.

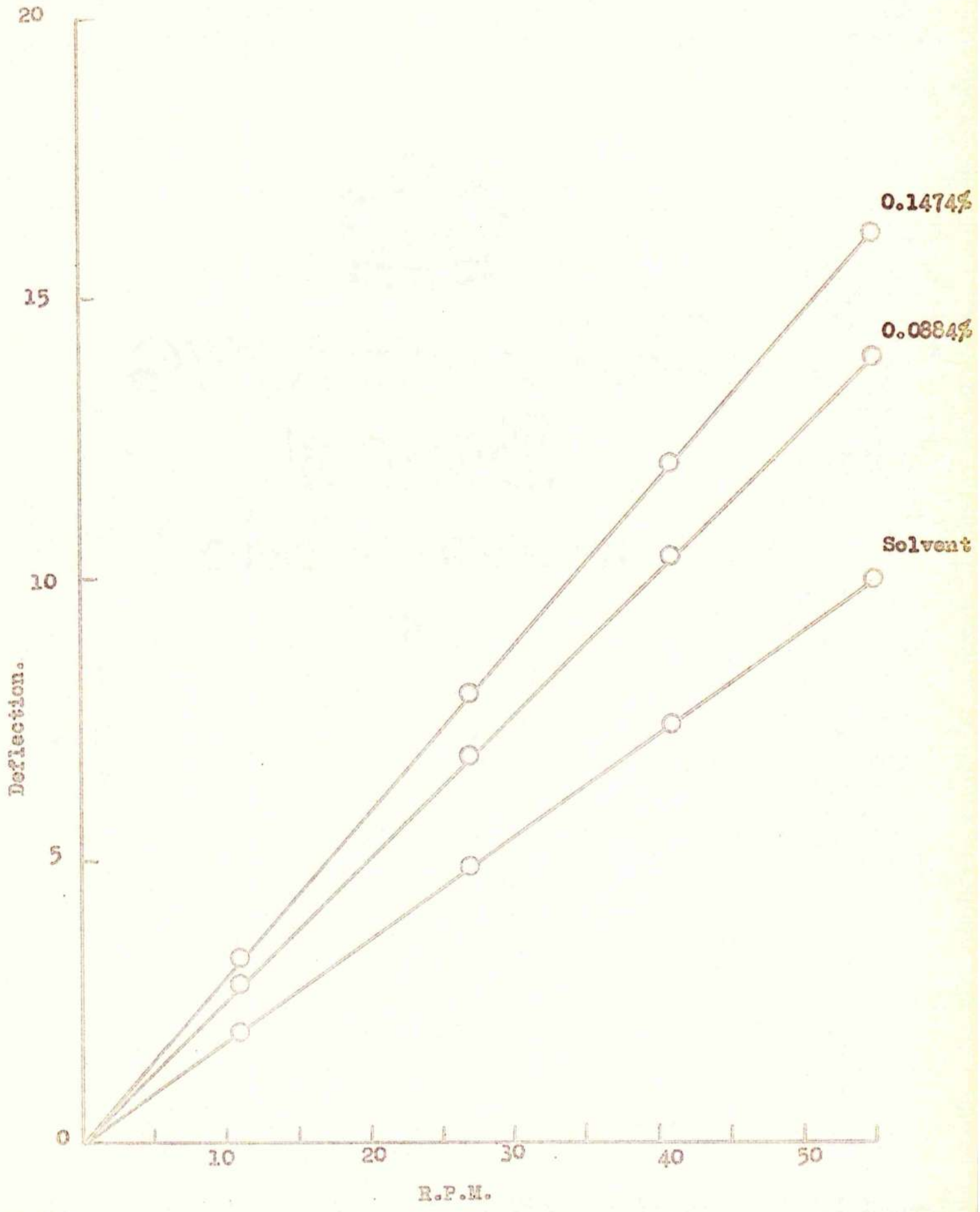

FIGURE 25.

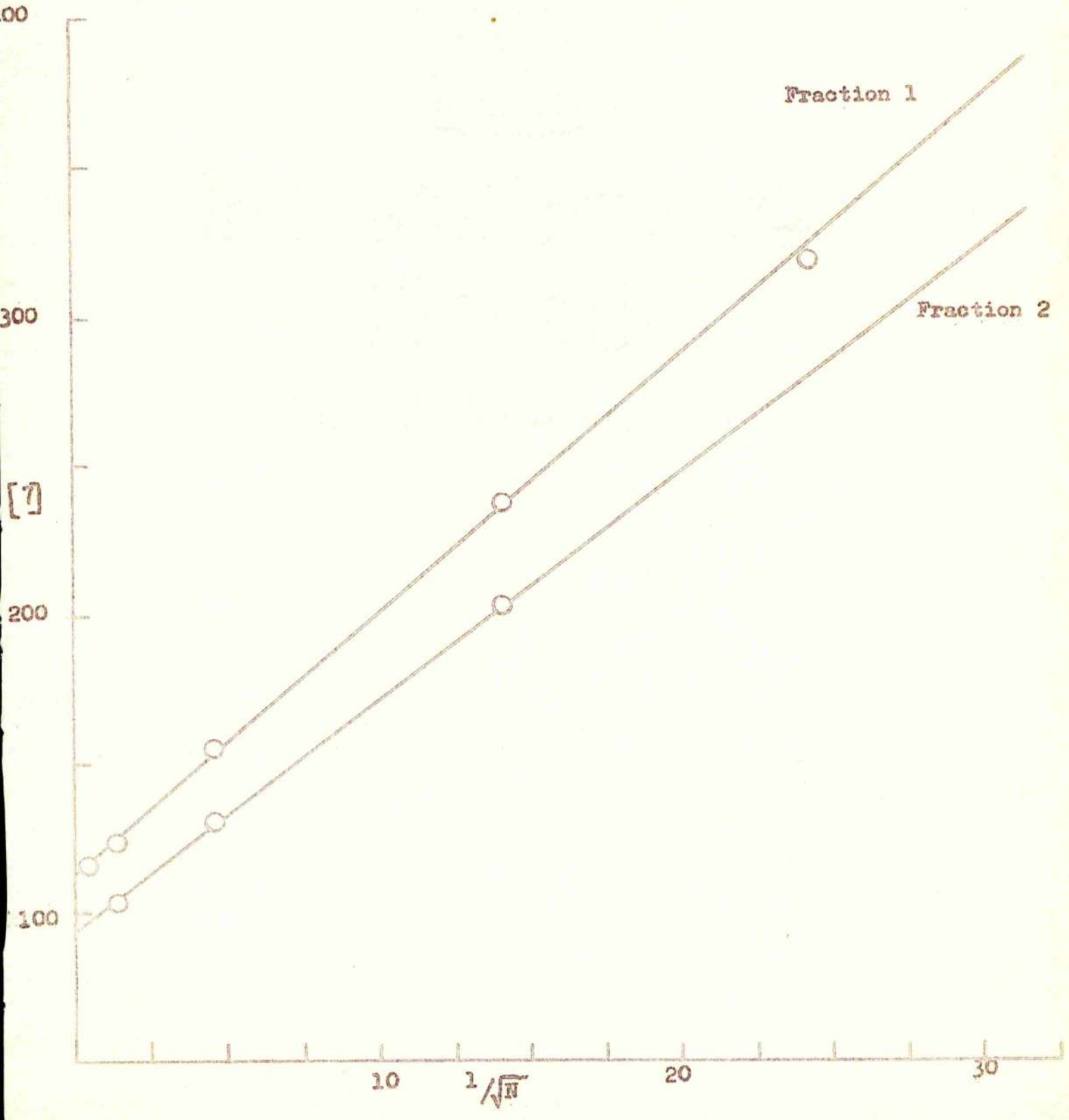

FIGURE 26.

Water Vapour Sorption Apparatus.

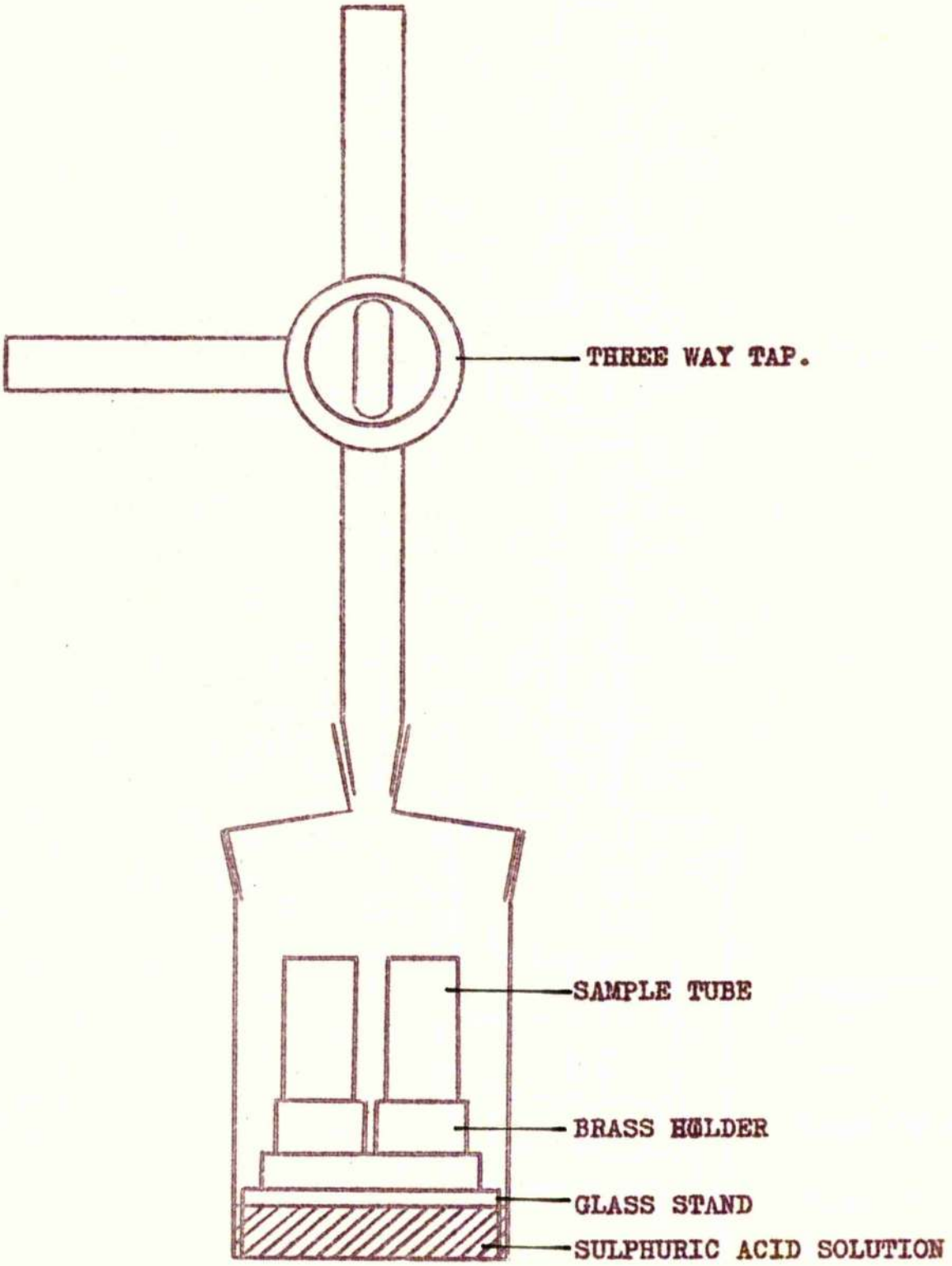

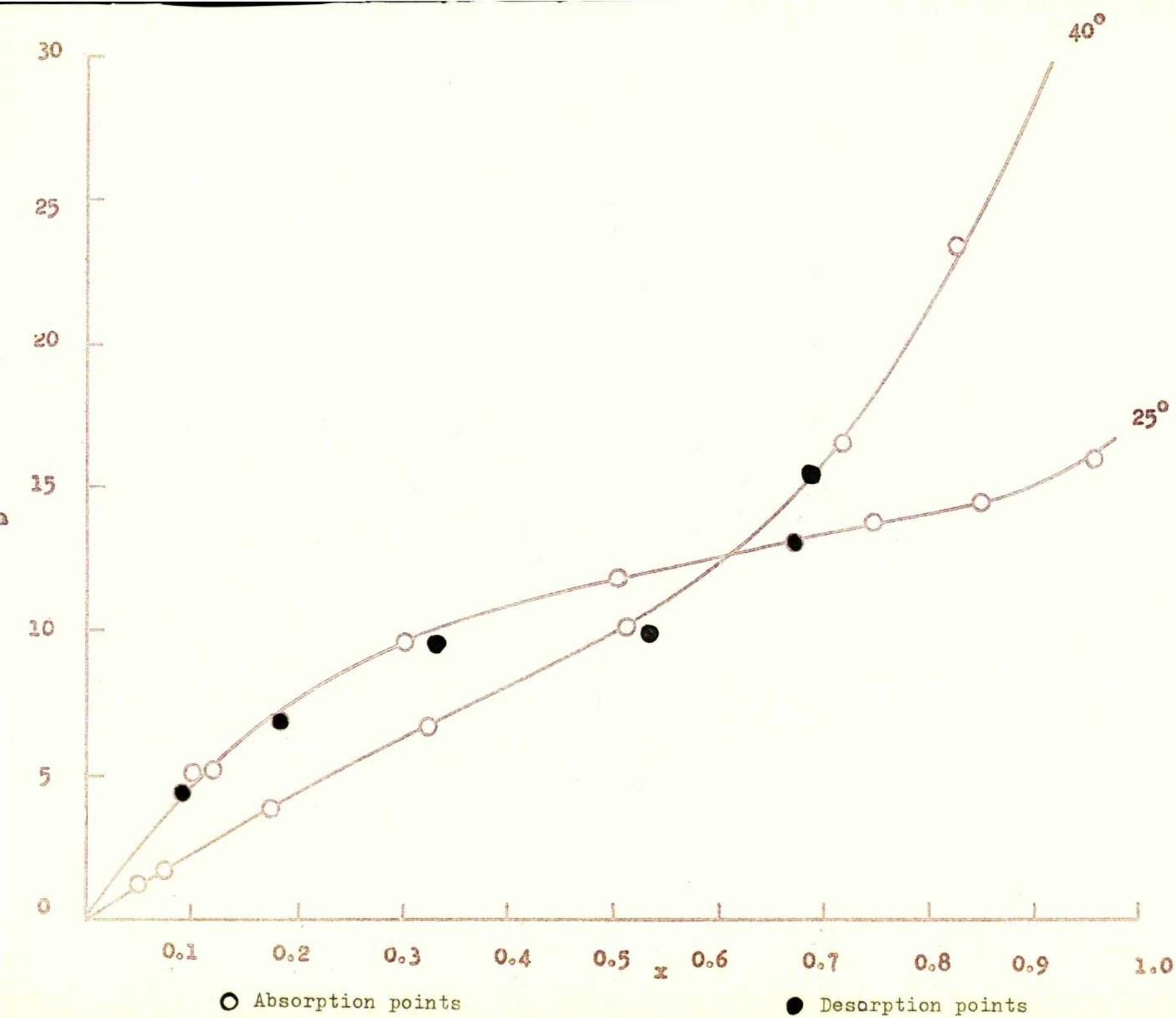

FIGURE 27a

Fraction 1.

FIGURE 27b

Fraction 2

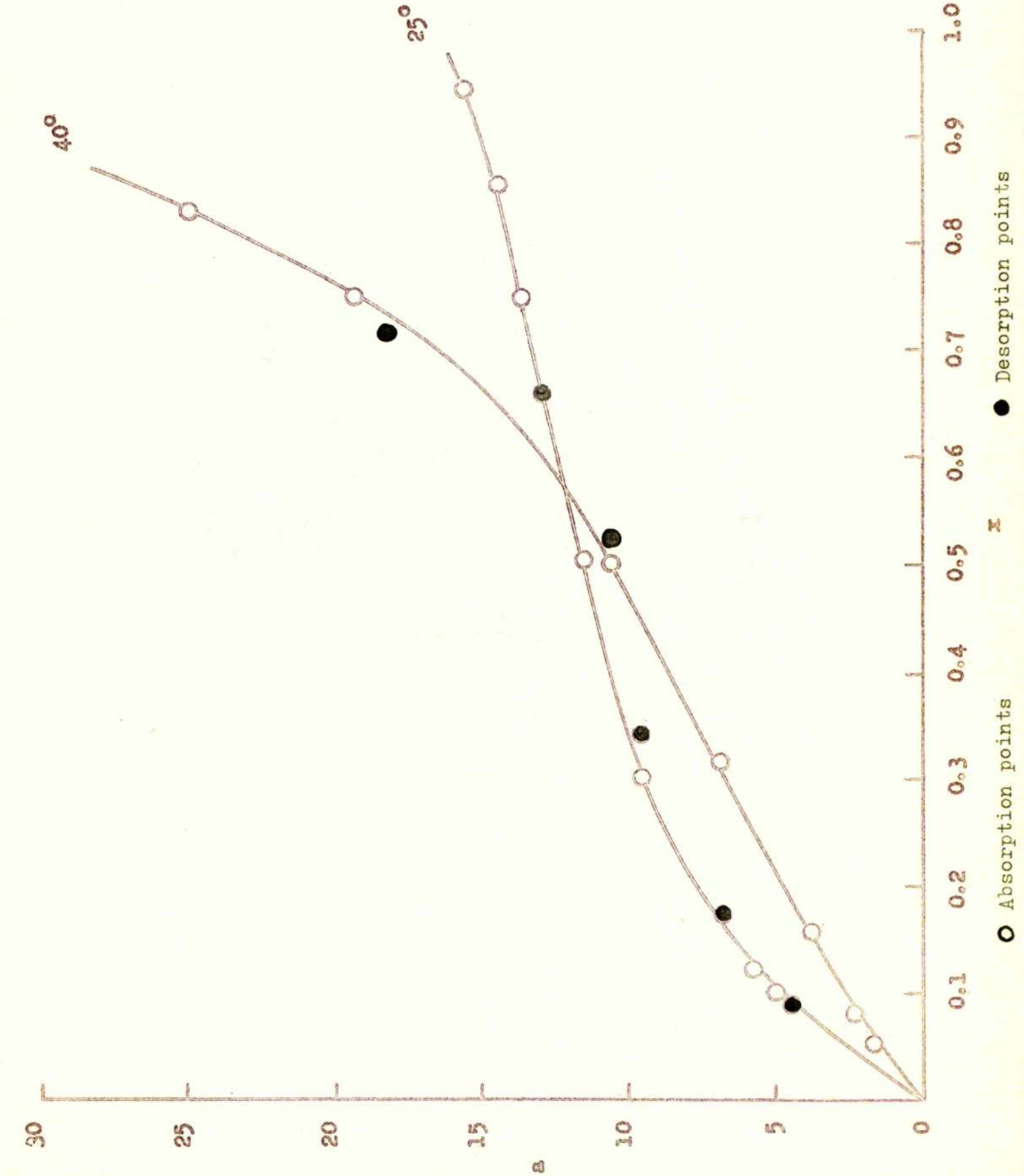

FIGURE 27c

Fraction 3.

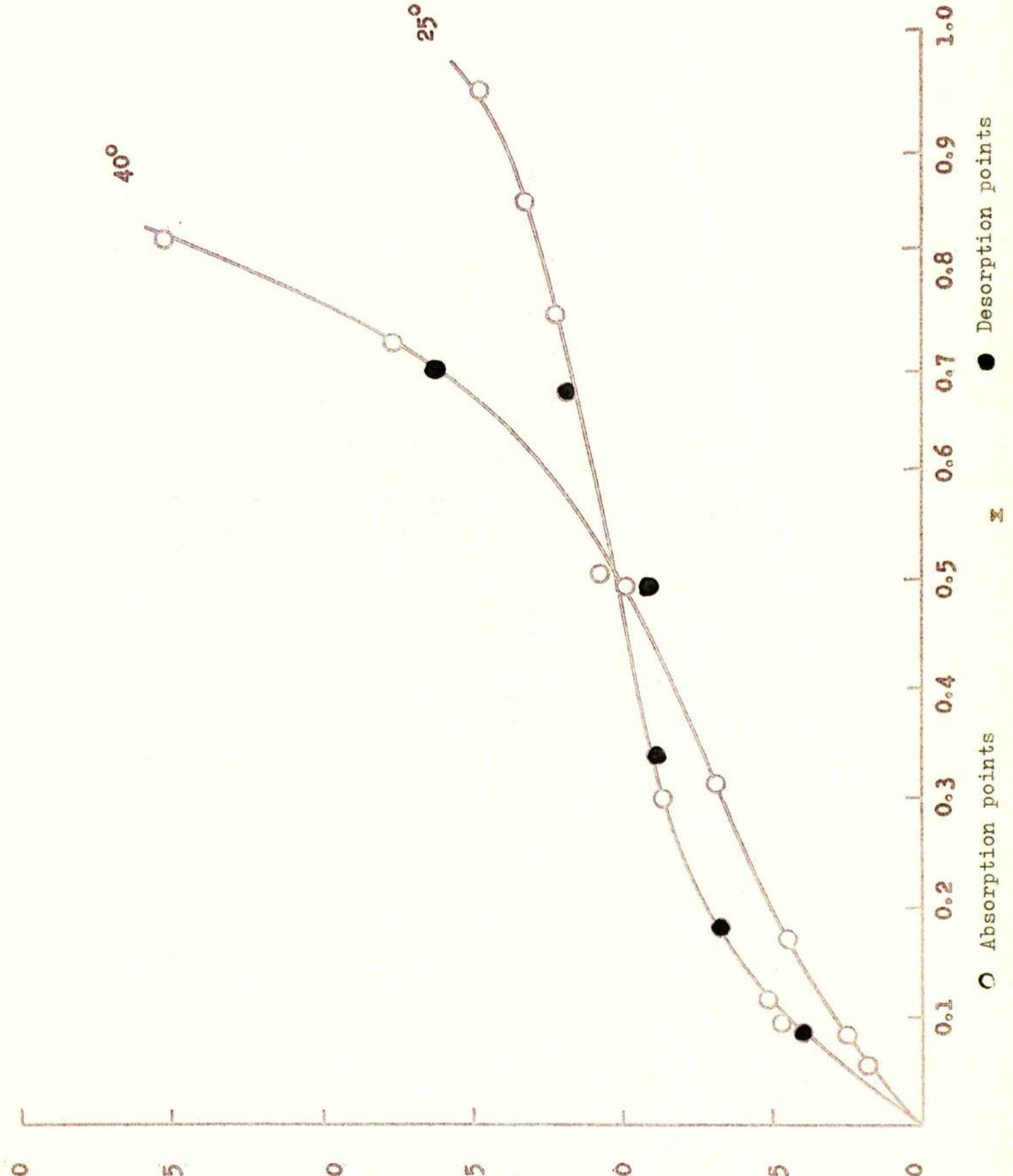

FIGURE 28a

Fraction 1.

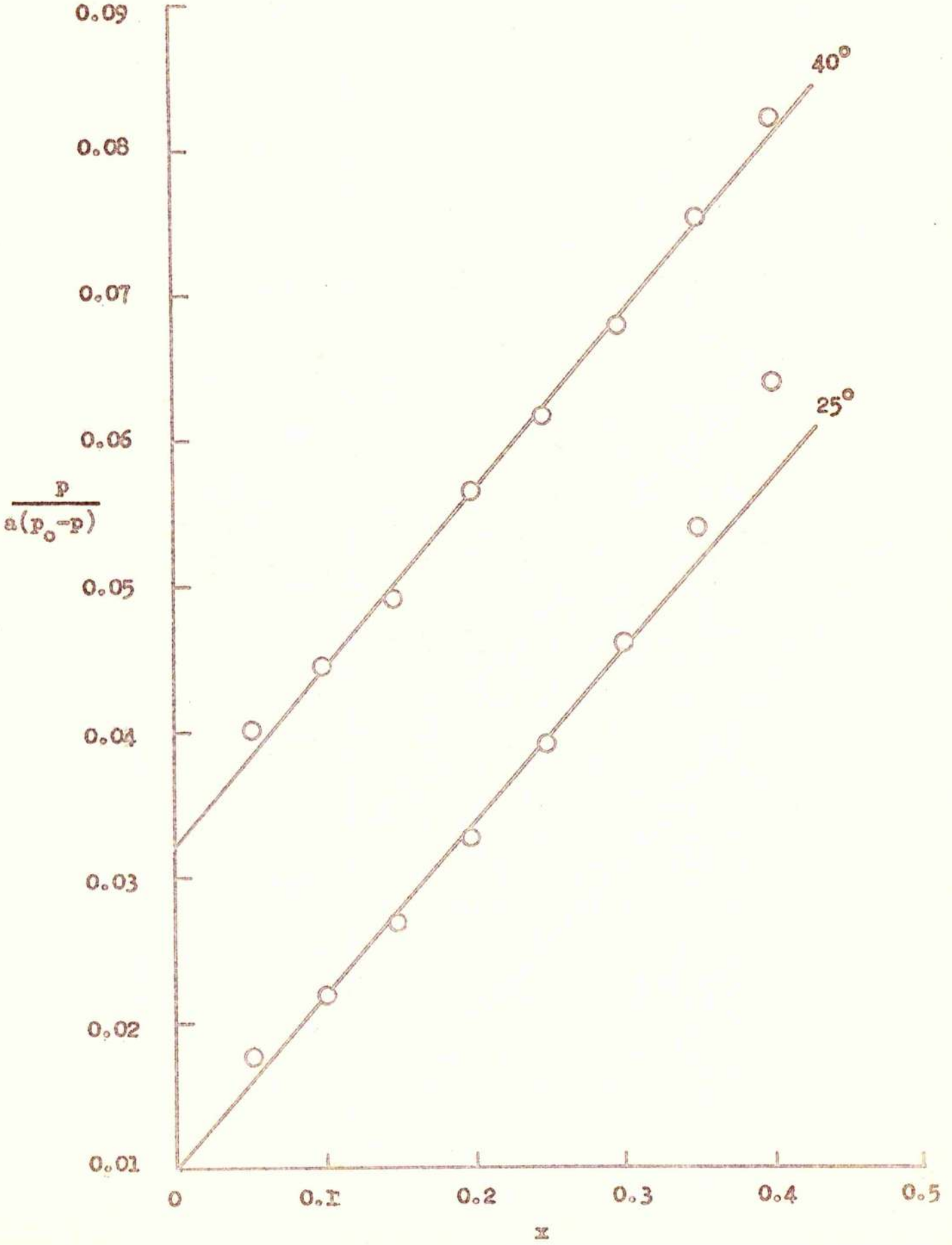

FIGURE 28b

Fraction 2.

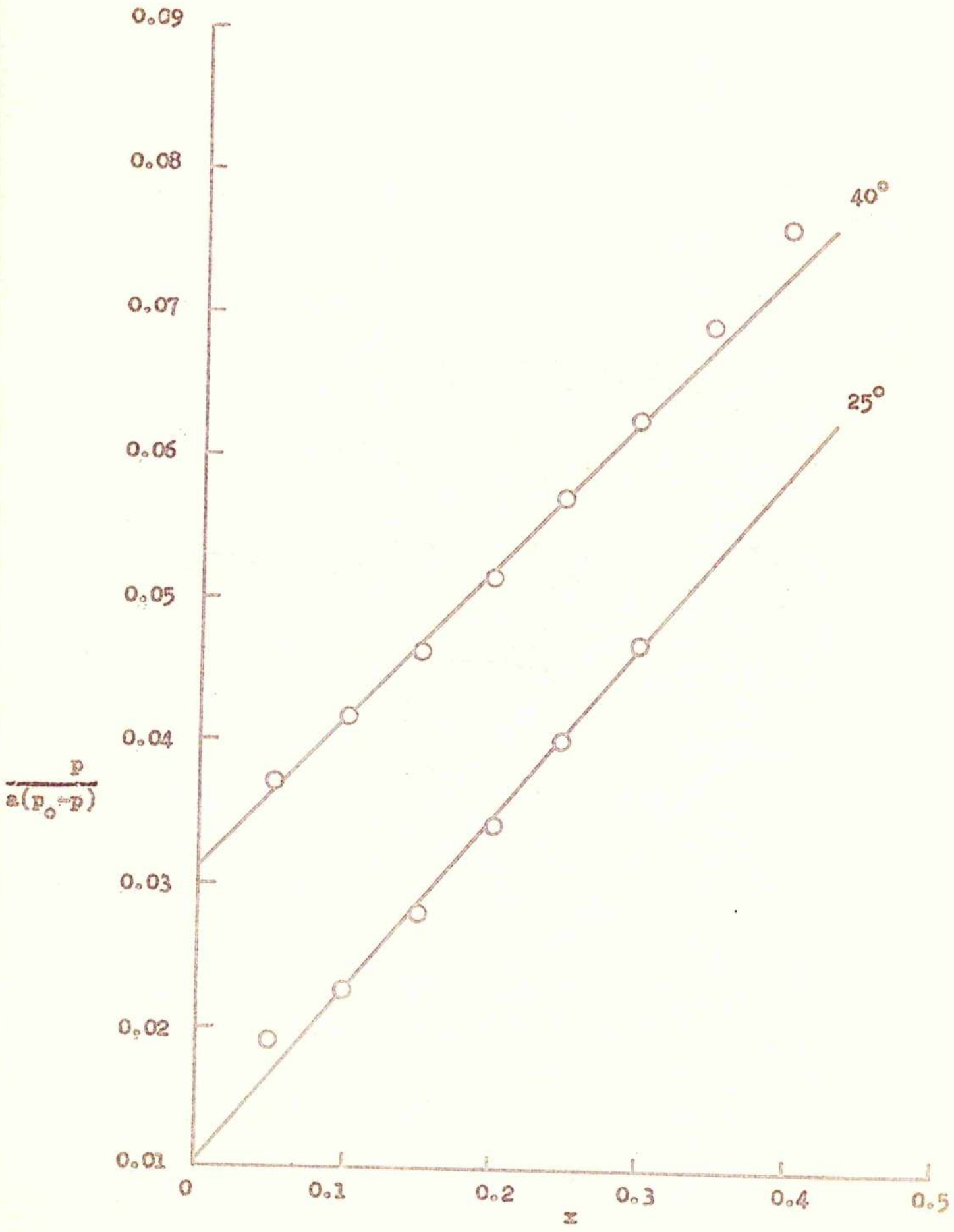

FIGURE 28c

Fraction 3.

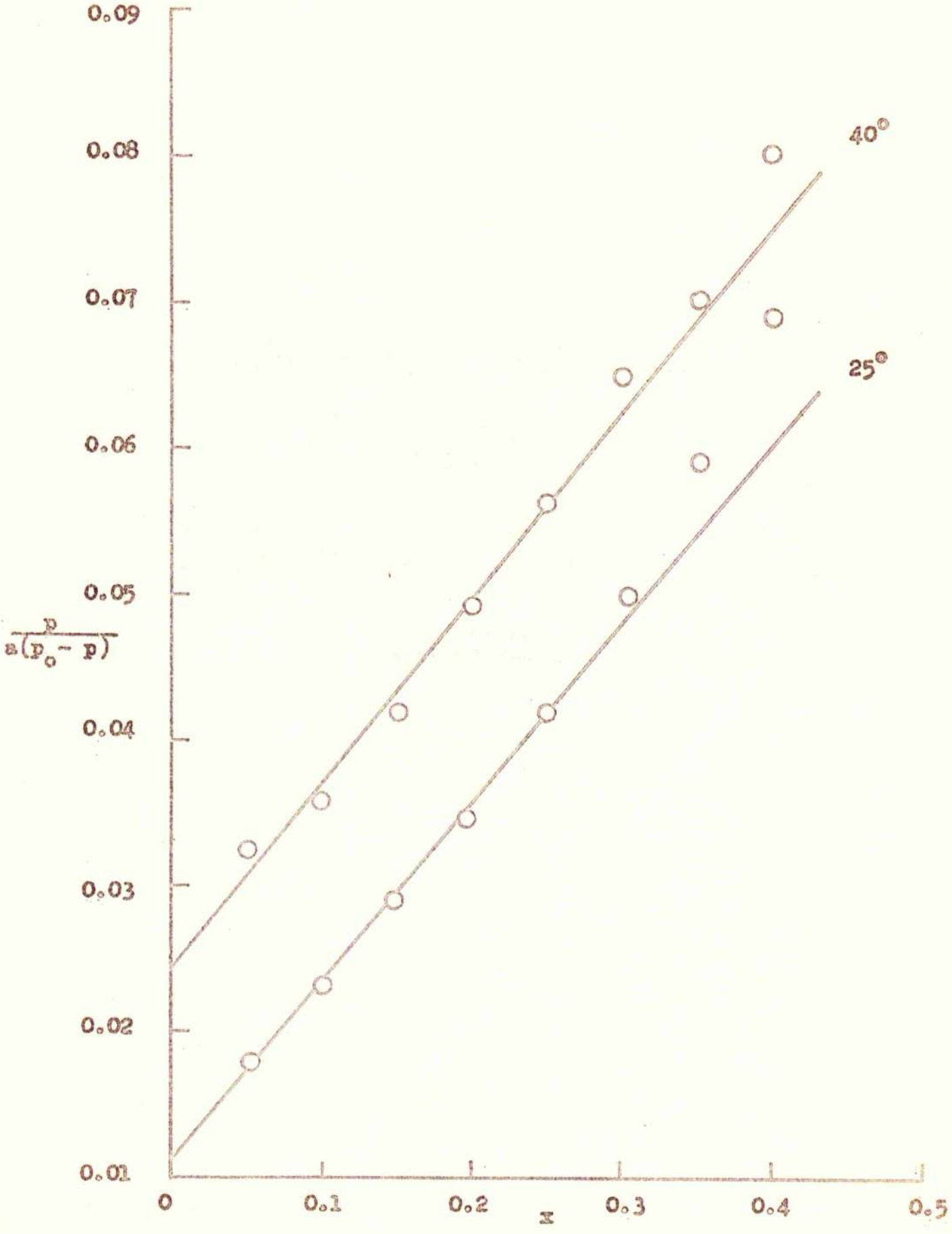

FIGURE 29a

Fraction 1.

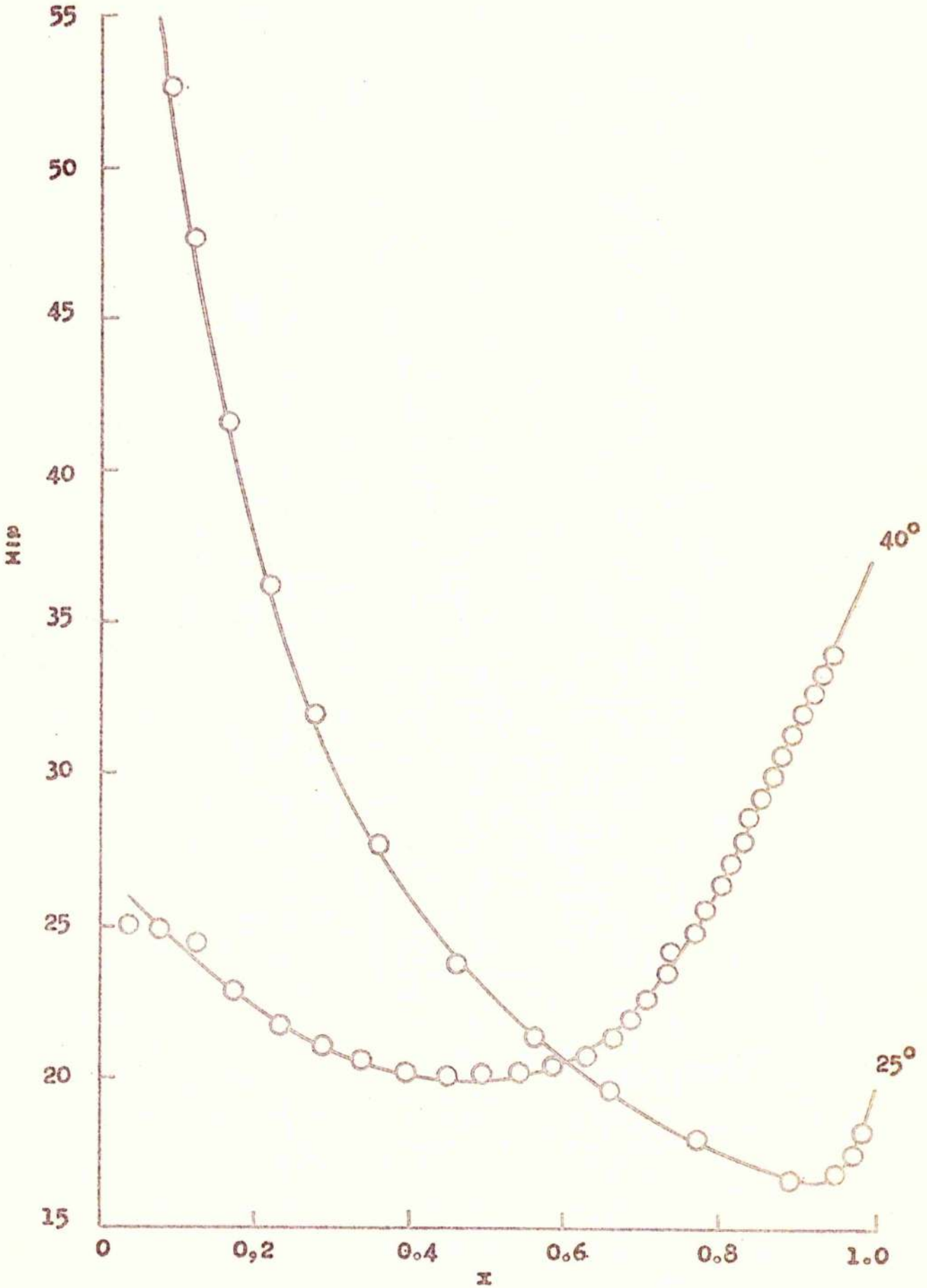

FIGURE 29b

Fraction 2.

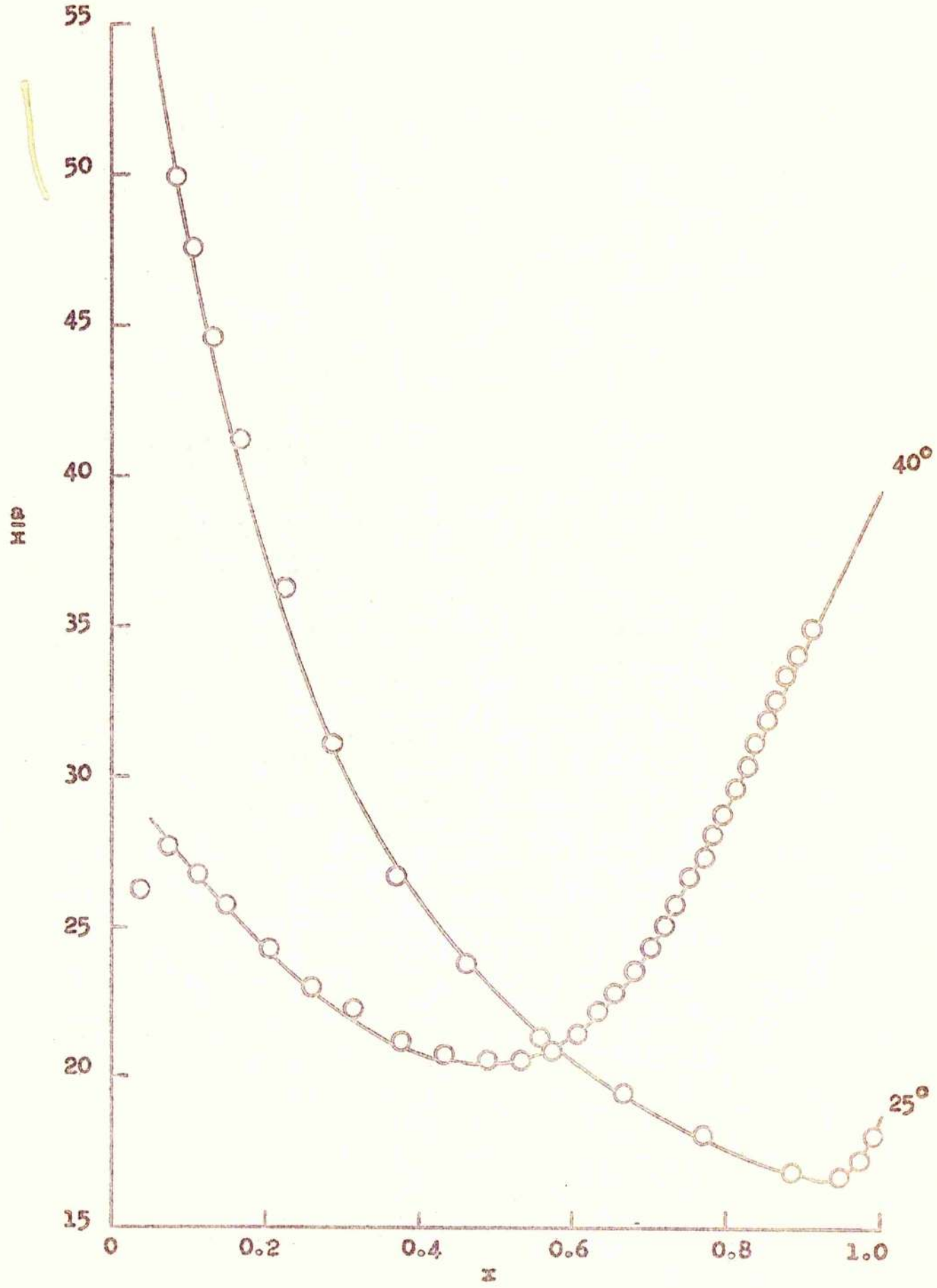

FIGURE 29c.

Fraction 3.

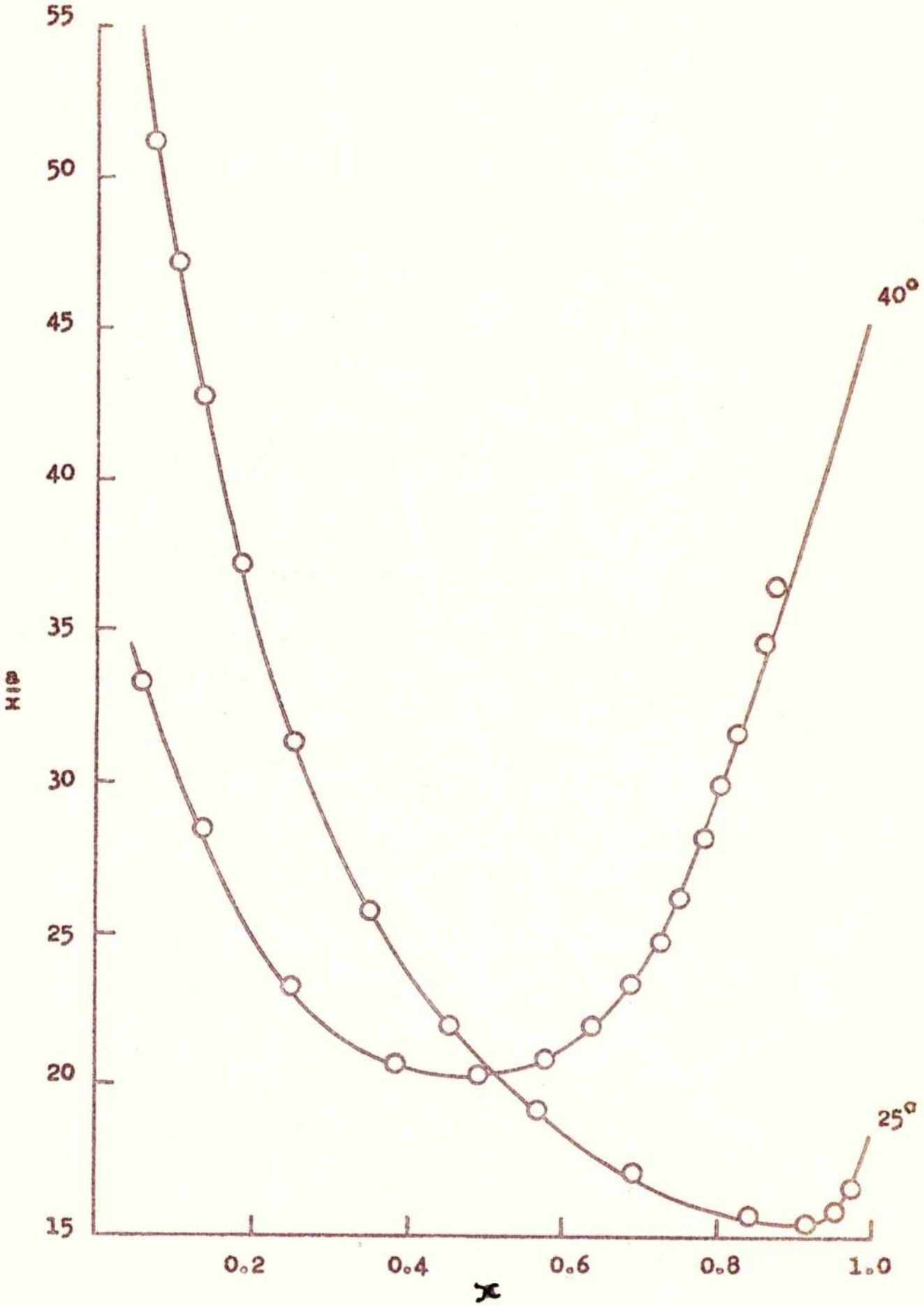

FIGURE 30a

Fraction 1.

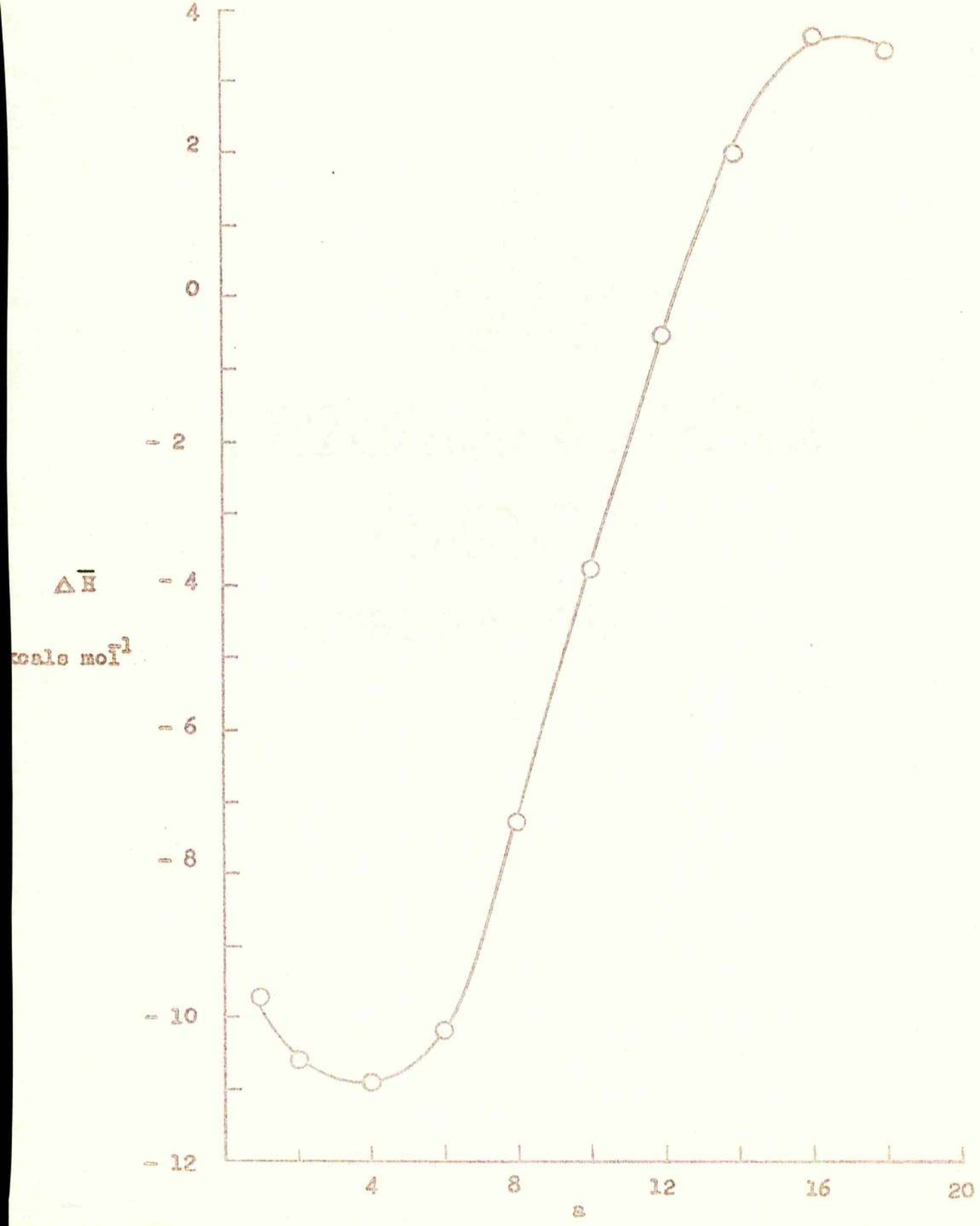

FIGURE 30b

Fraction 2

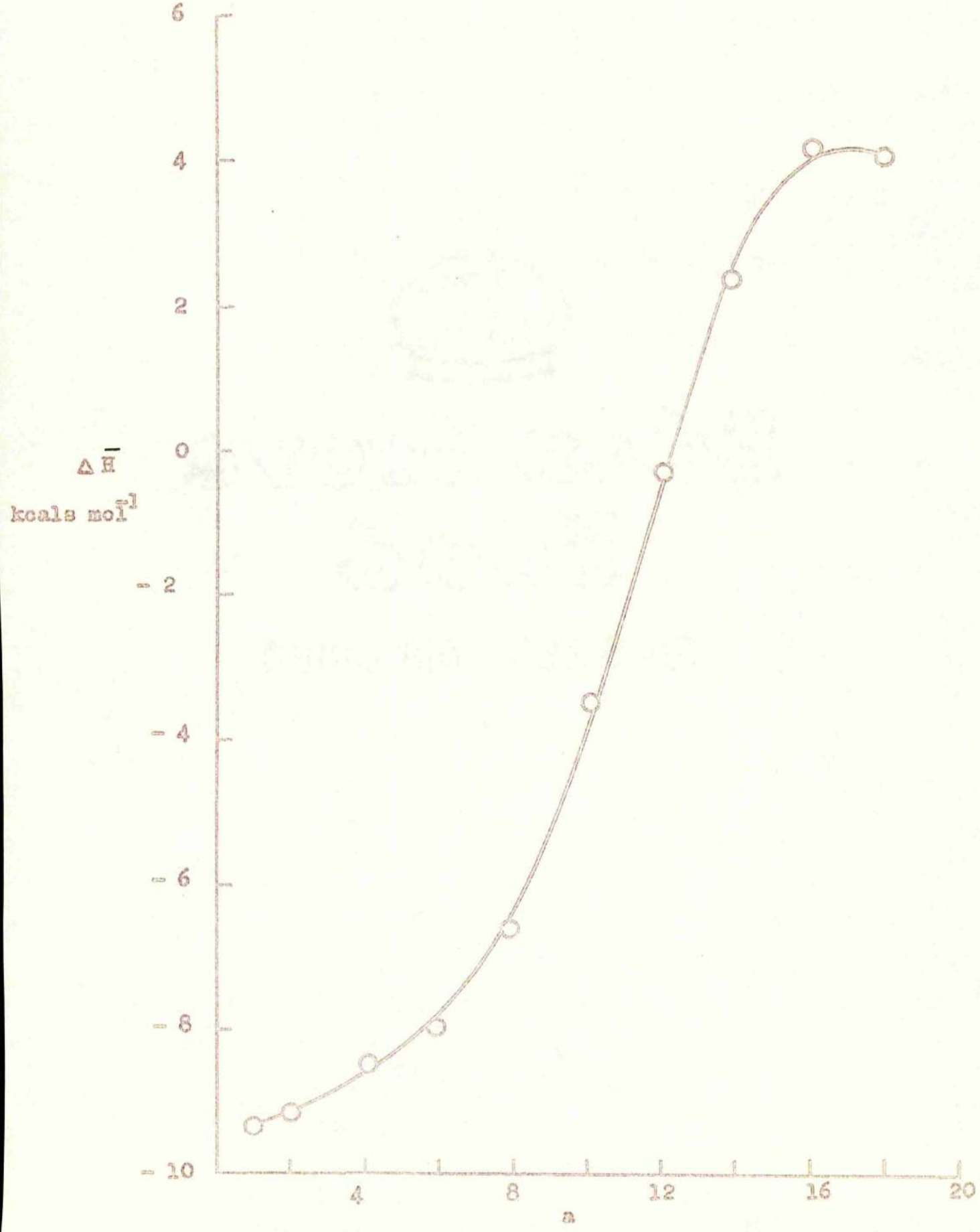

FIGURE 30c

Fraction 3.

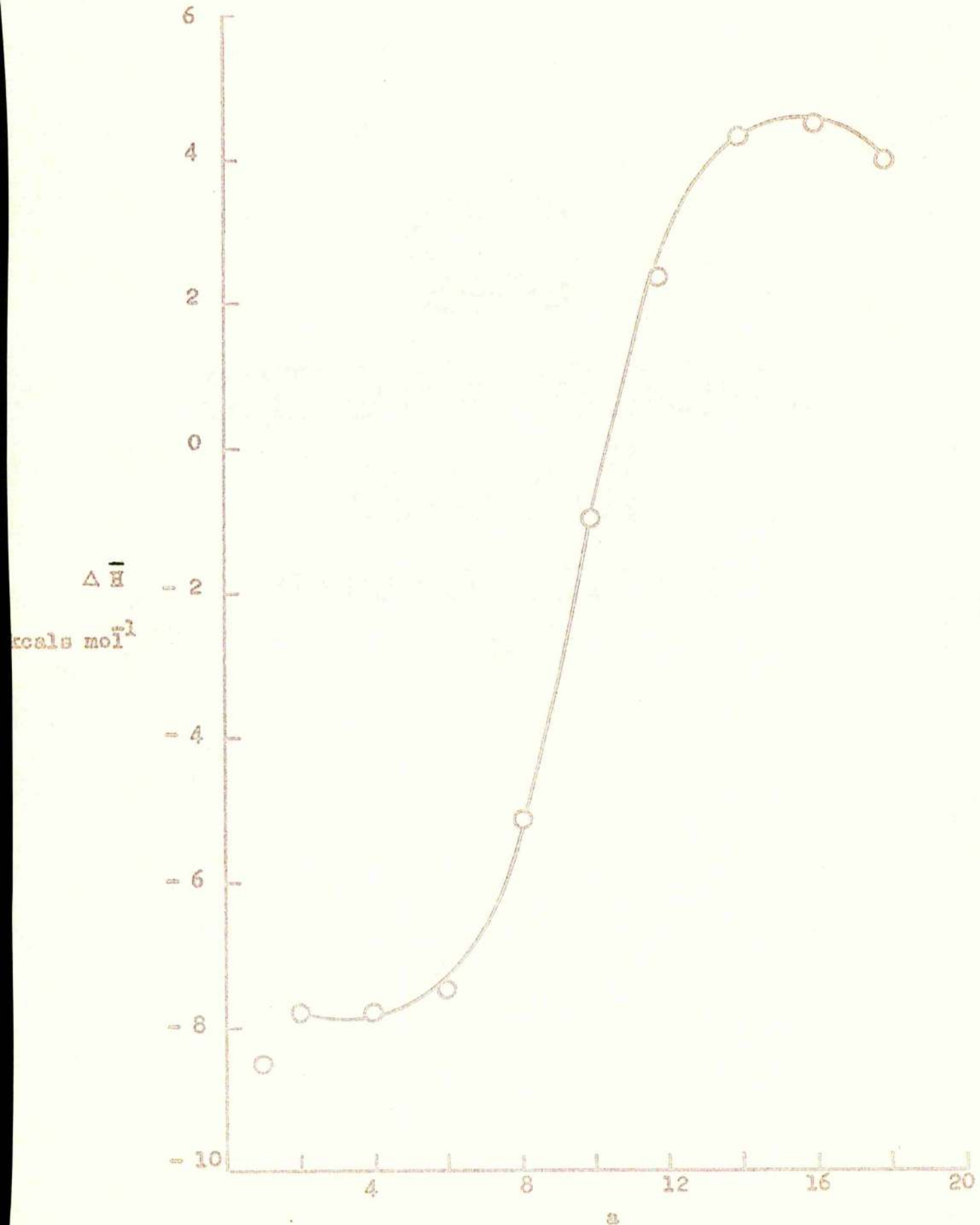

FIGURE 31a

Fraction 1

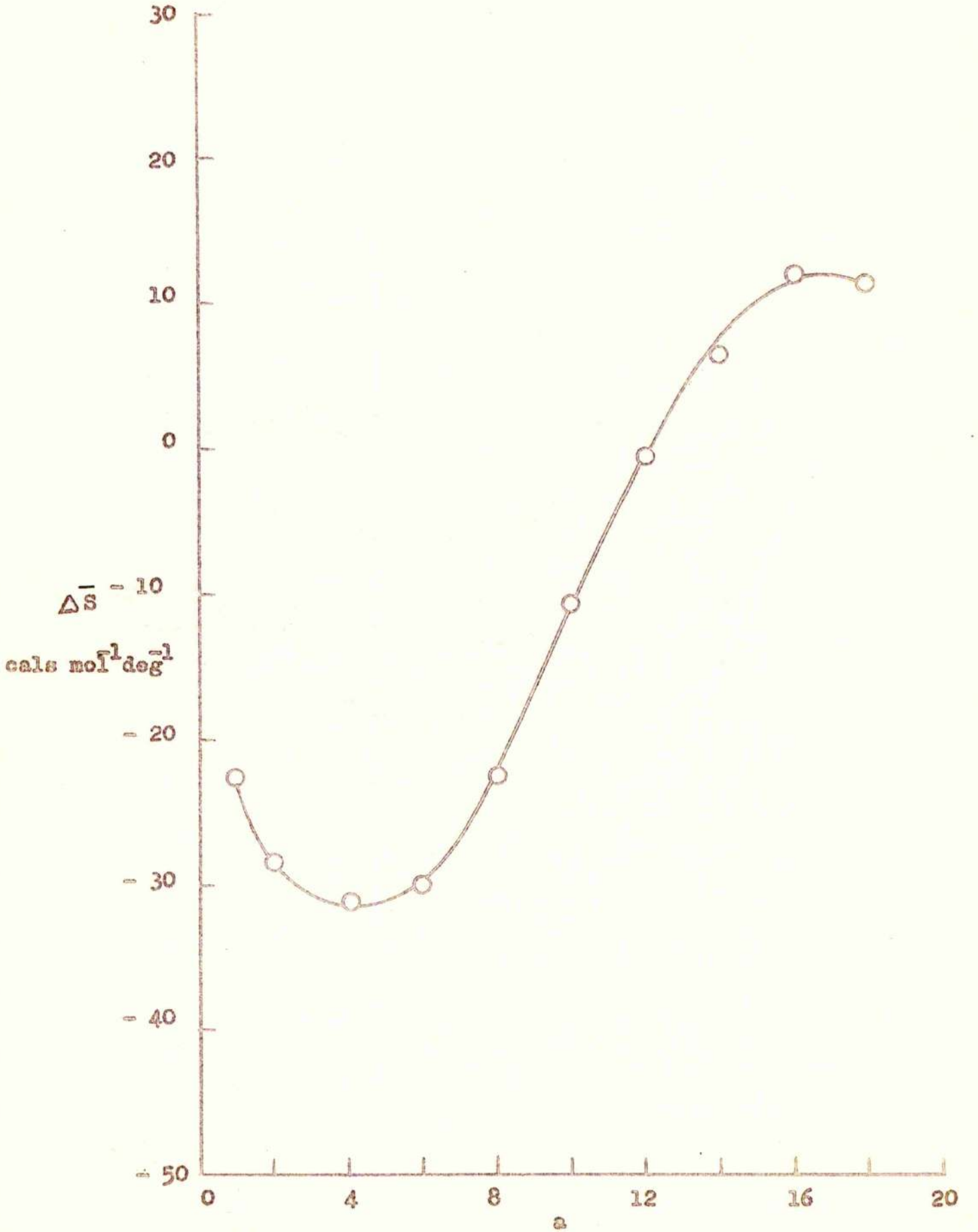

FIGURE 31b

Fraction 2.

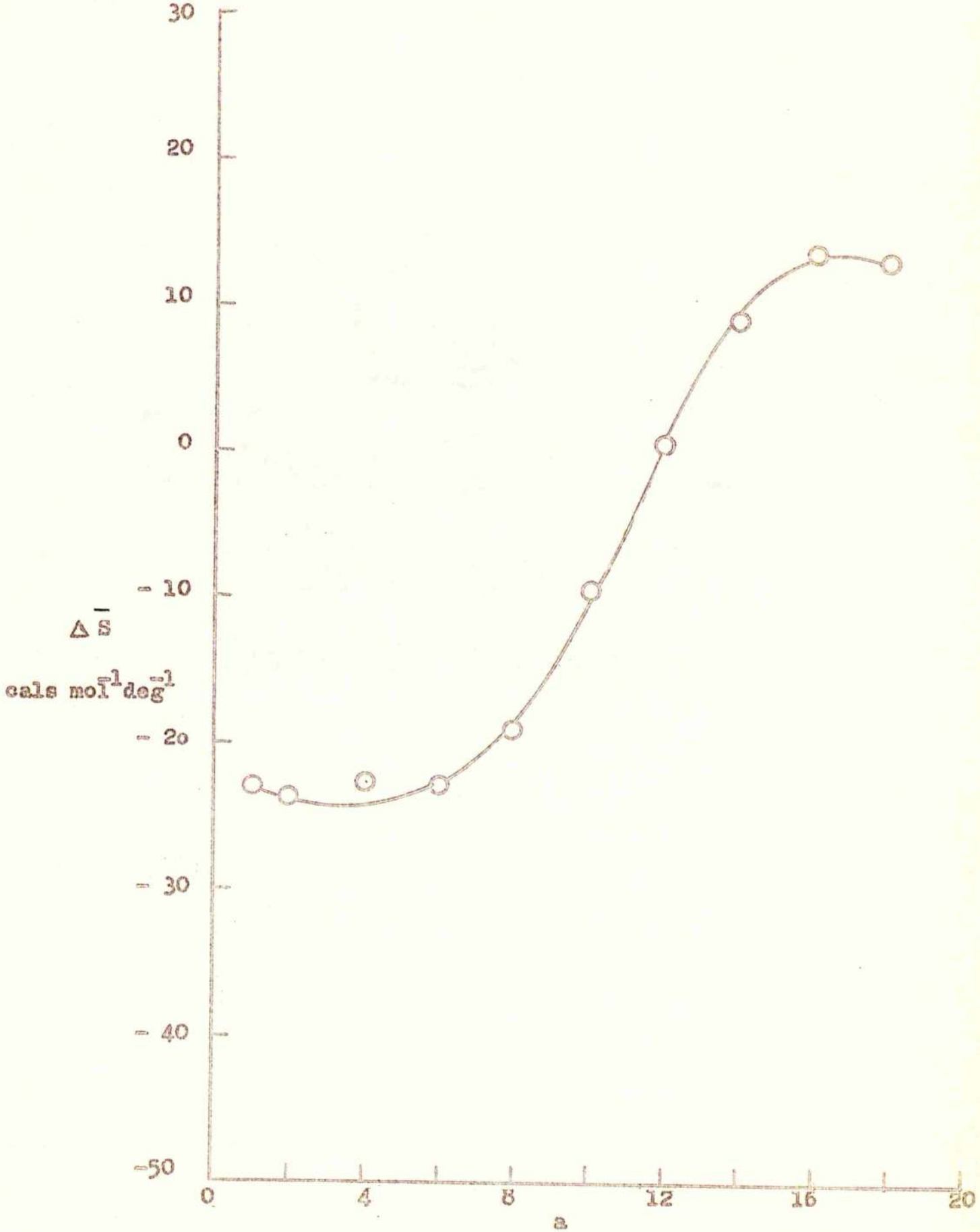

FIGURE 31c

Fraction 3.

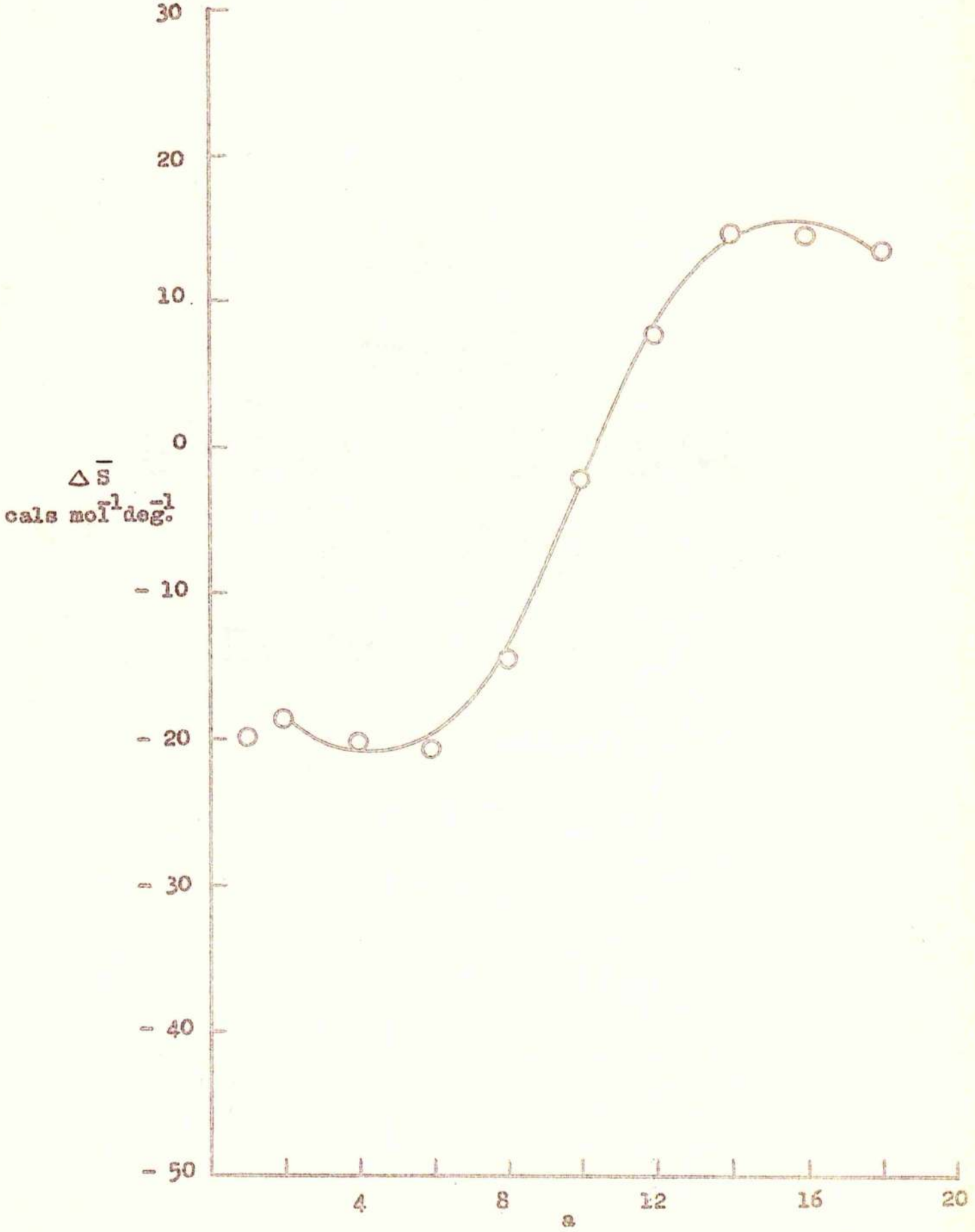

FIGURE 32.

(a)

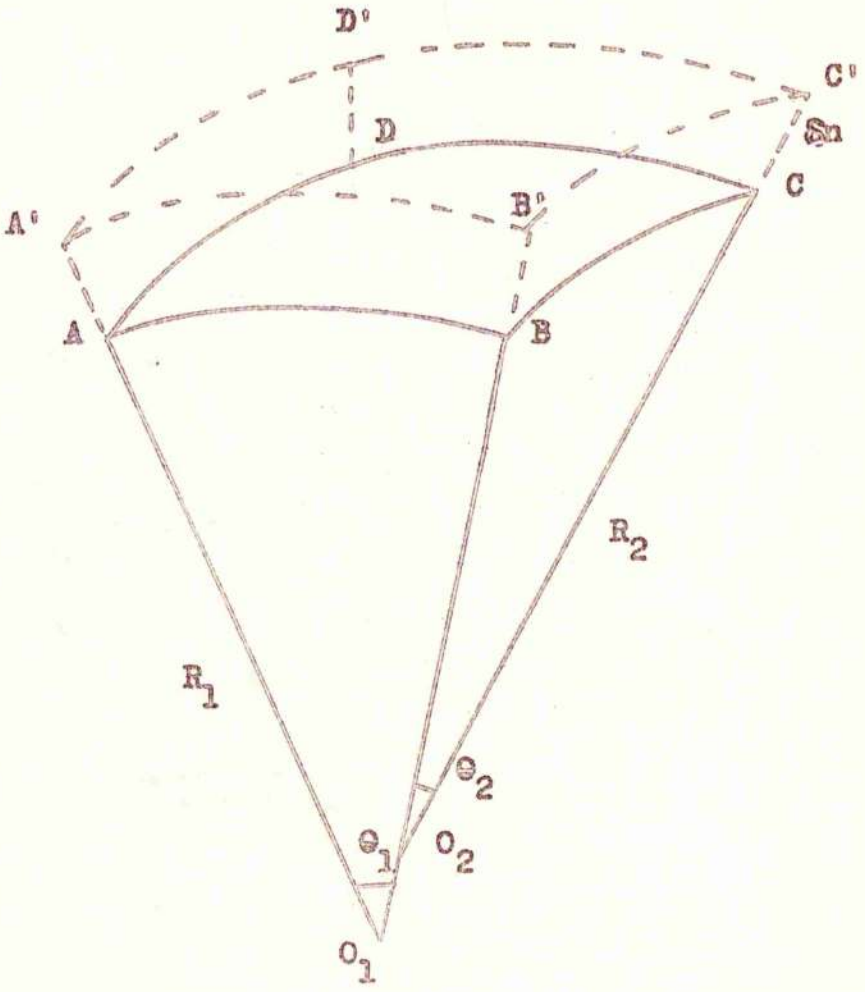
D'
C'
D
C
A'
B'
A
B
R_2
R_1
θ_2
θ_1
O_2
O_1

(b)

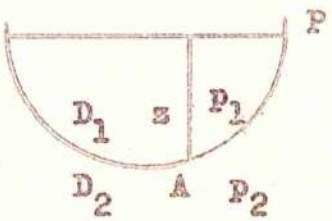
P
D_1
z
p_1
D_2
A
P_2

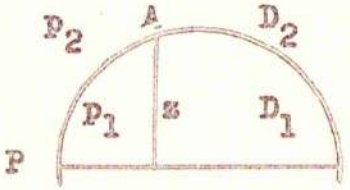
P_2
A
D_2
p_1
z
D_1
P

FIGURE 33

(a)

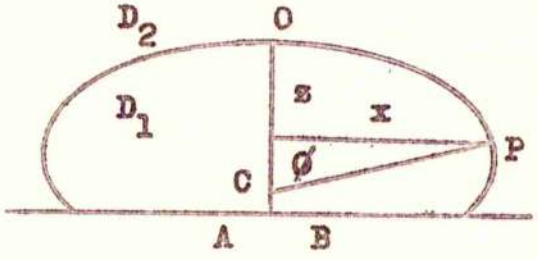

(b)

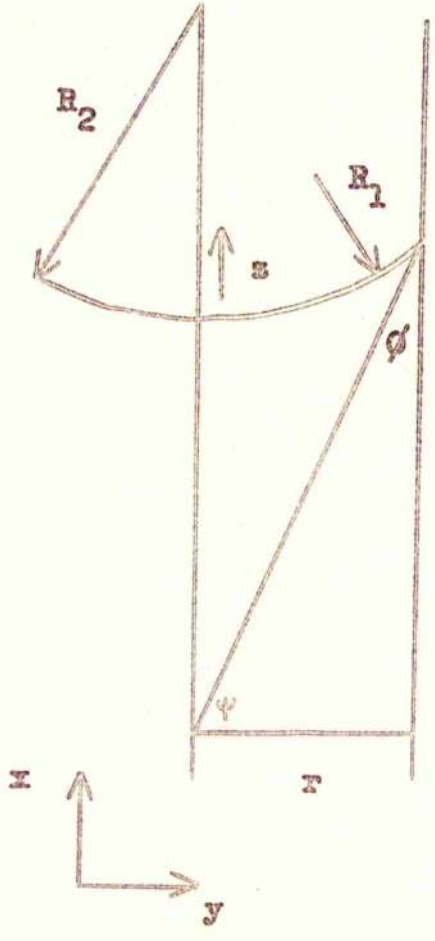

FIGURE 34.

Surface Tension Appàratus.

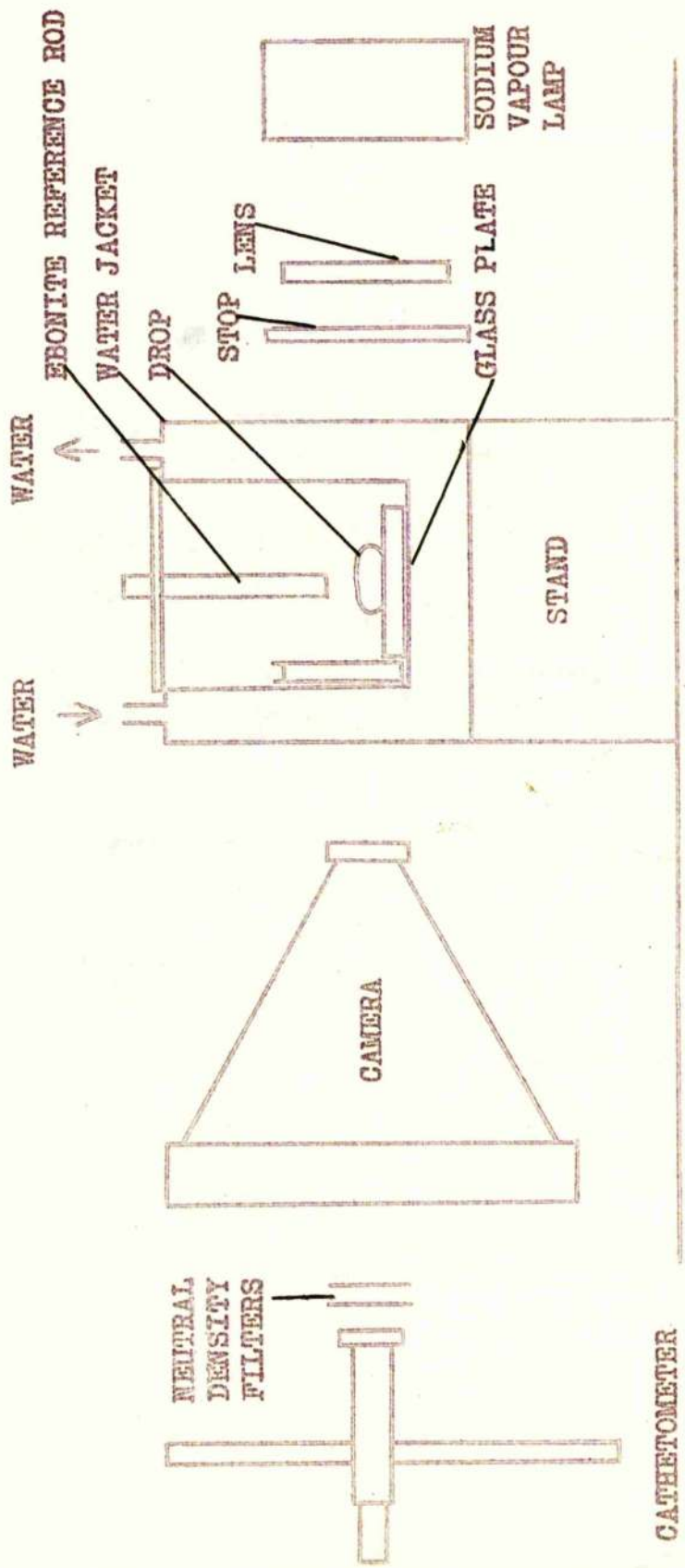

FIGURE 35

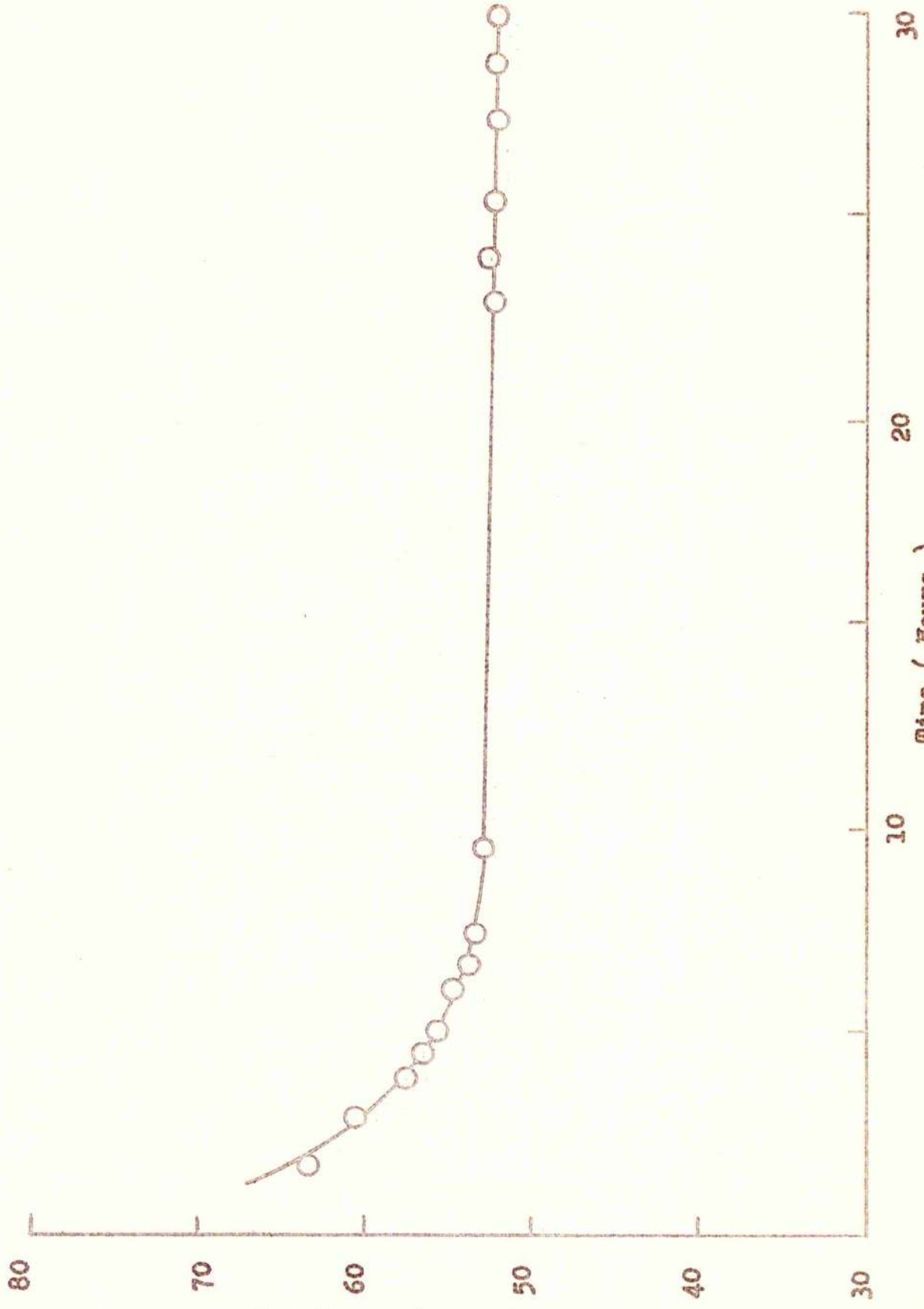

FIGURE 36

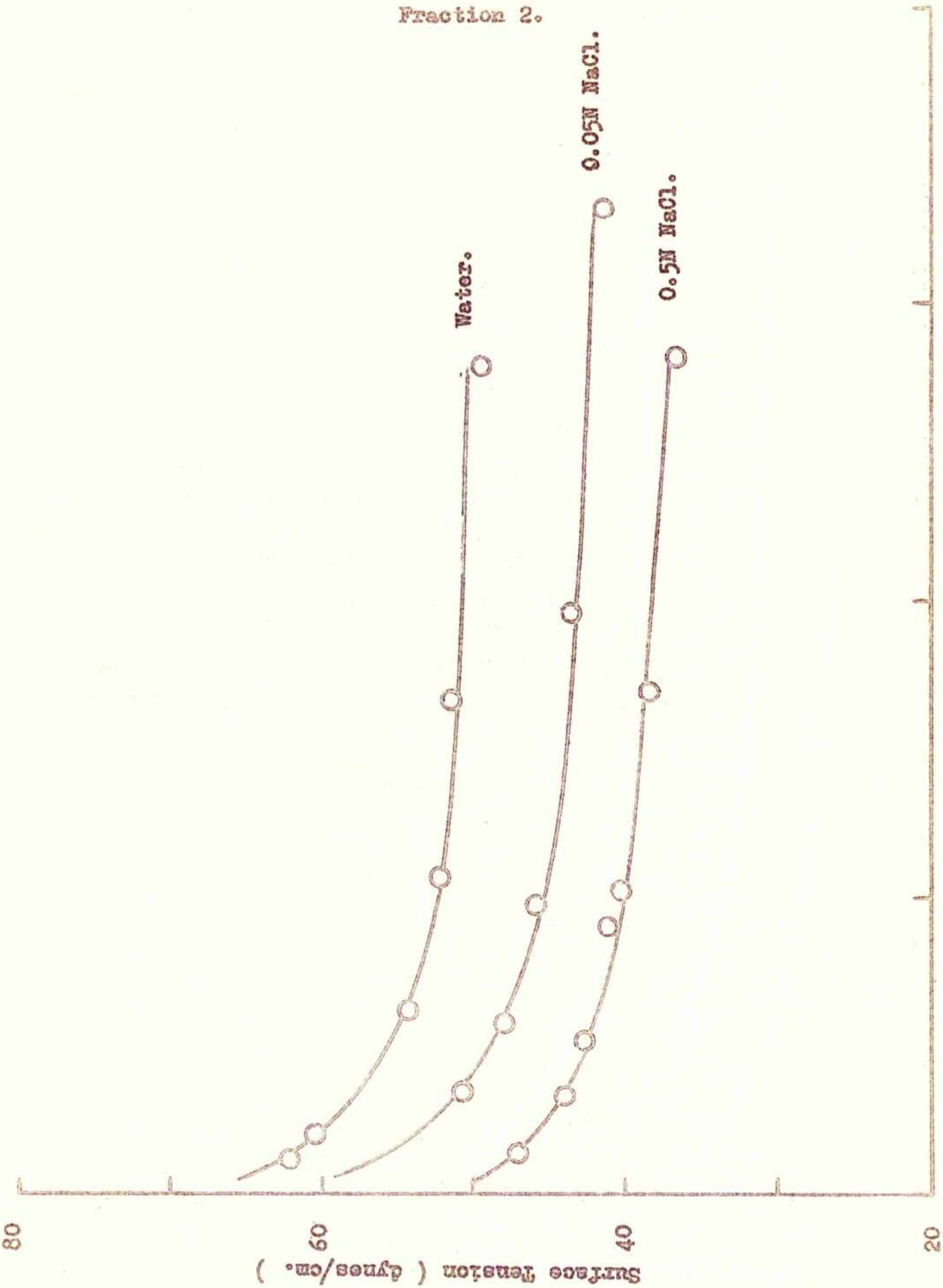
Fraction 2.
Water.
0.05N NaCl.
0.5N NaCl.
Surface Tension (dynes/cm.)
80
60
40
20
1.0
2.0
3.0
4.0
Concentration (%)